



THE UNIVERSITY *of* EDINBURGH

Edinburgh Research Explorer

Search for heavy Majorana or Dirac neutrinos and right-handed W gauge bosons in final states with two charged leptons and two jets at $\sqrt{s}=13$ TeV with the ATLAS detector

Citation for published version:

Clark, PJ, Farrington, S, Fauci Giannelli, M, Gao, Y, Hasib, A, Leonidopoulos, C, Martin, VJ, Mijovic, L, Wynne, B & Collaboration, A 2019, 'Search for heavy Majorana or Dirac neutrinos and right-handed W gauge bosons in final states with two charged leptons and two jets at $\sqrt{s}=13$ TeV with the ATLAS detector', *Journal of High Energy Physics*, vol. 1901, Aaboud:2018spl, pp. 016.
[https://doi.org/10.1007/JHEP01\(2019\)016](https://doi.org/10.1007/JHEP01(2019)016)

Digital Object Identifier (DOI):

[10.1007/JHEP01\(2019\)016](https://doi.org/10.1007/JHEP01(2019)016)

Link:

[Link to publication record in Edinburgh Research Explorer](#)

Document Version:

Publisher's PDF, also known as Version of record

Published In:

Journal of High Energy Physics

General rights

Copyright for the publications made accessible via the Edinburgh Research Explorer is retained by the author(s) and / or other copyright owners and it is a condition of accessing these publications that users recognise and abide by the legal requirements associated with these rights.

Take down policy

The University of Edinburgh has made every reasonable effort to ensure that Edinburgh Research Explorer content complies with UK legislation. If you believe that the public display of this file breaches copyright please contact openaccess@ed.ac.uk providing details, and we will remove access to the work immediately and investigate your claim.



RECEIVED: October 1, 2018

REVISED: December 5, 2018

ACCEPTED: December 12, 2018

PUBLISHED: January 3, 2019

Search for heavy Majorana or Dirac neutrinos and right-handed W gauge bosons in final states with two charged leptons and two jets at $\sqrt{s} = 13$ TeV with the ATLAS detector



The ATLAS collaboration

E-mail: atlas.publications@cern.ch

ABSTRACT: A search for heavy right-handed Majorana or Dirac neutrinos N_R and heavy right-handed gauge bosons W_R is performed in events with a pair of energetic electrons or muons, with the same or opposite electric charge, and two energetic jets. The events are selected from pp collision data with an integrated luminosity of 36.1 fb^{-1} collected by the ATLAS detector at $\sqrt{s} = 13 \text{ TeV}$. No significant deviations from the Standard Model are observed. The results are interpreted within the theoretical framework of a left-right symmetric model and lower limits are set on masses in the heavy right-handed W boson and neutrino mass plane. The excluded region extends to $m_{RR} = 4.7 \text{ TeV}$ for both Majorana and Dirac N_R neutrinos.

KEYWORDS: Hadron-Hadron scattering (experiments)

ARXIV EPRINT: [1809.11105](https://arxiv.org/abs/1809.11105)

Contents

1	Introduction	1
2	ATLAS detector	3
3	Dataset and simulated event samples	3
4	Object reconstruction	5
5	Event selection	6
6	Background estimation	7
7	Systematic uncertainties	11
8	Statistical analysis and results	12
9	Conclusion	19
	The ATLAS collaboration	26

1 Introduction

Left-right symmetric models [1–9] (LRSMs) attempt to explain the broken parity symmetry of the weak interaction in the Standard Model (SM) and can introduce, depending on the form of the LRSM, right-handed counterparts to the W and Z bosons (W_R and Z_R), and right-handed heavy neutrinos (N_R). A search for W_R boson and N_R neutrino production in a final state containing two charged leptons and two jets ($\ell\ell jj$) with $\ell = e, \mu$ is presented here. The exact process of interest is the Keung-Senjanović (KS) process [10], shown in figure 1. When the W_R boson is heavier than the N_R neutrino ($m_{W_R} > m_{N_R}$), the on-shell W_R mass can be reconstructed from the invariant mass of the $\ell\ell jj$ system, whereas, when $m_{N_R} > m_{W_R}$, the on-shell W_R mass can be reconstructed from the invariant mass of the jj system. Only ee and $\mu\mu$ lepton pairs, coupling respectively to N_R^e and N_R^μ , are considered as part of the $\ell\ell jj$ final state, since no mixing between flavours is assumed. Left- and right-handed weak gauge couplings are also defined to be equivalent ($g_L = g_R$).

In the minimal LRSM containing the type-I seesaw mechanism [6–9], N_R neutrinos are Majorana particles. The type-I seesaw mechanism accounts for the masses of the SM neutrinos by linking (heavy) N_R neutrinos and the SM neutrino masses through a mixing matrix. In this case, both the SM neutrinos and the hypothetical N_R neutrinos are required to be Majorana particles, allowing lepton-number-violating processes, such as the KS process, to occur. In LRSM variants, including the inverse seesaw mechanism [11–14],

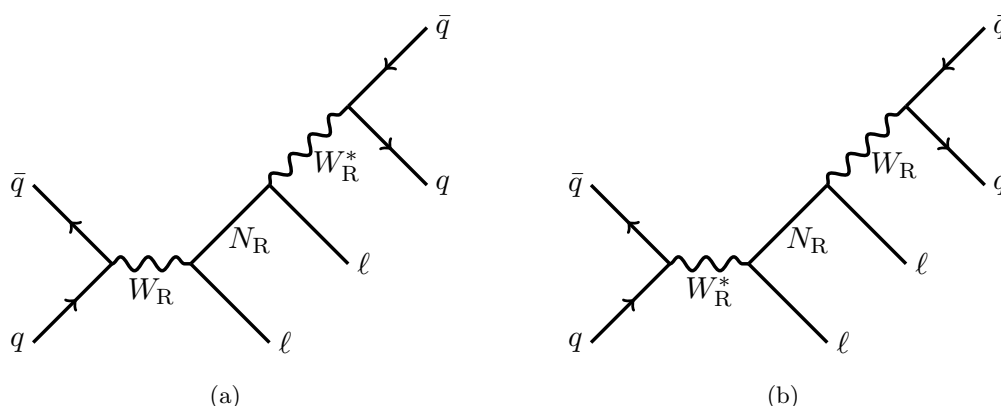


Figure 1. The KS process, for (a) the $m_{W_R} > m_{N_R}$ case and (b) the $m_{N_R} > m_{W_R}$ case.

N_R neutrinos are pseudo-Dirac particles¹ (referred to in this paper as “Dirac” particles for simplicity). For simple versions of LRSMs containing the inverse seesaw mechanism, lepton-number-violating processes are not expected [16]. The Majorana or Dirac nature of the N_R neutrino can be established by comparing the charges of the two final-state leptons. If the N_R neutrinos are Dirac particles, the leptons will always have opposite-sign (OS) charges. However, if they are Majorana particles, the N_R neutrinos are their own anti-particles, and their decay will give rise to an experimental signature of both opposite- and same-sign (SS) dileptons in a 50%-50% admixture.

The KS process resulting in an $\ell\ell jj$ final state in the electron and muon channels has been studied by both the ATLAS and CMS collaborations using $\sqrt{s} = 7$ TeV [17, 18], $\sqrt{s} = 8$ TeV [19, 20] and $\sqrt{s} = 13$ TeV [21] collision data. CMS also has results for the hadronic $\tau\tau jj$ final state at $\sqrt{s} = 13$ TeV [22, 23]. No evidence of a W_R boson or a N_R neutrino has emerged from these studies. The current most stringent exclusion limits on W_R boson and Majorana N_R neutrino masses are derived by the CMS experiment [21] at $\sqrt{s} = 13$ TeV, in both the electron and muon channels, regions extending to $m_{W_R} \sim 4.4$ TeV (for a range of m_{N_R} values) are excluded, whilst the m_{N_R} limits reach ~ 2.9 TeV in the electron channel (for $m_{W_R} \sim 3.8$ TeV) and ~ 3 TeV in the muon channel (for $m_{W_R} \sim 3.6$ TeV). The analysis presented here extends the ATLAS searches to 36.1 fb^{-1} of data at $\sqrt{s} = 13$ TeV and also provides lower limits on the masses for the Dirac case of the N_R neutrino. The cross-section of the KS process varies, depending on the masses of the W_R boson and the N_R neutrino, from a few pb to about 3×10^{-4} pb for high-mass signal points at the end of the sensitivity of this analysis. The analysis uses a new MADGRAPH generator model [24, 25] which overcomes known limitations of PYTHIA [26] as employed in previous searches by ATLAS and CMS, and also allows the exploration of the scenario in which the N_R neutrino is heavier than the W_R boson for the first time.

¹A pseudo-Dirac particle is formed by two Majorana particles with identical masses [15].

2 ATLAS detector

The ATLAS experiment [27] is a multipurpose particle detector with a forward-backward symmetric cylindrical geometry and a near 4π coverage in solid angle.² It consists of an inner tracking detector (ID) surrounded by a thin superconducting solenoid providing a 2 T axial magnetic field, electromagnetic (EM) and hadron calorimeters, and a muon spectrometer (MS). The ID covers the pseudorapidity range $|\eta| < 2.5$. It consists of silicon pixel, silicon microstrip, and straw-tube transition-radiation tracking detectors. A new innermost layer of pixel detectors [28, 29] was installed prior to the start of data taking in 2015. Lead/liquid-argon (LAr) sampling calorimeters provide electromagnetic energy measurements with high granularity and cover $|\eta| < 3.2$. A hadron (steel/scintillator-tile) calorimeter covers the central pseudorapidity range ($|\eta| < 1.7$). The endcap and forward regions are instrumented with LAr calorimeters for EM and hadronic energy measurements up to $|\eta| = 4.9$. The MS surrounds the calorimeters and is based on three large air-core toroidal superconducting magnets with eight coils each. The field integral of the toroidal magnets ranges between 2.0 and 6.0 Tm across most of the detector. The MS includes a system of precision tracking chambers covering $|\eta| < 2.7$ and fast detectors ($|\eta| < 2.4$) for triggering. A two-level trigger system [30] is used to select events for offline physics analyses. The first-level trigger is implemented in hardware and uses a subset of the detector information. This is followed by the software-based high-level trigger, reducing the event rate to about 1 kHz.

3 Dataset and simulated event samples

The data used in this analysis were collected at a centre-of-mass energy of 13 TeV during 2015 and 2016, and correspond to an integrated luminosity of 36.1 fb^{-1} . Only high-quality data with all detectors in normal operating conditions are analysed.

Simulated signal and background events are used to optimise the event selection and to estimate the background contributions.

Signal events with matrix elements calculated by MG5_aMC@NLO v2.2.2 [24, 25] were simulated by PYTHIA8.186 [26] using the NNPDF2.3 [31] parton distribution function (PDF) set and the A14 set of tuned parton shower parameters [32]. A version of an LRSM model produced with FeynRules [33] was implemented in MG5_aMC@NLO [34] and further modified as described in ref. [35]. Events were generated containing only Majorana N_R neutrinos. For the Dirac neutrino case, only the OS events are used in the analysis as no other differences are expected. Signal samples were generated for different W_R boson and N_R neutrino mass hypotheses, covering a range from 600 GeV to 5800 GeV for m_{W_R} and 50 GeV to 8000 GeV for m_{N_R} . Only samples with $m_{N_R} \leq 2m_{W_R}$ are used as the cross-section for the KS process drops off rapidly with increasing N_R neutrino mass.

²ATLAS uses a right-handed coordinate system with its origin at the nominal interaction point (IP) in the centre of the detector and the z -axis along the beam pipe. The x -axis points from the IP to the centre of the LHC ring, and the y -axis points upwards. Cylindrical coordinates (r, ϕ) are used in the transverse plane, ϕ being the azimuthal angle around the z -axis. The pseudorapidity is defined in terms of the polar angle θ as $\eta = -\ln \tan(\theta/2)$. The angular distance is measured in units of $\Delta R \equiv \sqrt{(\Delta\eta)^2 + (\Delta\phi)^2}$.

For the OS channel, the dominant SM backgrounds are $Z + \text{jet(s)}$ and $t\bar{t}$ processes. In the SS channel, the main backgrounds arise from misidentified leptons, electron charge misidentification, and leptons from diboson processes such as ZW , ZZ , or WW (including $W^\pm W^\pm jj$) production. Other backgrounds taken into the account are $t\bar{t}V$ ($V = W, Z, H$) and single-top production. Additional rare backgrounds such as the production of four or three top quarks as well as $t\bar{t}WW$, $t\bar{t}WZ$, tZ , and tWZ production, were found to be negligible in both the OS and SS channels.

Various SM backgrounds were simulated using different generators and the dominant backgrounds are evaluated using data-driven techniques, as described in section 6.

The $Z + \text{jet(s)}$ process (with $Z/\gamma^* \rightarrow ee/\mu\mu/\tau\tau$) was modelled using SHERPA 2.2.1 [36] with the NNPDF3.0 [37] PDF set. The matrix element (ME) was calculated for up to two partons with next-to-leading-order (NLO) accuracy in QCD and up to four partons with leading-order (LO) accuracy using Comix [38] and OpenLoops [39].

For the generation of $t\bar{t}$ events, POWHEG-BOX v2 [40–42] was used with the NNPDF3.0 PDF set in the ME calculation. The parton shower was modelled with PYTHIA8.186 [26] with the NNPDF2.3 [31] PDF set and the A14 set of tuned parameters [32]. Single-top-quark events produced in Wt final states were generated with POWHEG-BOX v2 with the CT10 PDF set [43] used in the ME calculations. Single top-quark production via s - or t -channels was generated by POWHEG-BOX v1 [40–42]. This generator uses the four-flavour scheme for the NLO QCD matrix element calculations together with the fixed four-flavour PDF set CT10f4 [43]. The parton shower, fragmentation, and underlying event were simulated with PYTHIA6.428 [44] using the CTEQ6L1 PDF sets [45] and the Perugia 2012 set of tuned parameters [46]. The top-quark mass was set to 172.5 GeV. The EvtGen v1.2.0 [47] program was used to model bottom and charm hadron decays. The $t\bar{t}V$ ($V = W, Z$) processes were generated at LO with MG5_aMC@NLO v2.2.2 [24] and the $t\bar{t}H$ process was generated at LO with MG5_aMC@NLO v2.3.2. For both, the NNPDF2.3 PDF set was used and the parton shower was modelled using PYTHIA8.186, configured with the A14 tune.

Diboson processes with four charged leptons (4ℓ), three charged leptons and one neutrino ($3\ell+1\nu$), or two charged leptons and two neutrinos ($2\ell+2\nu$) in the final state were generated using SHERPA 2.2.2 with the NNPDF3.0 PDF set. The matrix elements considered contained all diagrams with four electroweak vertices. The various processes were evaluated for up to three partons at LO accuracy and up to one (4ℓ , $2\ell+2\nu$) or zero partons ($3\ell+1\nu$) at NLO in QCD using the Comix and OpenLoops matrix element generators. Diboson processes with one boson decaying hadronically and the other one decaying leptonically were generated with SHERPA 2.2.1 using the NNPDF3.0 PDF set. The various processes were calculated for up to three additional partons at LO accuracy and up to one (ZZ) or zero (WW , WZ) additional partons at NLO using the Comix and OpenLoops matrix element generators. Loop-induced and electroweak processes with two weak gauge bosons (W/Z) plus two jets were simulated with SHERPA 2.1.1. The calculation is made at LO accuracy in QCD while up to one additional parton is merged with the matrix element. The CT10 PDF set was used in conjunction with a dedicated parton shower tuning. The SHERPA 2.1.1 diboson prediction was scaled by a factor of 0.91 to account for

Lepton flavour	Electrons		Muons	
Channel	OS	SS	OS	SS
Identification	LHMedium		Medium	
Isolation	LooseTrackOnly	Loose	LooseTrackOnly	FixedCutTightTrackOnly
$p_{\text{T}}(\mu), E_{\text{T}}(e)$	$E_{\text{T}} > 25 \text{ GeV}$	$E_{\text{T}} > 30 \text{ GeV}$	$p_{\text{T}} > 25 \text{ GeV}$	$p_{\text{T}} > 30 \text{ GeV}$
η	$ \eta < 2.47$ and veto $1.37 < \eta < 1.52$		$ \eta < 2.5$	
$ d_0 /\sigma_{d_0}$	$ d_0 /\sigma_{d_0} < 5$		$ d_0 /\sigma_{d_0} < 3$	
$ z_0 \sin \theta $	$ z_0 \sin \theta < 0.5 \text{ mm}$			

Table 1. Object reconstruction selection in the OS and the SS channels. The requirements corresponding to the identification and isolation working points are described in ref. [53] under the same names.

differences between the internal electroweak scheme used in this SHERPA version and the default scheme.

A single event recorded by the ATLAS detector consists of the superposition of a hard-scattering pp collision and several additional pp interaction vertices referred to as ‘pile-up.’ The effect of the pile-up was included by overlaying minimum-bias collisions, simulated by PYTHIA 8.186 with a set of tuned parameters referred to as the A2 tune [48] and the MSTW2008LO PDF [49], on each generated signal and background event. The average number of interactions per pp bunch crossing is 24 and simulated samples are weighted to reproduce the distribution observed in data.

The detector response for background events was simulated within a framework [50] based on GEANT4 [51]. Monte Carlo signal samples were instead processed with a fast simulation [50] which relies on a parameterisation of the calorimeter response [52]. Furthermore, simulated events were processed with the same reconstruction software used for data. In order to account for the different particle reconstruction efficiencies measured in data and simulation, correction factors are derived in dedicated measurements and applied to simulated events.

4 Object reconstruction

The electron and muon selection criteria are summarised in table 1.

Electron candidates are reconstructed from energy deposits in the EM calorimeter which are matched to a track reconstructed in the ID [54]. Candidate electrons must have transverse energy $E_T > 25$ (30) GeV in the OS (SS) channel, $|\eta| < 2.47$ and satisfy the LHMedium identification criterion based on a multivariate likelihood discriminant [53, 55]. Electrons falling in the transition region between the barrel and endcap EM calorimeters ($1.37 < |\eta| < 1.52$) are excluded. The transverse impact parameter (d_0) of the track associated with the electron must have a significance $|d_0|/\sigma(d_0) < 5$ relative to the beam line [56], where $\sigma(d_0)$ is the uncertainty on d_0 . All tracks with transverse momentum $p_T > 400$ MeV associated with electron candidates must have a longitudinal impact parameter multiplied by the sine of the polar angle $|z_0 \sin \theta|$ of less than 0.5 mm. Electrons are further required to satisfy the track-based (track- and calorimeter-based) isolation criteria for the OS (SS) channel. The isolation selection efficiencies are found to exceed 99% using $Z \rightarrow e^+e^-$ events [53].

Muons are reconstructed from a combined fit of a track in the ID matched to a track in the MS. The **Medium** quality criterion, described in ref. [57], is applied. Candidate muons must have $p_T > 25$ (30) GeV in the OS (SS) channel, $|\eta| < 2.5$, $|d_0|/\sigma(d_0) < 3$, and $|z_0 \sin \theta| < 0.5$ mm. Muon isolation in the OS channel is based on track isolation and has a 99% efficiency, independent of the muon p_T and $|\eta|$. In the SS channel, the track isolation provides an efficiency exceeding 99% for high- p_T muons and decreasing to $\sim 95\%$ for muons with $p_T < 40$ GeV [57].

The tighter selection criteria applied to leptons used in the SS channel are designed to suppress the contribution from background events with misidentified leptons (as discussed in section 6), which are negligible in the OS channel.

Jets are reconstructed with the anti- k_t algorithm [58] using a radius parameter of 0.4 from energy deposits in the topological clusters of the calorimeter, calibrated as described in ref. [59]. Jets must satisfy $p_T > 20$ GeV and $|\eta| < 2.5$. The majority of jets from pile-up are rejected using the jet-vertex-tagger [60], a likelihood discriminant combining information from several track-based variables, which is only applied to jets with $p_T < 60$ GeV and $|\eta| < 2.4$. The tagging efficiency of pile-up jets with the jet-vertex-tagger is determined in simulated $Z \rightarrow \mu\mu + \text{jet(s)}$ events to be 95%.

The identification of jets containing b -hadrons (b -jets) is based on a multivariate tagging algorithm [61]. This algorithm uses a set of tracks with loose impact parameter constraints in a region of interest around each jet axis to enable the reconstruction of the b -hadron decay vertex. The b -tagging working point used in the OS (SS) channel results in an efficiency of 70% (77%) for jets containing b -hadrons. The expected rejection factors against light-quark and gluon jets, c -quark jets and hadronically decaying tau leptons are respectively 381, 12, 55 for a 70% efficiency and 134, 6, 22 for a 77% efficiency. These efficiencies and rejection factors are determined in a sample of simulated $t\bar{t}$ events [62].

After the electron, muon and jet reconstruction and selection, possible overlaps between reconstructed objects are resolved. First, electrons are removed if they share a track with a muon. Next, ambiguities between electrons and jets are resolved by removing jets with an angular distance $\Delta R < 0.2$ from electrons; if $0.2 < \Delta R < 0.4$, the electron is removed. Finally, if a muon and a jet have $\Delta R < 0.4$, the jet is removed if it has less than three associated tracks, otherwise the muon is discarded.

5 Event selection

Events were collected using single-lepton or dilepton triggers during the 2015 and 2016 data-taking periods. For data collected in 2015, the lowest E_T and lowest p_T trigger thresholds are 24 GeV and 20 GeV for single-electron and single-muon triggers, respectively. For 2016 data, the thresholds are 26 GeV and 24 GeV for electron and muon triggers, respectively. Dielectron triggers with a E_T threshold of 17 GeV are used in the $e^\pm e^\pm$ case since a different background strategy is considered for the SS channel (see section 6). After satisfying the offline selections, the signal efficiency of the employed triggers is higher than 99% (95%) for the ee ($\mu\mu$) channel. Events are required to have at least one reconstructed primary vertex with at least two associated tracks with $p_T \gtrsim 400$ MeV. Among all the vertices in the event,

the one with the highest sum of squared transverse momenta of the associated tracks is chosen as the primary vertex. Events containing b -jets are vetoed to reduce contamination from top-quark background.

All selected events are required to have exactly two same-flavour leptons ($ee, \mu\mu$) and two jets with $p_T > 100$ GeV and $|\eta| < 2.0$. The main SM background after these requirements is the $Z + \text{jet(s)}$ process in the OS and electron SS channels, while diboson production is the main background in the muon SS channel. The $Z + \text{jet(s)}$ process enters the SS channel due to misidentification of electron charge.

Selected events are classified into orthogonal categories, called analysis regions, which serve different purposes. Signal regions (SR) are designed to contain the majority of expected signal events and are used to extract the signal yields. Control regions (CR) and validation regions (VR) are defined by reversing some of the SR event selection criteria and are used to constrain and validate background predictions respectively. The analysis region selection criteria are summarised in table 2. To suppress background from $Z + \text{jet(s)}$ processes in the $\text{SR}(e^\pm e^\mp)$, $\text{SR}(\mu^\pm \mu^\mp)$, $\text{SR}(e^\pm e^\pm)$ and $\text{SR}(\mu^\pm \mu^\pm)$ signal regions, the invariant masses of the two leptons ($m_{\ell\ell}$) and the two jets (m_{jj}) must be larger than 400 GeV and 110 GeV, respectively. In addition, the scalar p_T sum of the selected two leptons (E_T for electrons) and the two most energetic jets (H_T) must be larger than 400 GeV to further reject the SM background, which exhibits lower transverse energies than the signal. Since the expected event yields in the OS channel are larger than those in the SS channel, the CR and VR definitions differ slightly, as shown in table 2. The variable used to ensure the orthogonality between CRs, VRs and SRs is $m_{\ell\ell}$, except in the $\text{CR}(e^\pm \mu^\mp)$ which has the same kinematic selection as the SRs, but with different-flavour leptons. The $\text{CR}(e^\pm e^\mp)$ and $\text{CR}(\mu^\pm \mu^\mp)$ provide a high-purity sample of $Z + \text{jet(s)}$ events and are used to constrain the yields from this process. Similarly, the $\text{CR}(e^\pm \mu^\mp)$ is used to constrain events from top-quark processes. For the SS channel, the main prompt SM background is diboson production and its yield is constrained in both the $\text{CR}(e^\pm e^\pm)$ and $\text{CR}(\mu^\pm \mu^\pm)$. The rate of $Z + \text{jet(s)}$ events, which enter the analysis regions only through charge misidentification, as described in section 6, is constrained only in the $\text{CR}(e^\pm e^\pm)$.³ The invariant mass window used to define the $\text{CR}(e^\pm e^\pm)$ is reduced to the interval $[110, 300]$ GeV, to avoid overlap with the region around the Z mass peak, used to estimate the electron charge misidentification probability.

Once all selections are applied, the signal acceptance times efficiency — evaluated with simulated signal events — varies from 54% in the (W_R, N_R) high-mass regime to $\sim 30\%$ at the edge of the already excluded (W_R, N_R) low-mass region.

6 Background estimation

The composition of the SM background is substantially different in the OS and SS channels, requiring different background estimation techniques in the two cases, although SM back-

³The probability of muon charge misidentification is negligible because muon bremsstrahlung radiation is greatly reduced compared to electron, and muon tracks are measured in both the inner detector and the muon spectrometer, which provides a much larger lever arm for the curvature measurement.

Region	Control region			Validation region		Signal region	
Channel	CR($\ell^\pm \ell^\mp$)	CR($\ell^\pm \ell'^\mp$)	CR($\ell^\pm \ell^\pm$)	VR($\ell^\pm \ell^\mp$)	VR($\ell^\pm \ell^\pm$)	SR($\ell^\pm \ell^\mp$)	SR($\ell^\pm \ell^\pm$)
m_{ee} [GeV]	[60, 110]	—	[110, 300]	[110, 400]	[300, 400]	> 400	> 400
$m_{\mu\mu}$ [GeV]	[60, 110]	—	[60, 300]	[110, 400]	[300, 400]	> 400	> 400
$m_{e\mu}$ [GeV]	—	> 400	—	—	—	—	—
H_T [GeV]	> 400	> 400	—	> 400	—	> 400	> 400
m_{jj} [GeV]	> 110	> 110	—	> 110	—	> 110	> 110
Jet p_T [GeV]	> 100	> 100	> 50	> 100	> 50	> 100	> 100

Table 2. Summary of all regions defined in the analysis divided into the OS and SS channels. The table is split into two blocks: the top half indicates the mass range of the dilepton final state, whereas the bottom half indicates the event selection criteria used for a given region. The flavour combinations are summarised as follows: $\ell^\pm \ell^\mp = \{e^\pm e^\mp, \mu^\pm \mu^\mp\}$, $\ell^\pm \ell^\pm = \{e^\pm e^\pm, \mu^\pm \mu^\pm\}$, $\ell^\pm \ell'^\mp = \{e^\pm \mu^\mp\}$. Pairs of values $[X, Y]$ indicate the minimum and maximum values the quantity in question may take in the analysis region in question.

grounds containing a prompt lepton (referred to as ‘prompt SM backgrounds’ hereafter) are estimated using simulations in both channels. Prompt leptons are defined as leptons originating from Z , W , and H boson decays, or leptons from τ decays if the τ -lepton originates from a prompt decay (e.g. $Z \rightarrow \tau^+ \tau^-$). Unless otherwise stated, background processes are found to be well modelled by simulation.

The main prompt SM backgrounds contributing to the OS channel are from top-quark events (mainly $t\bar{t}$) and $Z + \text{jet(s)}$ production, with contributions of $\sim 49\%$ and $\sim 35\%$ respectively in the SR($e^\pm e^\mp$) and $\sim 55\%$ and $\sim 37\%$ in the SR($\mu^\pm \mu^\mp$). Minor contributions arise from diboson (mainly $ZW \rightarrow \ell^+ \ell^- jj$ and $ZZ \rightarrow \ell^+ \ell^- jj$) and $W + \text{jet(s)}$ events. The m_{jj} spectrum of simulated $Z + \text{jet(s)}$ events is not correctly modelled by the simulation samples in the CR($e^\pm e^\mp$) and CR($\mu^\pm \mu^\mp$). The effect is not visible in the SS channel because $Z + \text{jet(s)}$ production is a less dominant background and therefore the statistical uncertainty is much larger. A data-driven procedure is applied to the simulated $Z + \text{jet(s)}$ events to correct for this mismodelling. A reweighting factor is derived from the regions CR($e^\pm e^\mp$) and CR($\mu^\pm \mu^\mp$) and applied to all OS regions. It ranges from 1.1 in the low- m_{jj} region to 0.4 in the high- m_{jj} region above 3 TeV. The reweighting function is evaluated by fitting the ratio between data and simulation, after subtracting the non- $Z + \text{jet(s)}$ contributions from both of them. The function is a Novosibirsk-type function with three free parameters (peak and width, measured in TeV, and tail, unitless) and related to the weight by

$$k_1 = \ln \left[1.0 - \frac{(m_{jj} - \text{peak}) \cdot \text{tail}}{\text{width}} \right], \quad (6.1a)$$

$$k_2 = \frac{\sinh^{-1}(\sqrt{\ln 4} \cdot \text{tail})}{\sqrt{\ln 4}}, \quad (6.1b)$$

$$\text{weight} = \exp \left[-\frac{0.5}{k_2^2} k_1^2 - 0.5 k_2^2 \right]. \quad (6.1c)$$

The resulting reweighting factor with the best fit function is shown in figure 2.

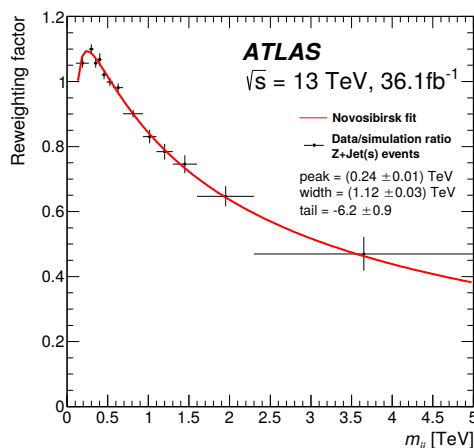


Figure 2. Ratio between data and simulation for $Z + \text{jet}(s)$ events collected in $\text{CR}(e^\pm e^\mp)$ and $\text{CR}(\mu^\pm \mu^\mp)$ as a function of the dijet invariant mass, with the result of the Novosibirsk fit superimposed. The fitted values for the peak and width in TeV, and tail (unitless) are shown. The binning is adjusted to minimise statistical fluctuations with 36.1 fb^{-1} of data.

In the SS channel, prompt SM processes such as $Z + \text{jet}(s)$ ($\sim 18\%$) and diboson ($\sim 22\%$) production contribute in the $\text{SR}(e^\pm e^\pm)$. Diboson production also contributes significantly ($\sim 37\%$) to the $\text{SR}(\mu^\pm \mu^\pm)$. A small fraction of top-quark events is present in both $\text{SR}(e^\pm e^\pm)$ ($\sim 7\%$) and $\text{SR}(\mu^\pm \mu^\pm)$ ($\sim 3\%$). The largest contribution, $\sim 53\%$ in $\text{SR}(e^\pm e^\pm)$ and $\sim 60\%$ in $\text{SR}(\mu^\pm \mu^\pm)$, is a reducible background arising from events with misidentified or non-prompt electrons and muons, collectively called ‘fakes’. A data-driven approach is used to assess the fake-lepton contributions as described in the following.

In the electron SS channel, electron charge misidentification is an additional source of SM background events mainly coming from $Z + \text{jet}(s)$ and top-quark production. A discrepancy between data and simulation is observed in these events, and data-driven correction factors are applied to simulated events. The charge misidentification of electrons is mainly due to bremsstrahlung radiation, with subsequent photon conversion into an electron-positron pair. The probability of charge misidentification is measured in data using $Z \rightarrow e^+ e^-$ events by comparing the numbers of OS and SS events. The probability is parameterised in terms of the electron E_T and $|\eta|$ [63]. It is measured in narrow E_T bins with the last bin extending above 250 GeV.

The misidentified-lepton background is estimated with the ‘fake-factor’ method, implemented in the same way as in ref. [63]. The implementation of the method requires two different lepton samples. The first one is defined by the leptons entering any analysis region, selected as in table 1, and called ‘tight’ (T). The second one is orthogonal to the tight selection and is called ‘loose’ (L). It is constructed by loosening some of the tight lepton requirements and by requiring that these leptons fail to satisfy the tight lepton criteria. The identification criteria for electrons are loosened to **LHLoose** [53, 55] and the isolation criteria are not imposed. Similarly, loose muons have a relaxed impact parameter requirement, $|d_0|/\sigma_{d_0} < 10$, and no isolation requirement. The fake-factor (F), quantifying the probability for a misidentified lepton to be reconstructed as a prompt lepton, is defined

Selection for fake-enriched regions	
Electrons	Muons
Single-electron trigger	Single-muon trigger
b -jet veto	b -jet veto
One electron and at least two jets	One muon and one jet
$p_T(\text{jet}) > 50 \text{ GeV}$	$p_T(\text{jet}) > 35 \text{ GeV}$
—	$\Delta\phi(\mu, \text{jet}) > 2.7$
$E_T^{\text{miss}} < 25 \text{ GeV}$	$E_T^{\text{miss}} < 40 \text{ GeV}$

Table 3. Selection criteria defining the dedicated fake-enriched regions, used to measure the electron and muon fake-factors as described in the text.

as the ratio of the number of tight to loose leptons $F = N_T/N_L$ and measured in dedicated ‘fake-enriched’ regions.

The regions, summarised in table 3, are enriched in fake leptons originating from dijet and $W + \text{jet(s)}$ production. They are selected using single-lepton triggers and must satisfy low missing transverse momentum (E_T^{miss}) requirements, to suppress $W + \text{jet(s)}$ production where a real lepton from a W boson decay is present. One charged lepton and at least one (two) jet(s) must be present in the event in the muon (electron) channel. Furthermore, contamination from prompt leptons in fake-enriched regions is subtracted using simulated events. This contamination is up to 40% in the electron channel, and in the muon channel for $p_T (< 100 \text{ GeV})$, while it becomes dominant for high p_T muons. The selection criteria for the electron fake-enriched region are designed to mimic as much as possible the signal region selection in order to ensure a similar composition of various sources of fake electrons: decays of light-flavour hadrons into light leptons, photon conversions, and jets faking electrons. In the muon channel, the major source of fake muons originates from decays of heavy-flavour hadrons and the muon fake-enriched region is optimised to maximise the number of such events. The fake-factors are parameterised in terms of lepton flavour (e or μ), E_T (p_T) for electrons (muons), and η . For electrons, they vary from 0.3 to 0.5 in the barrel region and from 0.4 to 0.9 in the endcap region. For muons, they are about 0.4 for $p_T < 50 \text{ GeV}$ and rise to 1.0 for $p_T > 50 \text{ GeV}$.

Once the factor F is measured, the contribution of the number of events with at least one misidentified lepton in the analysis regions (N^{fake}) is evaluated using:

$$N^{\text{fake}} = \left[F(N_{TL}^{\text{data}} + N_{LT}^{\text{data}}) - F^2 N_{LL}^{\text{data}} \right] - \left[F(N_{TL}^{\text{MC}} + N_{LT}^{\text{MC}}) - F^2 N_{LL}^{\text{MC}} \right]^{\text{prompt only}}. \quad (6.2)$$

In these regions the factor F is applied to events containing at least one loose lepton, N_{TL} , N_{LT} and N_{LL} , populating the ‘sideband’ regions, namely TL , LT and LL . In these events, either the subleading lepton is loose (TL), or the leading lepton is loose (LT), or both leptons are loose (LL). The residual prompt-lepton components in the sideband regions are subtracted using simulated events. The estimated backgrounds due to fakes and electron charge misidentification are validated in the dedicated VRs defined in table 2.

7 Systematic uncertainties

Several sources of systematic uncertainty are considered. They correspond to experimental and theoretical sources affecting both the background and signal predictions. All the sources of systematic uncertainty considered here affect the total event yield. They also alter the distributions of the variables used in the statistical analysis (section 8) with the exception of the uncertainties in the luminosity and cross-sections.

The uncertainty in the 2015 and 2016 integrated luminosity is 2.1%, derived with the methodology described in ref. [64], and using the LUCID-2 detector for the baseline luminosity measurements [65], from a calibration of the luminosity scale using x - y beam-separation scans.

A set of experimental systematic uncertainties arise from the calibrations of the lepton and jet energy and momentum, the lepton detection efficiencies and isolation, and the trigger efficiency. The largest uncertainty in the total SM yield arises from the energy calibration and smearing of jets, derived in ref. [59], and is between 5% and 10% depending on the invariant mass of the $\ell\ell jj$ system. Experimental systematic uncertainties associated with lepton reconstruction, identification, isolation and trigger efficiencies, as well as energy or momentum calibration and b -jet tagging, vary between 0.5% and 4% of the total SM yield.

There are two additional experimental sources of systematic uncertainty in the SS channel due to the data-driven background estimation techniques. The uncertainty related to the charge misidentification probability of electrons arises from the statistical uncertainty of both the data and the simulated samples of Z + jet(s) events used to measure this probability. The uncertainty ranges between 10% and 20% as a function of the electron E_T and η . Next, the uncertainty on the fake estimation arises from the unknown composition of fakes, as well as from statistical uncertainty and prompt lepton subtraction used to derive F in the fake-enriched regions. The uncertainty due to the composition of fakes is estimated by varying the criteria to select the nominal sample for the fake-factor measurement (table 3). In the electron channel, the E_T^{miss} requirement is increased to <100 GeV, the two-jet requirement is dropped and one jet recoiling against the electron (analogous to the nominal muon fake-factor measurement) is required. In the muon channel, the nominal $|d_0|/\sigma_{d_0}$ and E_T^{miss} requirements are varied up and down respectively by one unit and 10 GeV. Furthermore, the uncertainty in the yield of prompt leptons from W and Z boson decays is estimated by varying the total SM prediction of the simulated samples by $\pm 10\%$ in the muon channel and $\pm 30\%$ in the electron channel. These values represent the size of the uncertainty due to the choice of QCD renormalisation (μ_R) and factorisation (μ_F) scales, α_s , and PDF uncertainties. The different size of the uncertainty between channels arises from the different fake-enriched region definitions (table 3), requiring exactly one jet and at least two jets for the muon and electron channels respectively. The total uncertainty in the fake-factors ranges between 10% and 50% across all $E_T(e, \mu)$ and η bins for both flavours.

In the OS channel, an additional uncertainty is taken into account for the m_{jj} reweighting of the Z + jet(s) process. This is evaluated by comparing the shape difference between

the simulated and reweighted m_{jj} distribution and that measured in data, using the corresponding OS VR: the uncertainty in the reweighting factor is found to be between 5% and 20%, depending on the dijet invariant mass.

The theory uncertainties estimated for the $Z + \text{jet(s)}$ and diboson background processes include the choice of QCD renormalisation (μ_R) and factorisation (μ_F) scales, choice of the PDF set, α_S , and PDF uncertainty. The QCD scale uncertainty is estimated by varying μ_R and μ_F to half and twice their nominal values. The PDF uncertainty is estimated using the envelope of the NNPDF3.0 PDF set, as recommended in ref. [66]. In addition, the MMHT2014 [67] and CT14NNLO [68] PDF sets are used to estimate the uncertainty due to the PDF choice. Moreover, the uncertainty due to α_S is evaluated by varying its nominal value of 0.118 by ± 0.001 . The largest theory uncertainty generally originates from the QCD scales variations, and is between 20% and 40%, depending on the simulated process and the invariant mass of the $\ell\ell jj$ system.

The theory uncertainties estimated for $t\bar{t}$ processes are as follows. The uncertainty from hard-scatter generation is evaluated by comparing the POWHEG-BOX and MG5_aMC@NLO generators, both interfaced to the PYTHIA8.186 parton shower model, as recommended in ref. [66]. The uncertainty due to the hadronisation and fragmentation model is determined by comparing the nominal POWHEG-BOX + PYTHIA8.186 generated sample with the one generated by POWHEG-BOX interfaced to HERWIG [69] (version 7.0.1). The uncertainty related to the amount of initial- and final-state radiation is assessed by varying parton shower settings. The largest theory uncertainty generally originates from the amount of initial- and final-state radiation and is between 2% and 5% of the $t\bar{t}$ process yield.

Finally, the theory uncertainty of the signal efficiency times acceptance amounts to 10%. It is evaluated by varying renormalisation and factorisation scales as described above and by using alternative PDF sets, CTEQ6 [45] and MSTW [49]. The α_S emission scale factor is also varied to half and twice the nominal value. The uncertainty is dominated by the variation in factorisation scale. The variations are performed using SYSCALC [70].

8 Statistical analysis and results

The statistical analysis package HISTFITTER [71] is used to implement a binned maximum-likelihood fit of the data distributions in the control and signal regions for the evaluation of the numbers of signal and background events. For the scenario in which the N_R neutrino is a Majorana particle, the OS and SS channels are fitted simultaneously, whereas for the Dirac neutrino, only the OS channel is used in the fit. The analysis regions are optimised for the high-mass regime, where the CRs and the VRs have negligible signal contribution. On the other hand, it is found that lower mass points yield some signal events in the CRs. This effect is accounted for in the statistical analysis when evaluating the signal strength by simultaneously fitting the CRs and SRs. The VRs are not used in the fit, but are only employed to confirm the validity of the background modelling before the fit is carried out in the SRs.

In the OS channel, different distributions are used in the likelihood fit depending on the mass hierarchy of the signal sample. The $m_{\ell\ell jj}$ distribution is used as the discriminant

SM background yield	CR($e^\pm e^\mp$)	CR($e^\pm \mu^\mp$)	CR($\mu^\pm \mu^\mp$)	CR($e^\pm e^\pm$)	CR($\mu^\pm \mu^\pm$)
OS $Z + \text{jet(s)}$	✓	—	✓	—	—
SS $Z + \text{jet(s)}$	—	—	—	✓	—
OS Top	—	✓	—	—	—
SS Diboson	—	—	—	✓	✓

Table 4. Summary of the control regions used to fit the yields of the dominant SM background predictions. CRs used to fit a certain SM prediction yield are marked with a check-mark (✓) and CRs not used for this SM prediction are marked with a dash (—).

	CR ($e^\pm e^\mp$)	CR ($e^\pm \mu^\mp$)	CR ($\mu^\pm \mu^\mp$)	VR ($\mu^\pm \mu^\mp$)	VR ($\mu^\pm \mu^\mp$)
Data	29178	201	37378	2794	3327
Total background	29200 ± 170	202 ± 14	37360 ± 190	2700 ± 130	3290 ± 140
$Z + \text{jet(s)}$	27900 ± 190	1.2 ± 0.1	35790 ± 220	1306 ± 28	1729 ± 36
$t\bar{t}$, single- t , $t\bar{t}V$	524 ± 71	162 ± 14	628 ± 88	1250 ± 130	1400 ± 140
Diboson and W+jets	775 ± 28	39.1 ± 2.0	937 ± 35	149.1 ± 6.5	160.9 ± 5.9

Table 5. Numbers of expected background events in control and validation regions after the background-only fit in the opposite-charge channel, compared to the data. The quoted uncertainties correspond to the total uncertainty in the predicted event yield including correlations between the various sources of systematic uncertainties. Due to rounding the total background can differ from the sums of components. Top-quark and $Z + \text{jet(s)}$ yields are floating in the fit.

for the $m_{W_R} > m_{N_R}$ hypothesis, and the m_{jj} spectrum is used as the discriminant for the $m_{W_R} < m_{N_R}$ hypothesis.⁴ In both cases, the same discriminant variable is used in the control region and the signal region. In the SS channel, m_{jj} is used in the CRs and H_T is used in the SR, regardless of the mass hierarchy, as it yields a better separation between the signal and the background. Additional mass hypotheses are added by interpolating the discriminating distributions obtained for existing signal simulation samples using a moment morphing technique [72].

The likelihood is the product of a Poisson probability density function describing the observed number of events, and Gaussian distributions to constrain the nuisance parameters associated with the systematic uncertainties. The widths of the Gaussian distributions correspond to the magnitudes of these uncertainties, whereas Poisson distributions are used for the simulation statistical uncertainties. Additional free parameters are introduced to normalise the contributions of $Z + \text{jet(s)}$, diboson, and top-quark backgrounds to the data in the analysis control regions. The fitted normalisation parameters are applied simultaneously in SRs. The fitted normalisations are consistent with their SM predictions within the uncertainties.

Due to the different object definitions and background components in the OS and SS channels, separate nuisance parameters are used for all sources of uncertainties and fitted

⁴For the CR($e^\pm e^\mp$) and CR($\mu^\pm \mu^\mp$), the event yields are integrated into a single-bin and then fed into the fit.

	SR ($e^\pm e^\mp$)	SR ($\mu^\pm \mu^\mp$)
Data	156	169
Total background	152.2 ± 8.4	165.9 ± 8.9
$Z + \text{jet(s)}$	53.9 ± 5.1	61.8 ± 4.8
$t\bar{t}$, single- t , $t\bar{t}V$	74.0 ± 7.6	89.6 ± 8.3
Diboson and $W + \text{jet(s)}$	24.5 ± 1.6	12.8 ± 0.7

Table 6. Numbers of expected background events in signal regions after the background-only fit in the opposite-charge channel, compared to the data. The quoted uncertainties correspond to the total uncertainty in the predicted event yield including correlations between the various sources of systematic uncertainties. Due to rounding the total background can differ from the sums of components. Top-quark and $Z + \text{jet(s)}$ yields are floating in the fit.

	CR ($e^\pm e^\pm$)		CR ($\mu^\pm \mu^\pm$)		VR ($e^\pm e^\pm$)		VR ($\mu^\pm \mu^\pm$)		SR ($e^\pm e^\pm$)		SR ($\mu^\pm \mu^\pm$)	
Data	304		119		33		11		11		5	
Total background	306 ± 17		119 ± 11		31.1 ± 5.5		10.3 ± 2.4		11.2 ± 2.0		5.5 ± 1.7	
$Z + \text{jet(s)}$	100 ± 31	—	—		4.3 ± 2.0	—	—		2.0 ± 0.9	—	—	
Fakes	119 ± 23		40.4 ± 9.6		14.1 ± 4.6		4.1 ± 2.0		5.9 ± 1.9		3.3 ± 1.7	
Diboson	61 ± 13		74 ± 14		7.3 ± 1.6		5.8 ± 1.4		2.6 ± 0.6		2.0 ± 0.5	
$t\bar{t}$, single- t , $t\bar{t}V$	25.8 ± 5.9		4.3 ± 0.8		5.4 ± 1.7		0.35 ± 0.08		0.8 ± 0.3		0.14 ± 0.05	

Table 7. Numbers of expected background events in analysis regions after the background-only fit in the same-charge channel, compared to the data. The quoted uncertainties correspond to the total uncertainty in the predicted event yield including correlations between the various sources of systematic uncertainties. Due to rounding the total background can differ from the sums of components. Diboson and $Z + \text{jet(s)}$ yields are floating in the fit. Background processes with a negligible yield are marked with the dash (—).

yields for the largest backgrounds, as summarised in table 4. Observed and predicted event yields and the corresponding uncertainties of the dominant backgrounds in all analysis regions are presented in tables 5, 6 and 7. The information on observed and expected yields, along with their ratio for pre- (black filled markers) and post-fit (red hollow markers) yields, is presented in figure 3 in all the analysis regions. The $\text{CR}(e^\pm e^\mp)$ and $\text{CR}(\mu^\pm \mu^\mp)$ are used to extract the yield of $Z + \text{jet(s)}$ background, as the purity is above 95%. The $\text{CR}(e^\pm \mu^\mp)$ is mostly populated by top-quark background events (80% purity) and used to extract their normalisation. In the SS channel, the $Z + \text{jet(s)}$ contribution is estimated to be $\sim 33\%$, determined in a fit using the $\text{CR}(e^\pm e^\pm)$ only, and with the diboson normalisation factor free to vary. The data-driven fake background normalisation is fixed, which allows for the measurement of the $Z + \text{jet(s)}$ normalisation despite its low contribution in the control region.

To check the validity of the background prediction in the validation regions and to estimate the SM background in the signal regions, a background-only fit is performed where the nuisance parameters are constrained only in the CRs and are extrapolated to VRs after the fit. Figures 4 and 5 show the distributions in the CRs and VRs after

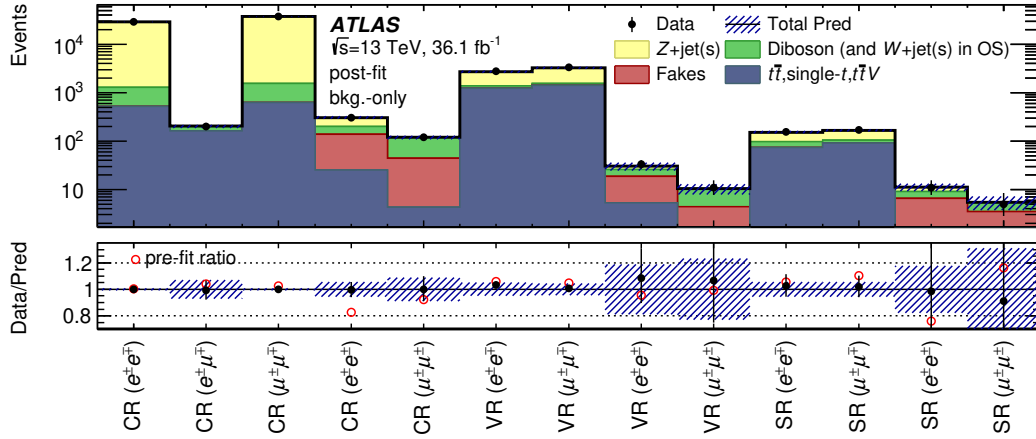


Figure 3. Number of observed and expected events in the control (CR), validation (VR), and signal (SR) regions for all channels considered after the background-only fit. The background expectation is the result of the fit described in the text using both OS and SS control regions. The hatched bands include all post-fit systematic uncertainties. The correlation between sources of systematic uncertainties are taken into account. The pre-fit ratio is indicated with the red hollow markers in the ratio plot.

this background-only fit (the binning used in figures corresponds to the one used in the fit). When performing the CR+SR fit to obtain the upper limit on the signal strength, the nuisance parameters are constrained both in CRs and SRs. For example, the SS diboson normalisation is constrained using both $\text{CR}(e^\pm e^\pm)$ and $\text{CR}(\mu^\pm \mu^\pm)$. This diboson normalisation factor is validated in the $\text{VR}(\mu^\pm \mu^\pm)$, as shown in figure 5(f), where the expected background and observed number of events agree within the uncertainties. In the fit, the Majorana and the Dirac case are distinguished by using both the OS and SS regions or only the OS regions, respectively. The SR distributions after the CR+SR fit are shown in figure 6.

No significant deviation from the SM predictions is observed in any of the signal regions. The most significant local excess is observed in the $m_{\ell\ell jj}$ spectrum of the $e^\pm e^\mp$ channel, with a $\sim 2\sigma$ local significance ($\sim 1\sigma$ global significance) between 3.5 and 4 TeV. After the fit, the compatibility between the data and the expected background is assessed. The global p -values for the background-only hypothesis are 0.67 and 0.62 for the $e^\pm e^\pm$ and $\mu^\pm \mu^\pm$ channels respectively and 0.16 and 0.59 for the $e^\pm e^\mp$ and $\mu^\pm \mu^\mp$ channels. Upper limits at 95% CL are calculated for the KS process cross-section using the CL_s method [73] and the profile likelihood-ratio [74] as the test statistic. Exclusion limits are calculated in separate fits for the ee and $\mu\mu$ channels since there is no theoretical requirement that N_R^e and N_R^μ have the same mass.

When setting exclusion limits for the two models the Dirac case is assumed to give twice as many OS events as the Majorana case. Results are shown in figure 7 for both Majorana and Dirac N_R neutrino cases. In both cases, W_R bosons with masses up to 4.7 TeV are excluded at 95% CL, for m_{N_R} in the 0.5–3.0 TeV region. The two jets in the W_R boson decay chain, for $m_{W_R} \sim 3–3.5$ TeV and m_{N_R} neutrino masses below 0.5 TeV, tend

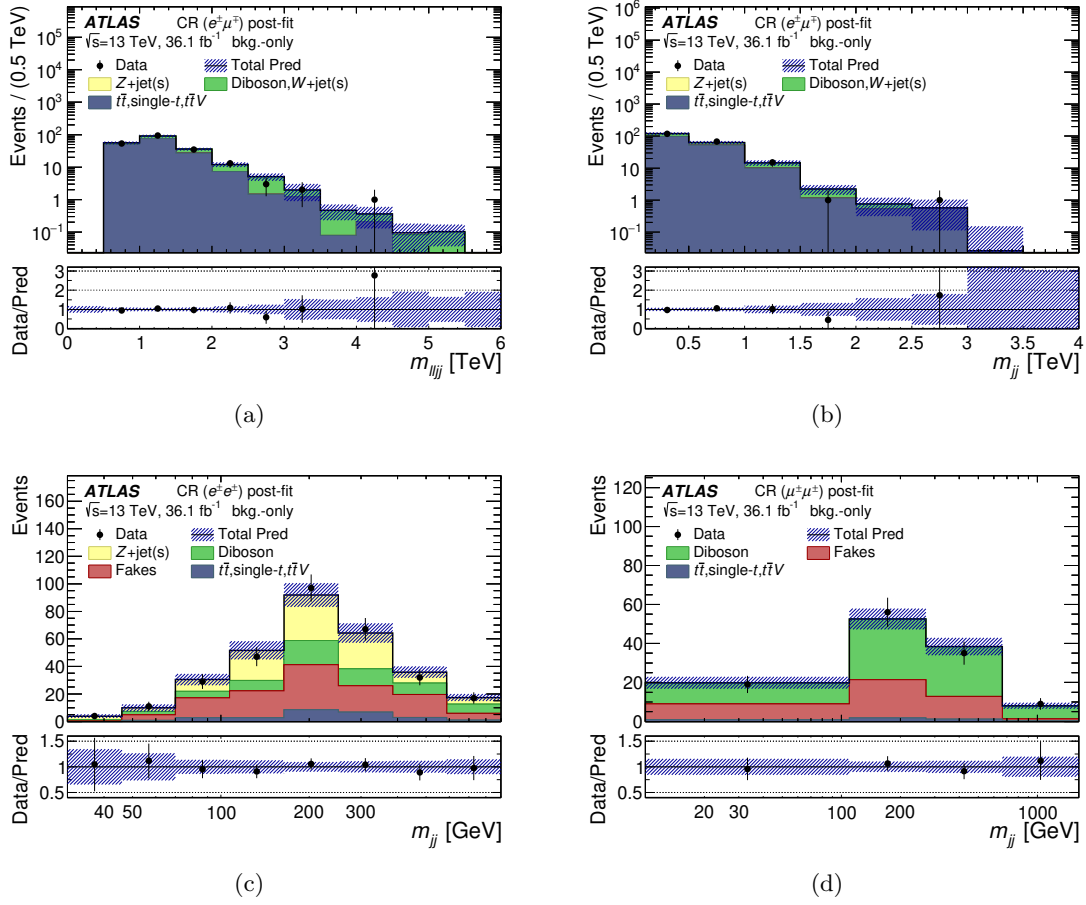


Figure 4. Distributions for data and background predictions for discriminant variables in various control regions and channels after the background-only fit: (a) $m_{\ell\ell jj}$ in $\text{CR}(e^\pm\mu^\mp)$, (b) m_{jj} in $\text{CR}(e^\pm\mu^\mp)$, (c) m_{jj} in $\text{CR}(e^\pm e^\pm)$, and (d) m_{jj} in $\text{CR}(\mu^\pm\mu^\pm)$. The hatched bands include all post-fit systematic uncertainties. The correlation between sources of systematic uncertainties are taken into account. The last bin in each histogram contains the overflow.

to overlap, resulting in a rapidly changing sensitivity and narrow 1σ and 2σ uncertainty bands in the exclusion limit plot, as visible in figures 7(a) and 7(c). Figure 8 shows the exclusion limits separately for the OS and SS analyses in the Majorana N_R neutrino case. The two analyses generally exhibit a similar sensitivity across the two-dimensional mass plane. Under the inverted hierarchy hypothesis ($m_{N_R} > m_{W_R}$) the SS analysis is more sensitive due to the lower expected background (figures 6(b), 6(d), 6(e) and 6(f)).

In the electron channel (figure 8(a)), the OS observed limit around $m_{W_R} \sim 4.2$ TeV and $m_{N_R} \sim 3$ TeV is weaker than expected due to three events observed at $m_{\ell\ell jj} \sim 3.8$ TeV, compared to an expected background of 1.1 ± 0.4 events for $m_{\ell\ell jj} > 3.5$ TeV (figure 6(a)). The opposite effect is observed in the muon channel (figure 8(b)), where no events are observed in the $m_{\ell\ell jj} > 3$ TeV region (figure 6(c)).

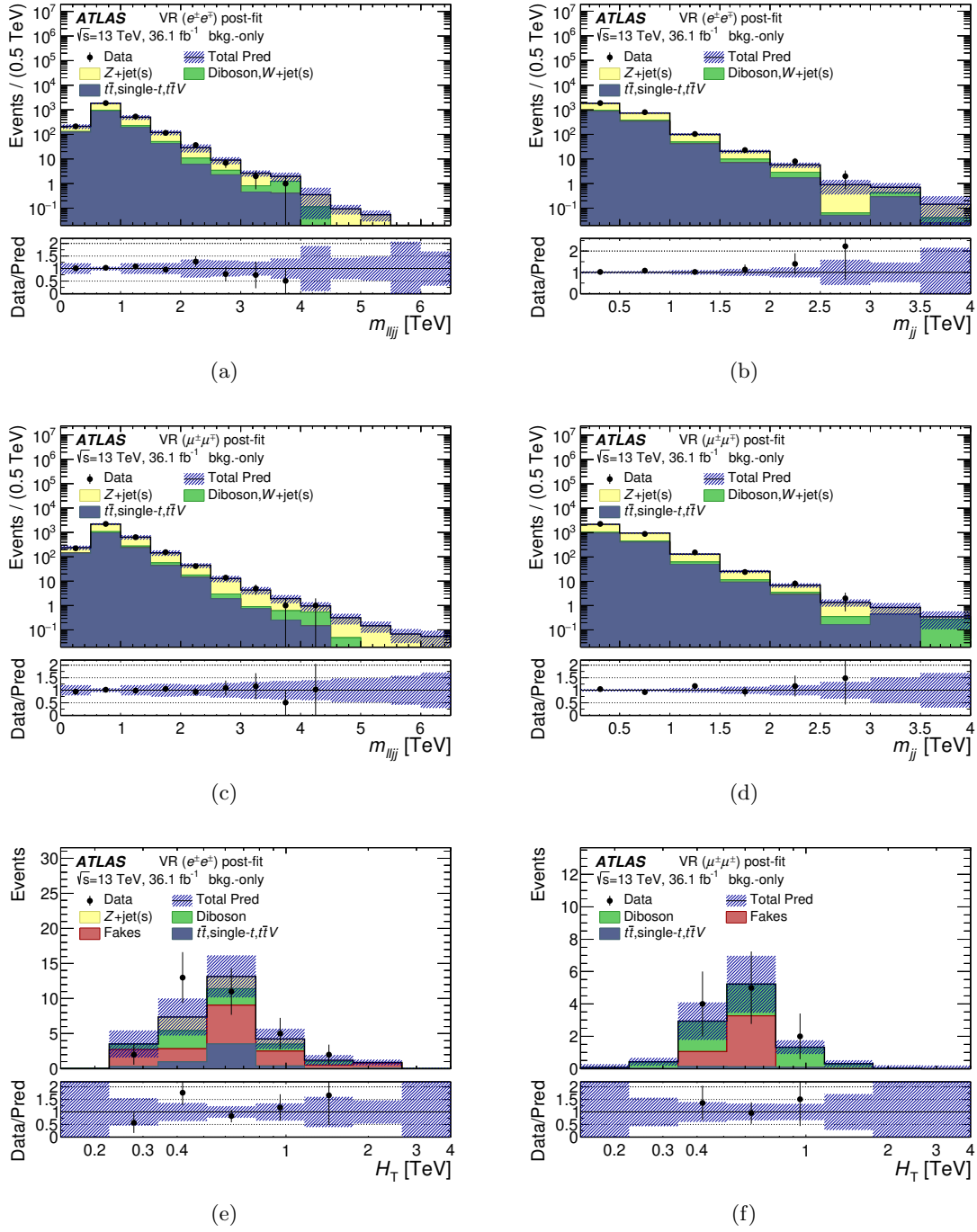


Figure 5. Distributions for data and background predictions for discriminant variables in various validation regions and channels after the background-only fit: (a) $m_{\ell j j}$ in VR($e^{\pm}e^{\mp}$), (b) $m_{j j}$ in VR($e^{\pm}e^{\mp}$), (c) $m_{\ell j j}$ in VR($\mu^{\pm}\mu^{\mp}$), (d) $m_{j j}$ in VR($\mu^{\pm}\mu^{\mp}$), (e) H_T in VR($e^{\pm}e^{\pm}$), and (f) H_T in VR($\mu^{\pm}\mu^{\pm}$). The hatched bands include all post-fit systematic uncertainties. The correlation between sources of systematic uncertainties are taken into account. The last bin in each histogram contains the overflow.

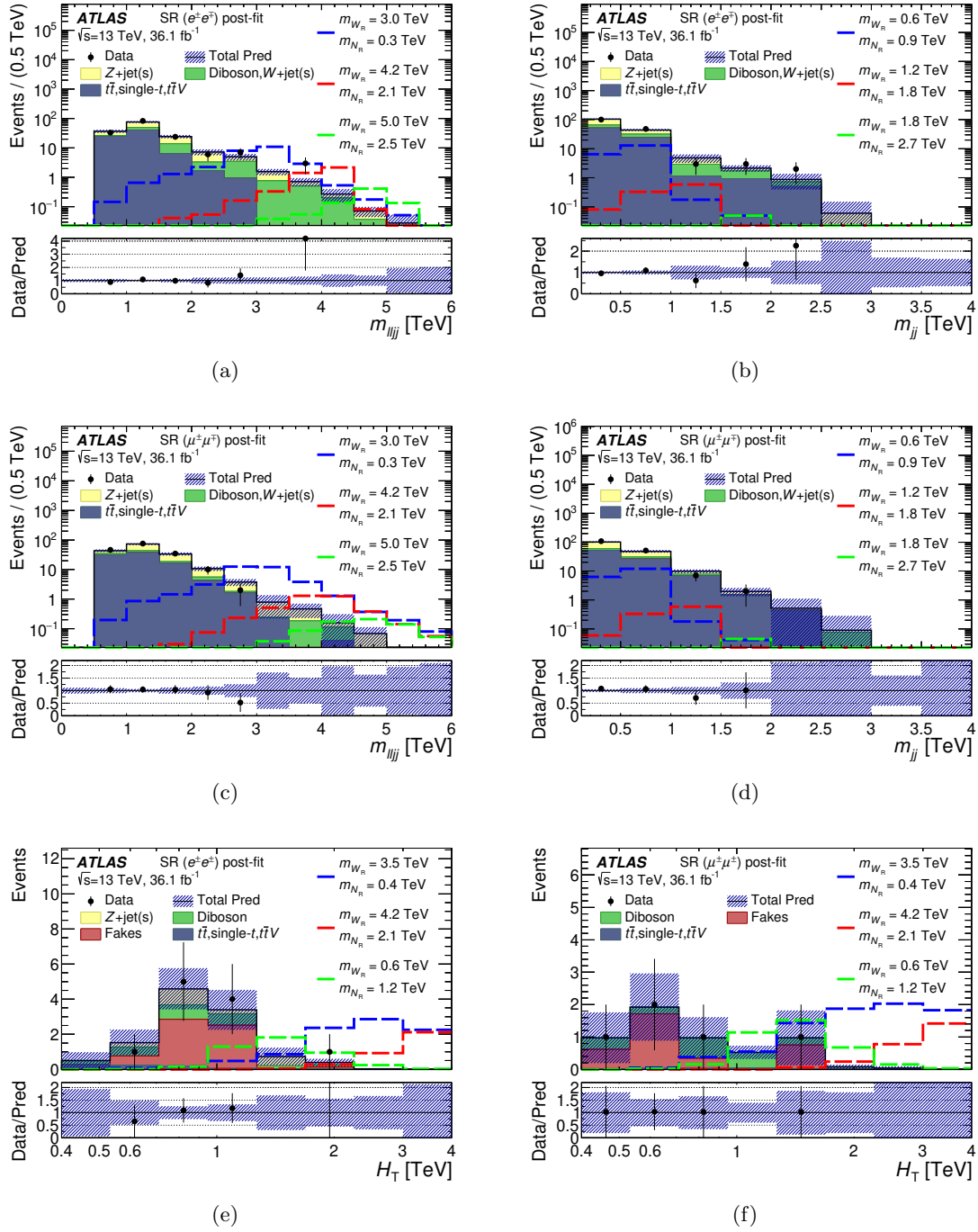


Figure 6. Distributions for data and background predictions after the CR+SR fit for discriminant variables in various signal regions and channels: (a) $m_{\ell\ell jj}$ in $\text{SR}(e^\pm e^\mp)$, (b) m_{jj} in $\text{SR}(e^\pm e^\mp)$, (c) $m_{\ell\ell jj}$ in $\text{SR}(\mu^\pm \mu^\mp)$, (d) m_{jj} in $\text{SR}(\mu^\pm \mu^\mp)$, (e) H_T in $\text{SR}(e^\pm e^\pm)$, and (f) H_T in $\text{SR}(\mu^\pm \mu^\pm)$. The hatched bands include all post-fit systematic uncertainties. The correlation between sources of systematic uncertainties are taken into account. A few simulated signal distributions, normalised to the predicted cross-section, are overlaid on top of the background prediction in the plots. The last bin in each histogram contains the overflow.

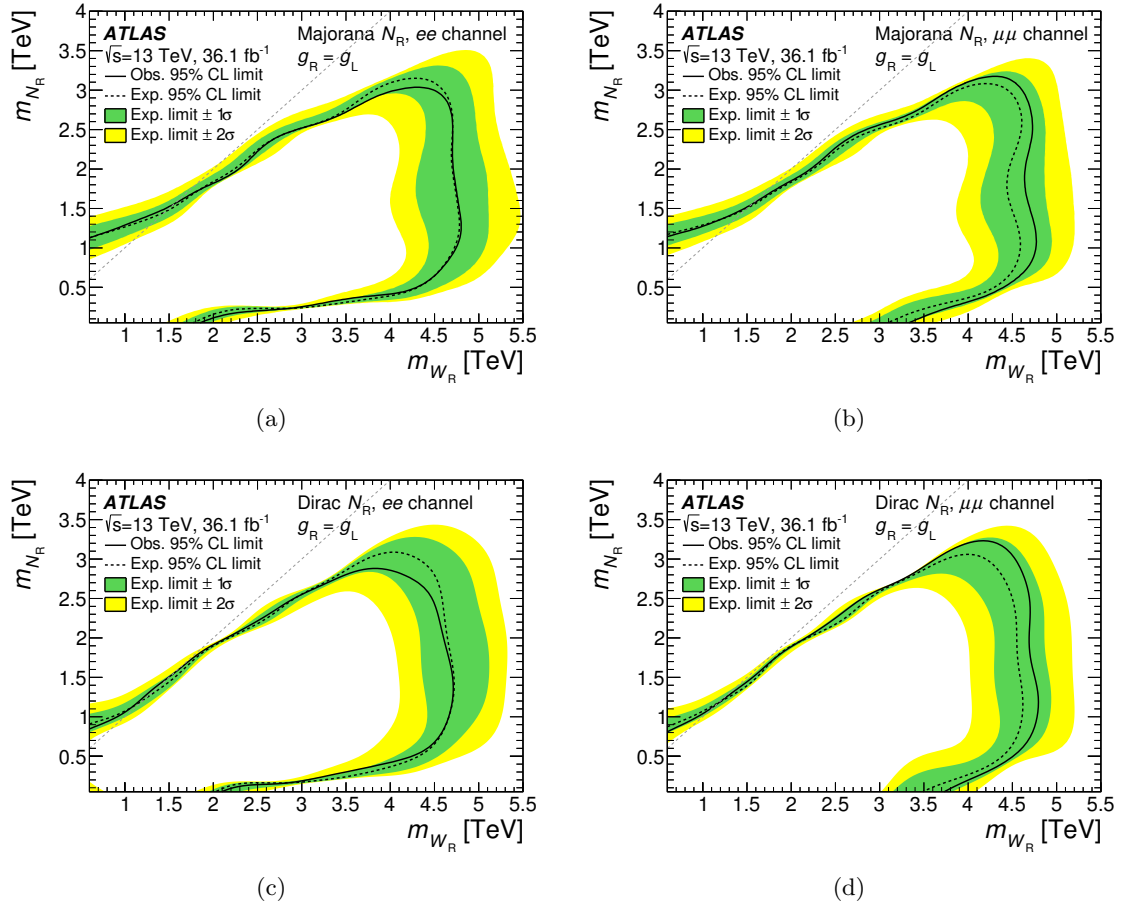


Figure 7. Observed (continuous line) and expected (dashed line) 95% CL exclusion contours in the m_{W_R} – m_{N_R} plane, along with the one- and two-standard-deviation uncertainty bands around the expected exclusion contour in the (a) ee and (b) $\mu\mu$ channels for Majorana N_R neutrinos, (c) ee and (d) $\mu\mu$ channels for Dirac N_R neutrinos. The dashed gray line indicates the region of the plane where $m_{W_R} = m_{N_R}$. The left- and right-handed weak gauge couplings are assumed to be the same, as indicated by $g_L = g_R$.

9 Conclusion

A search for right-handed W bosons and heavy right-handed Majorana or Dirac neutrinos is presented using a final state containing a pair of charged leptons, electrons or muons, and two jets ($\ell\ell jj$), with $\ell = e, \mu$, in a 36.1 fb $^{-1}$ sample of pp collisions recorded by the ATLAS detector at $\sqrt{s} = 13$ TeV at LHC. No evidence of W_R bosons or Majorana or Dirac heavy neutrinos, N_R , is found assuming the KS production and lower limits are set on the m_{W_R} and m_{N_R} masses, assuming equality of left- and right-handed weak gauge couplings ($g_L = g_R$). The excluded region for the Majorana N_R neutrinos extends to about $m_{W_R} = 4.7$ TeV, for $m_{N_R} = 1.2$ TeV in the electron channel and for $m_{N_R} = 1$ TeV in the muon channel. The m_{N_R} limits reach about 2.9 TeV in the electron channel and 3.1 TeV in the muon channel (for $m_{W_R} = 4.3$ TeV). For Dirac N_R neutrinos, limits reach

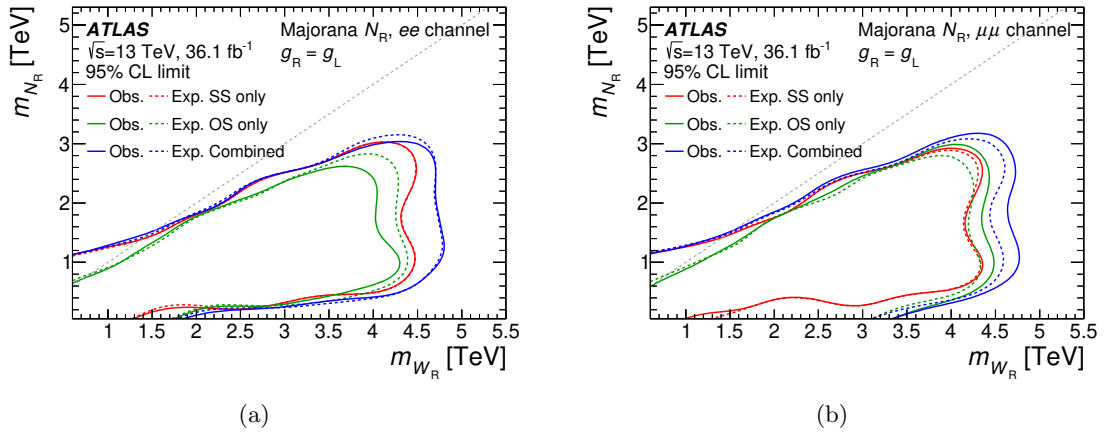


Figure 8. Observed (continuous line) and expected (dashed line) 95% CL exclusion contours in the m_{W_R} – m_{N_R} plane for Majorana N_R neutrinos calculated in the OS and SS analyses, and their combination, in the (a) ee and (b) $\mu\mu$ channels. The dashed gray line indicates the region of the plane where $m_{W_R} = m_{N_R}$. The left- and right-handed weak gauge couplings are assumed to be the same ($g_L = g_R$).

about $m_{W_R} = 4.7$ TeV, for $m_{N_R} = 1$ TeV in the electron channel and for $m_{N_R} = 1.2$ TeV in the muon channel. Limits on m_{N_R} up to about 2.8 TeV (for $m_{W_R} = 3.7$ TeV) in the electron channel and up to 3.2 TeV (for $m_{W_R} = 4.1$ TeV) in the muon channel are set. In the low-mass regime ($m_{W_R} < 1.5$ TeV), under the hierarchy hypothesis $m_{N_R} > m_{W_R}$, N_R masses up to 1.5 TeV are excluded at 95% CL. These results improve upon previous ATLAS searches [19] and extend the exclusion limits on m_{W_R} by 1–2 TeV. Additionally, the scenario in which the N_R neutrino is heavier than the W_R boson is explored for the first time.

Acknowledgments

We thank CERN for the very successful operation of the LHC, as well as the support staff from our institutions without whom ATLAS could not be operated efficiently.

We acknowledge the support of ANPCyT, Argentina; YerPhI, Armenia; ARC, Australia; BMWFW and FWF, Austria; ANAS, Azerbaijan; SSTC, Belarus; CNPq and FAPESP, Brazil; NSERC, NRC and CFI, Canada; CERN; CONICYT, Chile; CAS, MOST and NSFC, China; COLCIENCIAS, Colombia; MSMT CR, MPO CR and VSC CR, Czech Republic; DNRF and DNSRC, Denmark; IN2P3-CNRS, CEA-DRF/IRFU, France; SRNSFG, Georgia; BMBF, HGF, and MPG, Germany; GSRT, Greece; RGC, Hong Kong SAR, China; ISF and Benoziyo Center, Israel; INFN, Italy; MEXT and JSPS, Japan; CNRST, Morocco; NWO, Netherlands; RCN, Norway; MNiSW and NCN, Poland; FCT, Portugal; MNE/IFA, Romania; MES of Russia and NRC KI, Russian Federation; JINR; MESTD, Serbia; MSSR, Slovakia; ARRS and MIZŠ, Slovenia; DST/NRF, South Africa; MINECO, Spain; SRC and Wallenberg Foundation, Sweden; SERI, SNSF and Cantons of Bern and Geneva, Switzerland; MOST, Taiwan; TAEK, Turkey; STFC, United Kingdom;

DOE and NSF, United States of America. In addition, individual groups and members have received support from BCKDF, CANARIE, CRC and Compute Canada, Canada; COST, ERC, ERDF, Horizon 2020, and Marie Skłodowska-Curie Actions, European Union; Investissements d’Avenir Labex and Idex, ANR, France; DFG and AvH Foundation, Germany; Herakleitos, Thales and Aristeia programmes co-financed by EU-ESF and the Greek NSRF, Greece; BSF-NSF and GIF, Israel; CERCA Programme Generalitat de Catalunya, Spain; The Royal Society and Leverhulme Trust, United Kingdom.

The crucial computing support from all WLCG partners is acknowledged gratefully, in particular from CERN, the ATLAS Tier-1 facilities at TRIUMF (Canada), NDGF (Denmark, Norway, Sweden), CC-IN2P3 (France), KIT/GridKA (Germany), INFN-CNAF (Italy), NL-T1 (Netherlands), PIC (Spain), ASGC (Taiwan), RAL (U.K.) and BNL (U.S.A.), the Tier-2 facilities worldwide and large non-WLCG resource providers. Major contributors of computing resources are listed in ref. [75].

Open Access. This article is distributed under the terms of the Creative Commons Attribution License ([CC-BY 4.0](https://creativecommons.org/licenses/by/4.0/)), which permits any use, distribution and reproduction in any medium, provided the original author(s) and source are credited.

References

- [1] J.C. Pati and A. Salam, *Lepton number as the fourth color*, *Phys. Rev. D* **10** (1974) 275 [*Erratum ibid.* **11** (1975) 703] [[INSPIRE](#)].
- [2] R.N. Mohapatra and J.C. Pati, *Left-right gauge symmetry and an isoconjugate model of CP-violation*, *Phys. Rev. D* **11** (1975) 566 [[INSPIRE](#)].
- [3] R.N. Mohapatra and J.C. Pati, *A natural left-right symmetry*, *Phys. Rev. D* **11** (1975) 2558 [[INSPIRE](#)].
- [4] G. Senjanović and R.N. Mohapatra, *Exact left-right symmetry and spontaneous violation of parity*, *Phys. Rev. D* **12** (1975) 1502 [[INSPIRE](#)].
- [5] G. Senjanović, *Spontaneous breakdown of parity in a class of gauge theories*, *Nucl. Phys. B* **153** (1979) 334 [[INSPIRE](#)].
- [6] P. Minkowski, *$\mu \rightarrow e\gamma$ at a rate of one out of 10^9 muon decays?*, *Phys. Lett.* **67B** (1977) 421 [[INSPIRE](#)].
- [7] R.N. Mohapatra and G. Senjanović, *Neutrino mass and spontaneous parity nonconservation*, *Phys. Rev. Lett.* **44** (1980) 912 [[INSPIRE](#)].
- [8] R.E. Marshak and R.N. Mohapatra, *Quark-lepton symmetry and B-L as the U(1) generator of the electroweak symmetry group*, *Phys. Lett.* **91B** (1980) 222 [[INSPIRE](#)].
- [9] R.N. Mohapatra and R.E. Marshak, *Local B-L Symmetry of electroweak interactions, Majorana neutrinos and neutron oscillations*, *Phys. Rev. Lett.* **44** (1980) 1316 [*Erratum ibid.* **44** (1980) 1643] [[INSPIRE](#)].
- [10] W.-Y. Keung and G. Senjanović, *Majorana neutrinos and the production of the right-handed charged gauge boson*, *Phys. Rev. Lett.* **50** (1983) 1427 [[INSPIRE](#)].
- [11] R.N. Mohapatra, *Mechanism for understanding small neutrino mass in superstring theories*, *Phys. Rev. Lett.* **56** (1986) 561 [[INSPIRE](#)].

- [12] R.N. Mohapatra and J.W.F. Valle, *Neutrino mass and baryon number nonconservation in superstring models*, *Phys. Rev. D* **34** (1986) 1642 [[INSPIRE](#)].
- [13] C.-Y. Chen and P.S.B. Dev, *Multi-lepton collider signatures of heavy Dirac and Majorana neutrinos*, *Phys. Rev. D* **85** (2012) 093018 [[arXiv:1112.6419](#)] [[INSPIRE](#)].
- [14] P.S. Bhupal Dev and R.N. Mohapatra, *Unified explanation of the $eejj$, diboson and dijet resonances at the LHC*, *Phys. Rev. Lett.* **115** (2015) 181803 [[arXiv:1508.02277](#)] [[INSPIRE](#)].
- [15] L. Wolfenstein, *Different varieties of massive Dirac neutrinos*, *Nucl. Phys. B* **186** (1981) 147 [[INSPIRE](#)].
- [16] A. Das, P.S.B. Dev and R.N. Mohapatra, *Same sign versus opposite sign dileptons as a probe of low scale seesaw mechanisms*, *Phys. Rev. D* **97** (2018) 015018 [[arXiv:1709.06553](#)] [[INSPIRE](#)].
- [17] ATLAS collaboration, *Search for heavy neutrinos and right-handed W bosons in events with two leptons and jets in pp collisions at $\sqrt{s} = 7$ TeV with the ATLAS detector*, *Eur. Phys. J. C* **72** (2012) 2056 [[arXiv:1203.5420](#)] [[INSPIRE](#)].
- [18] CMS collaboration, *Search for heavy neutrinos and $W[R]$ bosons with right-handed couplings in a left-right symmetric model in pp collisions at $\sqrt{s} = 7$ TeV*, *Phys. Rev. Lett.* **109** (2012) 261802 [[arXiv:1210.2402](#)] [[INSPIRE](#)].
- [19] ATLAS collaboration, *Search for heavy Majorana neutrinos with the ATLAS detector in pp collisions at $\sqrt{s} = 8$ TeV*, *JHEP* **07** (2015) 162 [[arXiv:1506.06020](#)] [[INSPIRE](#)].
- [20] CMS collaboration, *Search for heavy neutrinos and W bosons with right-handed couplings in proton-proton collisions at $\sqrt{s} = 8$ TeV*, *Eur. Phys. J. C* **74** (2014) 3149 [[arXiv:1407.3683](#)] [[INSPIRE](#)].
- [21] CMS collaboration, *Search for a heavy right-handed W boson and a heavy neutrino in events with two same-flavor leptons and two jets at $\sqrt{s} = 13$ TeV*, *JHEP* **05** (2018) 148 [[arXiv:1803.11116](#)] [[INSPIRE](#)].
- [22] CMS collaboration, *Search for heavy neutrinos or third-generation leptoquarks in final states with two hadronically decaying τ leptons and two jets in proton-proton collisions at $\sqrt{s} = 13$ TeV*, *JHEP* **03** (2017) 077 [[arXiv:1612.01190](#)] [[INSPIRE](#)].
- [23] CMS collaboration, *Search for third-generation scalar leptoquarks and heavy right-handed neutrinos in final states with two tau leptons and two jets in proton-proton collisions at $\sqrt{s} = 13$ TeV*, *JHEP* **07** (2017) 121 [[arXiv:1703.03995](#)] [[INSPIRE](#)].
- [24] J. Alwall et al., *MadGraph 5: going beyond*, *JHEP* **06** (2011) 128 [[arXiv:1106.0522](#)] [[INSPIRE](#)].
- [25] J. Alwall et al., *The automated computation of tree-level and next-to-leading order differential cross sections and their matching to parton shower simulations*, *JHEP* **07** (2014) 079 [[arXiv:1405.0301](#)] [[INSPIRE](#)].
- [26] T. Sjöstrand, S. Mrenna and P.Z. Skands, *A brief introduction to PYTHIA 8.1*, *Comput. Phys. Commun.* **178** (2008) 852 [[arXiv:0710.3820](#)] [[INSPIRE](#)].
- [27] ATLAS collaboration, *The ATLAS experiment at the CERN Large Hadron Collider*, 2008 *JINST* **3** S08003 [[INSPIRE](#)].
- [28] ATLAS collaboration, *ATLAS insertable b -layer technical design report*, ATLAS-TDR-19 (2010).

- [29] ATLAS IBL collaboration, *Production and integration of the ATLAS insertable B-layer*, [*2018 JINST* **13** T05008](#) [[arXiv:1803.00844](#)] [[INSPIRE](#)].
- [30] ATLAS collaboration, *Performance of the ATLAS trigger system in 2015*, [*Eur. Phys. J. C* **77** \(2017\) 317](#) [[arXiv:1611.09661](#)] [[INSPIRE](#)].
- [31] R.D. Ball et al., *Parton distributions with LHC data*, [*Nucl. Phys. B* **867** \(2013\) 244](#) [[arXiv:1207.1303](#)] [[INSPIRE](#)].
- [32] ATLAS collaboration, *ATLAS Run 1 PYTHIA8 tunes*, [ATL-PHYS-PUB-2014-021](#) (2014).
- [33] A. Alloul et al., *FeynRules 2.0 — A complete toolbox for tree-level phenomenology*, [*Comput. Phys. Commun.* **185** \(2014\) 2250](#) [[arXiv:1310.1921](#)] [[INSPIRE](#)].
- [34] A. Roitgrund, G. Eilam and S. Bar-Shalom, *Implementation of the left-right symmetric model in FeynRules*, [*Comput. Phys. Commun.* **203** \(2016\) 18](#) [[arXiv:1401.3345](#)] [[INSPIRE](#)].
- [35] M. Nemešsek, F. Nesti and G. Popara, *Keung-Senjanović process at the LHC: from lepton number violation to displaced vertices to invisible decays*, [*Phys. Rev. D* **97** \(2018\) 115018](#) [[arXiv:1801.05813](#)] [[INSPIRE](#)].
- [36] T. Gleisberg et al., *Event generation with SHERPA 1.1*, [*JHEP* **02** \(2009\) 007](#) [[arXiv:0811.4622](#)] [[INSPIRE](#)].
- [37] NNPDF collaboration, R.D. Ball et al., *Parton distributions for the LHC Run II*, [*JHEP* **04** \(2015\) 040](#) [[arXiv:1410.8849](#)] [[INSPIRE](#)].
- [38] T. Gleisberg and S. Hoeche, *Comix, a new matrix element generator*, [*JHEP* **12** \(2008\) 039](#) [[arXiv:0808.3674](#)] [[INSPIRE](#)].
- [39] F. Cascioli, P. Maierhofer and S. Pozzorini, *Scattering amplitudes with open loops*, [*Phys. Rev. Lett.* **108** \(2012\) 111601](#) [[arXiv:1111.5206](#)] [[INSPIRE](#)].
- [40] S. Alioli, P. Nason, C. Oleari and E. Re, *A general framework for implementing NLO calculations in shower Monte Carlo programs: the POWHEG BOX*, [*JHEP* **06** \(2010\) 043](#) [[arXiv:1002.2581](#)] [[INSPIRE](#)].
- [41] P. Nason, *A new method for combining NLO QCD with shower Monte Carlo algorithms*, [*JHEP* **11** \(2004\) 040](#) [[hep-ph/0409146](#)] [[INSPIRE](#)].
- [42] S. Frixione, P. Nason and C. Oleari, *Matching NLO QCD computations with Parton Shower simulations: the POWHEG method*, [*JHEP* **11** \(2007\) 070](#) [[arXiv:0709.2092](#)] [[INSPIRE](#)].
- [43] H.-L. Lai et al., *New parton distributions for collider physics*, [*Phys. Rev. D* **82** \(2010\) 074024](#) [[arXiv:1007.2241](#)] [[INSPIRE](#)].
- [44] T. Sjöstrand, S. Mrenna and P.Z. Skands, *PYTHIA 6.4 Physics and Manual*, [*JHEP* **05** \(2006\) 026](#) [[hep-ph/0603175](#)] [[INSPIRE](#)].
- [45] J. Pumplin et al., *New generation of parton distributions with uncertainties from global QCD analysis*, [*JHEP* **07** \(2002\) 012](#) [[hep-ph/0201195](#)] [[INSPIRE](#)].
- [46] P.Z. Skands, *Tuning Monte Carlo generators: the Perugia tunes*, [*Phys. Rev. D* **82** \(2010\) 074018](#) [[arXiv:1005.3457](#)] [[INSPIRE](#)].
- [47] D.J. Lange, *The EvtGen particle decay simulation package*, [*Nucl. Instrum. Meth. A* **462** \(2001\) 152](#) [[INSPIRE](#)].
- [48] ATLAS collaboration, *Summary of ATLAS PYTHIA 8 tunes*, [ATL-PHYS-PUB-2012-003](#) (2012).

- [49] A.D. Martin, W.J. Stirling, R.S. Thorne and G. Watt, *Parton distributions for the LHC*, *Eur. Phys. J. C* **63** (2009) 189 [[arXiv:0901.0002](#)] [[INSPIRE](#)].
- [50] ATLAS collaboration, *The ATLAS simulation infrastructure*, *Eur. Phys. J. C* **70** (2010) 823 [[arXiv:1005.4568](#)] [[INSPIRE](#)].
- [51] GEANT4 collaboration, S. Agostinelli et al., *GEANT4: A Simulation toolkit*, *Nucl. Instrum. Meth. A* **506** (2003) 250 [[INSPIRE](#)].
- [52] ATLAS collaboration, *The simulation principle and performance of the ATLAS fast calorimeter simulation FastCaloSim*, [ATL-PHYS-PUB-2010-013](#) (2010).
- [53] ATLAS collaboration, *Electron efficiency measurements with the ATLAS detector using the 2015 LHC proton-proton collision data*, [ATLAS-CONF-2016-024](#) (2016).
- [54] ATLAS collaboration, *Electron and photon energy calibration with the ATLAS detector using data collected in 2015 at $\sqrt{s} = 13$ TeV*, [ATL-PHYS-PUB-2016-015](#) (2016).
- [55] ATLAS collaboration, *Electron identification measurements in ATLAS using $\sqrt{s} = 13$ TeV data with 50 ns bunch spacing*, [ATL-PHYS-PUB-2015-041](#) (2015).
- [56] ATLAS collaboration, *Charged-particle distributions in $\sqrt{s} = 13$ TeV pp interactions measured with the ATLAS detector at the LHC*, *Phys. Lett. B* **758** (2016) 67 [[arXiv:1602.01633](#)] [[INSPIRE](#)].
- [57] ATLAS collaboration, *Muon reconstruction performance of the ATLAS detector in proton-proton collision data at $\sqrt{s} = 13$ TeV*, *Eur. Phys. J. C* **76** (2016) 292 [[arXiv:1603.05598](#)] [[INSPIRE](#)].
- [58] M. Cacciari, G.P. Salam and G. Soyez, *The anti- k_t jet clustering algorithm*, *JHEP* **04** (2008) 063 [[arXiv:0802.1189](#)] [[INSPIRE](#)].
- [59] ATLAS collaboration, *Jet energy scale measurements and their systematic uncertainties in proton-proton collisions at $\sqrt{s} = 13$ TeV with the ATLAS detector*, *Phys. Rev. D* **96** (2017) 072002 [[arXiv:1703.09665](#)] [[INSPIRE](#)].
- [60] ATLAS collaboration, *Performance of pile-up mitigation techniques for jets in pp collisions at $\sqrt{s} = 8, 13$ TeV using the ATLAS detector*, *Eur. Phys. J. C* **76** (2016) 581 [[arXiv:1510.03823](#)] [[INSPIRE](#)].
- [61] ATLAS collaboration, *Optimisation of the ATLAS b-tagging performance for the 2016 LHC Run*, [ATL-PHYS-PUB-2016-012](#) (2016).
- [62] ATLAS collaboration, *Measurements of b-jet tagging efficiency with the ATLAS detector using $t\bar{t}$ events at $\sqrt{s} = 13$ TeV*, *JHEP* **08** (2018) 089 [[arXiv:1805.01845](#)] [[INSPIRE](#)].
- [63] ATLAS collaboration, *Search for doubly charged Higgs boson production in multi-lepton final states with the ATLAS detector using proton-proton collisions at $\sqrt{s} = 13$ TeV*, *Eur. Phys. J. C* **78** (2018) 199 [[arXiv:1710.09748](#)] [[INSPIRE](#)].
- [64] ATLAS collaboration, *Luminosity determination in pp collisions at $\sqrt{s} = 8$ TeV using the ATLAS detector at the LHC*, *Eur. Phys. J. C* **76** (2016) 653 [[arXiv:1608.03953](#)] [[INSPIRE](#)].
- [65] G. Avoni et al., *The new LUCID-2 detector for luminosity measurement and monitoring in ATLAS*, [2018 JINST](#) **13** P07017 [[INSPIRE](#)].
- [66] M. Botje et al., *The PDF4LHC working group interim recommendations*, [arXiv:1101.0538](#) [[INSPIRE](#)].

- [67] L.A. Harland-Lang, A.D. Martin, P. Motylinski and R.S. Thorne, *Parton distributions in the LHC era: MMHT 2014 PDFs*, *Eur. Phys. J. C* **75** (2015) 204 [[arXiv:1412.3989](#)] [[INSPIRE](#)].
- [68] S. Dulat et al., *New parton distribution functions from a global analysis of quantum chromodynamics*, *Phys. Rev. D* **93** (2016) 033006 [[arXiv:1506.07443](#)] [[INSPIRE](#)].
- [69] M. Bahr et al., *HERWIG++ physics and manual*, *Eur. Phys. J. C* **58** (2008) 639 [[arXiv:0803.0883](#)] [[INSPIRE](#)].
- [70] A. Kalogeropoulos and J. Alwall, *The SysCalc code: a tool to derive theoretical systematic uncertainties*, [arXiv:1801.08401](#) [[INSPIRE](#)].
- [71] M. Baak et al., *HistFitter software framework for statistical data analysis*, *Eur. Phys. J. C* **75** (2015) 153 [[arXiv:1410.1280](#)] [[INSPIRE](#)].
- [72] M. Baak, S. Gadatsch, R. Harrington and W. Verkerke, *Interpolation between multi-dimensional histograms using a new non-linear moment morphing method*, *Nucl. Instrum. Meth. A* **771** (2015) 39 [[arXiv:1410.7388](#)] [[INSPIRE](#)].
- [73] A.L. Read, *Presentation of search results: the CL_s technique*, *J. Phys. G* **28** (2002) 2693 [[INSPIRE](#)].
- [74] G. Cowan, K. Cranmer, E. Gross and O. Vitells, *Asymptotic formulae for likelihood-based tests of new physics*, *Eur. Phys. J. C* **71** (2011) 1554 [Erratum *ibid.* **C 73** (2013) 2501] [[arXiv:1007.1727](#)] [[INSPIRE](#)].
- [75] ATLAS collaboration, *ATLAS computing acknowledgements*, [ATL-GEN-PUB-2016-002](#) (2016).

The ATLAS collaboration

M. Aaboud^{34d}, G. Aad⁹⁹, B. Abbott¹²⁴, O. Abdinov^{13,*}, B. Abeloos¹²⁸,
D.K. Abhayasinghe⁹¹, S.H. Abidi¹⁶⁴, O.S. AbouZeid³⁹, N.L. Abraham¹⁵³,
H. Abramowicz¹⁵⁸, H. Abreu¹⁵⁷, Y. Abulaiti⁶, B.S. Acharya^{64a,64b,n}, S. Adachi¹⁶⁰,
L. Adamczyk^{81a}, J. Adelman¹¹⁹, M. Adersberger¹¹², A. Adiguzel^{12c}, T. Adye¹⁴¹,
A.A. Affolder¹⁴³, Y. Afik¹⁵⁷, C. Agheorghiesei^{27c}, J.A. Aguilar-Saavedra^{136f,136a},
F. Ahmadov^{77,ad}, G. Aielli^{71a,71b}, S. Akatsuka⁸³, T.P.A. Åkesson⁹⁴, E. Akilli⁵²,
A.V. Akimov¹⁰⁸, G.L. Alberghi^{23b,23a}, J. Albert¹⁷³, P. Albicocco⁴⁹,
M.J. Alconada Verzini⁸⁶, S. Alderweireldt¹¹⁷, M. Aleksa³⁵, I.N. Aleksandrov⁷⁷,
C. Alexa^{27b}, T. Alexopoulos¹⁰, M. Alhroob¹²⁴, B. Ali¹³⁸, G. Alimonti^{66a}, J. Alison³⁶,
S.P. Alkire¹⁴⁵, C. Allaire¹²⁸, B.M.M. Allbrooke¹⁵³, B.W. Allen¹²⁷, P.P. Allport²¹,
A. Aloisio^{67a,67b}, A. Alonso³⁹, F. Alonso⁸⁶, C. Alpigiani¹⁴⁵, A.A. Alshehri⁵⁵,
M.I. Alstaty⁹⁹, B. Alvarez Gonzalez³⁵, D. Álvarez Piqueras¹⁷¹, M.G. Alviggi^{67a,67b},
B.T. Amadio¹⁸, Y. Amaral Coutinho^{78b}, L. Ambroz¹³¹, C. Amelung²⁶, D. Amidei¹⁰³,
S.P. Amor Dos Santos^{136a,136c}, S. Amoroso⁴⁴, C.S. Amrouche⁵², C. Anastopoulos¹⁴⁶,
L.S. Ancu⁵², N. Andari¹⁴², T. Andeen¹¹, C.F. Anders^{59b}, J.K. Anders²⁰, K.J. Anderson³⁶,
A. Andreazza^{66a,66b}, V. Andrei^{59a}, C.R. Anelli¹⁷³, S. Angelidakis³⁷, I. Angelozzi¹¹⁸,
A. Angerami³⁸, A.V. Anisenkov^{120b,120a}, A. Annovi^{69a}, C. Antel^{59a}, M.T. Anthony¹⁴⁶,
M. Antonelli⁴⁹, D.J.A. Antrim¹⁶⁸, F. Anulli^{70a}, M. Aoki⁷⁹, J.A. Aparisi Pozo¹⁷¹,
L. Aperio Bella³⁵, G. Arabidze¹⁰⁴, J.P. Araque^{136a}, V. Araujo Ferraz^{78b},
R. Araujo Pereira^{78b}, A.T.H. Arce⁴⁷, R.E. Ardell⁹¹, F.A. Arduh⁸⁶, J-F. Arguin¹⁰⁷,
S. Argyropoulos⁷⁵, A.J. Armbruster³⁵, L.J. Armitage⁹⁰, A. Armstrong¹⁶⁸, O. Arnaez¹⁶⁴,
H. Arnold¹¹⁸, M. Arratia³¹, O. Arslan²⁴, A. Artamonov^{109,*}, G. Artoni¹³¹, S. Artz⁹⁷,
S. Asai¹⁶⁰, N. Asbah⁵⁷, A. Ashkenazi¹⁵⁸, E.M. Asimakopoulou¹⁶⁹, L. Asquith¹⁵³,
K. Assamagan²⁹, R. Astalos^{28a}, R.J. Atkin^{32a}, M. Atkinson¹⁷⁰, N.B. Atlay¹⁴⁸,
K. Augsten¹³⁸, G. Avolio³⁵, R. Avramidou^{58a}, M.K. Ayoub^{15a}, G. Azuelos^{107,aq},
A.E. Baas^{59a}, M.J. Baca²¹, H. Bachacou¹⁴², K. Bachas^{65a,65b}, M. Backes¹³¹,
P. Bagnaia^{70a,70b}, M. Bahmani⁸², H. Bahrasemani¹⁴⁹, A.J. Bailey¹⁷¹, J.T. Baines¹⁴¹,
M. Bajic³⁹, C. Bakalis¹⁰, O.K. Baker¹⁸⁰, P.J. Bakker¹¹⁸, D. Bakshi Gupta⁹³,
E.M. Baldin^{120b,120a}, P. Balek¹⁷⁷, F. Balli¹⁴², W.K. Balunas¹³³, J. Balz⁹⁷, E. Banas⁸²,
A. Bandyopadhyay²⁴, S. Banerjee^{178,j}, A.A.E. Bannoura¹⁷⁹, L. Barak¹⁵⁸, W.M. Barbe³⁷,
E.L. Barberio¹⁰², D. Barberis^{53b,53a}, M. Barbero⁹⁹, T. Barillari¹¹³, M-S. Barisits³⁵,
J. Barkeloo¹²⁷, T. Barklow¹⁵⁰, N. Barlow³¹, R. Barnea¹⁵⁷, S.L. Barnes^{58c},
B.M. Barnett¹⁴¹, R.M. Barnett¹⁸, Z. Barnovska-Blenessy^{58a}, A. Baroncelli^{72a},
G. Barone²⁶, A.J. Barr¹³¹, L. Barranco Navarro¹⁷¹, F. Barreiro⁹⁶,
J. Barreiro Guimarães da Costa^{15a}, R. Bartoldus¹⁵⁰, A.E. Barton⁸⁷, P. Bartos^{28a},
A. Basalae¹³⁴, A. Bassalat¹²⁸, R.L. Bates⁵⁵, S.J. Batista¹⁶⁴, S. Batlamous^{34e},
J.R. Batley³¹, M. Battaglia¹⁴³, M. Bause^{70a,70b}, F. Bauer¹⁴², K.T. Bauer¹⁶⁸,
H.S. Bawa^{150,1}, J.B. Beacham¹²², T. Beau¹³², P.H. Beauchemin¹⁶⁷, P. Bechtel²⁴,
H.C. Beck⁵¹, H.P. Beck^{20,p}, K. Becker⁵⁰, M. Becker⁹⁷, C. Becot⁴⁴, A. Beddall^{12d},
A.J. Beddall^{12a}, V.A. Bednyakov⁷⁷, M. Bedognetti¹¹⁸, C.P. Bee¹⁵², T.A. Beermann³⁵,
M. Begalli^{78b}, M. Begel²⁹, A. Behera¹⁵², J.K. Behr⁴⁴, A.S. Bell⁹², G. Bella¹⁵⁸,
L. Bellagamba^{23b}, A. Bellerive³³, M. Bellomo¹⁵⁷, P. Bellos⁹, K. Belotskiy¹¹⁰,

N.L. Belyaev¹¹⁰, O. Benary^{158,*}, D. Benchechrone^{34a}, M. Bender¹¹², N. Benekos¹⁰,
 Y. Benhammou¹⁵⁸, E. Benhar Noccioli¹⁸⁰, J. Benitez⁷⁵, D.P. Benjamin⁴⁷, M. Benoit⁵²,
 J.R. Bensinger²⁶, S. Bentvelsen¹¹⁸, L. Beresford¹³¹, M. Beretta⁴⁹, D. Berge⁴⁴,
 E. Bergeaas Kuutmann¹⁶⁹, N. Berger⁵, L.J. Bergsten²⁶, J. Beringer¹⁸, S. Berlendis⁷,
 N.R. Bernard¹⁰⁰, G. Bernardi¹³², C. Bernius¹⁵⁰, F.U. Bernlochner²⁴, T. Berry⁹¹,
 P. Berta⁹⁷, C. Bertella^{15a}, G. Bertoli^{43a,43b}, I.A. Bertram⁸⁷, G.J. Besjes³⁹,
 O. Bessidskaia Bylund¹⁷⁹, M. Bessner⁴⁴, N. Besson¹⁴², A. Bethani⁹⁸, S. Bethke¹¹³,
 A. Betti²⁴, A.J. Bevan⁹⁰, J. Beyer¹¹³, R.M.B. Bianchi¹³⁵, O. Biebel¹¹², D. Biedermann¹⁹,
 R. Bielski³⁵, K. Bierwagen⁹⁷, N.V. Biesuz^{69a,69b}, M. Biglietti^{72a}, T.R.V. Billoud¹⁰⁷,
 M. Bindi⁵¹, A. Bingul^{12d}, C. Bini^{70a,70b}, S. Biondi^{23b,23a}, M. Birman¹⁷⁷, T. Bisanz⁵¹,
 J.P. Biswal¹⁵⁸, C. Bittrich⁴⁶, D.M. Bjergaard⁴⁷, J.E. Black¹⁵⁰, K.M. Black²⁵,
 T. Blazek^{28a}, I. Bloch⁴⁴, C. Blocker²⁶, A. Blue⁵⁵, U. Blumenschein⁹⁰, Dr. Blunier^{144a},
 G.J. Bobbink¹¹⁸, V.S. Bobrovnikov^{120b,120a}, S.S. Bocchetta⁹⁴, A. Bocci⁴⁷, D. Boerner¹⁷⁹,
 D. Bogavac¹¹², A.G. Bogdanchikov^{120b,120a}, C. Boehm^{43a}, V. Boisvert⁹¹, P. Bokan^{169,w},
 T. Bold^{81a}, A.S. Boldyrev¹¹¹, A.E. Bolz^{59b}, M. Bomben¹³², M. Bona⁹⁰, J.S. Bonilla¹²⁷,
 M. Boonekamp¹⁴², A. Borisov¹⁴⁰, G. Borissov⁸⁷, J. Bortfeldt³⁵, D. Bortoletto¹³¹,
 V. Bortolotto^{71a,71b}, D. Boscherini^{23b}, M. Bosman¹⁴, J.D. Bossio Sola³⁰, K. Bouaouda^{34a},
 J. Boudreau¹³⁵, E.V. Bouhova-Thacker⁸⁷, D. Boumediene³⁷, C. Bourdarios¹²⁸,
 S.K. Boutle⁵⁵, A. Boveia¹²², J. Boyd³⁵, D. Boye^{32b}, I.R. Boyko⁷⁷, A.J. Bozson⁹¹,
 J. Bracinik²¹, N. Brahimi⁹⁹, A. Brandt⁸, G. Brandt¹⁷⁹, O. Brandt^{59a}, F. Braren⁴⁴,
 U. Bratzler¹⁶¹, B. Brau¹⁰⁰, J.E. Brau¹²⁷, W.D. Breaden Madden⁵⁵, K. Brendlinger⁴⁴,
 A.J. Brennan¹⁰², L. Brenner⁴⁴, R. Brenner¹⁶⁹, S. Bressler¹⁷⁷, B. Brickwedde⁹⁷,
 D.L. Briglin²¹, D. Britton⁵⁵, D. Britzger^{59b}, I. Brock²⁴, R. Brock¹⁰⁴, G. Brooijmans³⁸,
 T. Brooks⁹¹, W.K. Brooks^{144b}, E. Brost¹¹⁹, J.H. Broughton²¹,
 P.A. Bruckman de Renstrom⁸², D. Bruncko^{28b}, A. Bruni^{23b}, G. Bruni^{23b}, L.S. Bruni¹¹⁸,
 S. Bruno^{71a,71b}, B.H. Brunt³¹, M. Bruschi^{23b}, N. Bruscino¹³⁵, P. Bryant³⁶,
 L. Bryngemark⁴⁴, T. Buanes¹⁷, Q. Buat³⁵, P. Buchholz¹⁴⁸, A.G. Buckley⁵⁵,
 I.A. Budagov⁷⁷, F. Buehrer⁵⁰, M.K. Bugge¹³⁰, O. Bulekov¹¹⁰, D. Bullock⁸, T.J. Burch¹¹⁹,
 S. Burdin⁸⁸, C.D. Burgard¹¹⁸, A.M. Burger⁵, B. Burghgrave¹¹⁹, K. Burka⁸², S. Burke¹⁴¹,
 I. Burmeister⁴⁵, J.T.P. Burr¹³¹, D. Büscher⁵⁰, V. Büscher⁹⁷, E. Buschmann⁵¹,
 P. Bussey⁵⁵, J.M. Butler²⁵, C.M. Buttar⁵⁵, J.M. Butterworth⁹², P. Butti³⁵,
 W. Buttinger³⁵, A. Buzatu¹⁵⁵, A.R. Buzykaev^{120b,120a}, G. Cabras^{23b,23a},
 S. Cabrera Urbán¹⁷¹, D. Caforio¹³⁸, H. Cai¹⁷⁰, V.M.M. Cairo², O. Cakir^{4a}, N. Calace⁵²,
 P. Calafiura¹⁸, A. Calandri⁹⁹, G. Calderini¹³², P. Calfayan⁶³, G. Callea^{40b,40a},
 L.P. Caloba^{78b}, S. Calvente Lopez⁹⁶, D. Calvet³⁷, S. Calvet³⁷, T.P. Calvet¹⁵²,
 M. Calvetti^{69a,69b}, R. Camacho Toro¹³², S. Camarda³⁵, P. Camarri^{71a,71b}, D. Cameron¹³⁰,
 R. Caminal Armadans¹⁰⁰, C. Camincher³⁵, S. Campana³⁵, M. Campanelli⁹²,
 A. Camplani³⁹, A. Campoverde¹⁴⁸, V. Canale^{67a,67b}, M. Cano Bret^{58c}, J. Cantero¹²⁵,
 T. Cao¹⁵⁸, Y. Cao¹⁷⁰, M.D.M. Capeans Garrido³⁵, I. Caprini^{27b}, M. Caprini^{27b},
 M. Capua^{40b,40a}, R.M. Carbone³⁸, R. Cardarelli^{71a}, F.C. Cardillo¹⁴⁶, I. Carli¹³⁹,
 T. Carli³⁵, G. Carlino^{67a}, B.T. Carlson¹³⁵, L. Carminati^{66a,66b}, R.M.D. Carney^{43a,43b},
 S. Caron¹¹⁷, E. Carquin^{144b}, S. Carrá^{66a,66b}, G.D. Carrillo-Montoya³⁵, D. Casadei^{32b},
 M.P. Casado^{14,f}, A.F. Casha¹⁶⁴, D.W. Casper¹⁶⁸, R. Castelijns¹¹⁸, F.L. Castillo¹⁷¹,

V. Castillo Gimenez¹⁷¹, N.F. Castro^{136a,136e}, A. Catinaccio³⁵, J.R. Catmore¹³⁰,
A. Cattai³⁵, J. Caudron²⁴, V. Cavaliere²⁹, E. Cavallaro¹⁴, D. Cavalli^{66a},
M. Cavalli-Sforza¹⁴, V. Cavasinni^{69a,69b}, E. Celebi^{12b}, F. Ceradini^{72a,72b},
L. Cerda Alberich¹⁷¹, A.S. Cerqueira^{78a}, A. Cerri¹⁵³, L. Cerrito^{71a,71b}, F. Cerutti¹⁸,
A. Cervelli^{23b,23a}, S.A. Cetin^{12b}, A. Chafaq^{34a}, D. Chakraborty¹¹⁹, S.K. Chan⁵⁷,
W.S. Chan¹¹⁸, Y.L. Chan^{61a}, J.D. Chapman³¹, B. Chargeishvili^{156b}, D.G. Charlton²¹,
C.C. Chau³³, C.A. Chavez Barajas¹⁵³, S. Che¹²², A. Chegwidan¹⁰⁴, S. Chekanov⁶,
S.V. Chekulaev^{165a}, G.A. Chelkov^{77,ap}, M.A. Chelstowska³⁵, C. Chen^{58a}, C.H. Chen⁷⁶,
H. Chen²⁹, J. Chen^{58a}, J. Chen³⁸, S. Chen¹³³, S.J. Chen^{15b}, X. Chen^{15c,ao}, Y. Chen⁸⁰,
Y-H. Chen⁴⁴, H.C. Cheng¹⁰³, H.J. Cheng^{15d}, A. Cheplakov⁷⁷, E. Cheremushkina¹⁴⁰,
R. Cherkaoui El Moursli^{34e}, E. Cheu⁷, K. Cheung⁶², L. Chevalier¹⁴², V. Chiarella⁴⁹,
G. Chiarelli^{69a}, G. Chiodini^{65a}, A.S. Chisholm³⁵, A. Chitan^{27b}, I. Chiu¹⁶⁰, Y.H. Chiu¹⁷³,
M.V. Chizhov⁷⁷, K. Choi⁶³, A.R. Chomont¹²⁸, S. Chouridou¹⁵⁹, Y.S. Chow¹¹⁸,
V. Christodoulou⁹², M.C. Chu^{61a}, J. Chudoba¹³⁷, A.J. Chuinard¹⁰¹, J.J. Chwastowski⁸²,
L. Chytka¹²⁶, D. Cinca⁴⁵, V. Cindro⁸⁹, I.A. Cioară²⁴, A. Ciocio¹⁸, F. Ciotto^{67a,67b},
Z.H. Citron¹⁷⁷, M. Citterio^{66a}, A. Clark⁵², M.R. Clark³⁸, P.J. Clark⁴⁸, C. Clement^{43a,43b},
Y. Coadou⁹⁹, M. Cobal^{64a,64c}, A. Coccaro^{53b,53a}, J. Cochran⁷⁶, H. Cohen¹⁵⁸,
A.E.C. Coimbra¹⁷⁷, L. Colasurdo¹¹⁷, B. Cole³⁸, A.P. Colijn¹¹⁸, J. Collot⁵⁶,
P. Conde Muiño^{136a,136b}, E. Coniavitis⁵⁰, S.H. Connell^{32b}, I.A. Connelly⁹⁸,
S. Constantinescu^{27b}, F. Conventi^{67a,ar}, A.M. Cooper-Sarkar¹³¹, F. Cormier¹⁷²,
K.J.R. Cormier¹⁶⁴, M. Corradi^{70a,70b}, E.E. Corrigan⁹⁴, F. Corriveau^{101,ab},
A. Cortes-Gonzalez³⁵, M.J. Costa¹⁷¹, D. Costanzo¹⁴⁶, G. Cottin³¹, G. Cowan⁹¹,
B.E. Cox⁹⁸, J. Crane⁹⁸, K. Cranmer¹²¹, S.J. Crawley⁵⁵, R.A. Creager¹³³, G. Cree³³,
S. Crépé-Renaudin⁵⁶, F. Crescioli¹³², M. Cristinziani²⁴, V. Croft¹²¹, G. Crosetti^{40b,40a},
A. Cueto⁹⁶, T. Cuhadar Donszelmann¹⁴⁶, A.R. Cukierman¹⁵⁰, J. Cúth⁹⁷, S. Czekierda⁸²,
P. Czodrowski³⁵, M.J. Da Cunha Sargedas De Sousa^{58b,136b}, C. Da Via⁹⁸,
W. Dabrowski^{81a}, T. Dado^{28a,w}, S. Dahbi^{34e}, T. Dai¹⁰³, F. Dallaire¹⁰⁷, C. Dallapiccola¹⁰⁰,
M. Dam³⁹, G. D'amen^{23b,23a}, J. Damp⁹⁷, J.R. Dandoy¹³³, M.F. Daneri³⁰, N.P. Dang^{178,j},
N.D. Dann⁹⁸, M. Danninger¹⁷², V. Dao³⁵, G. Darbo^{53b}, S. Darmora⁸, O. Dartsis⁵,
A. Dattagupta¹²⁷, T. Daubney⁴⁴, S. D'Auria⁵⁵, W. Davey²⁴, C. David⁴⁴, T. Davidek¹³⁹,
D.R. Davis⁴⁷, E. Dawe¹⁰², I. Dawson¹⁴⁶, K. De⁸, R. De Asmundis^{67a}, A. De Benedetti¹²⁴,
M. De Beurs¹¹⁸, S. De Castro^{23b,23a}, S. De Cecco^{70a,70b}, N. De Groot¹¹⁷, P. de Jong¹¹⁸,
H. De la Torre¹⁰⁴, F. De Lorenzi⁷⁶, A. De Maria^{51,r}, D. De Pedis^{70a}, A. De Salvo^{70a},
U. De Sanctis^{71a,71b}, M. De Santis^{71a,71b}, A. De Santo¹⁵³, K. De Vasconcelos Corga⁹⁹,
J.B. De Vivie De Regie¹²⁸, C. Debenedetti¹⁴³, D.V. Dedovich⁷⁷, N. Dehghanian³,
M. Del Gaudio^{40b,40a}, J. Del Peso⁹⁶, Y. Delabat Diaz⁴⁴, D. Delgove¹²⁸, F. Deliot¹⁴²,
C.M. Delitzsch⁷, M. Della Pietra^{67a,67b}, D. Della Volpe⁵², A. Dell'Acqua³⁵, L. Dell'Asta²⁵,
M. Delmastro⁵, C. Delporte¹²⁸, P.A. Delsart⁵⁶, D.A. DeMarco¹⁶⁴, S. Demers¹⁸⁰,
M. Demichev⁷⁷, S.P. Denisov¹⁴⁰, D. Denysiuk¹¹⁸, L. D'Eramo¹³², D. Derendarz⁸²,
J.E. Derkaoui^{34d}, F. Derue¹³², P. Dervan⁸⁸, K. Desch²⁴, C. Deterre⁴⁴, K. Dette¹⁶⁴,
M.R. Devesa³⁰, P.O. Deviveiros³⁵, A. Dewhurst¹⁴¹, S. Dhaliwal²⁶, F.A. Di Bello⁵²,
A. Di Ciaccio^{71a,71b}, L. Di Ciaccio⁵, W.K. Di Clemente¹³³, C. Di Donato^{67a,67b},
A. Di Girolamo³⁵, B. Di Micco^{72a,72b}, R. Di Nardo¹⁰⁰, K.F. Di Petrillo⁵⁷, R. Di Sipio¹⁶⁴,

D. Di Valentino³³, C. Diaconu⁹⁹, M. Diamond¹⁶⁴, F.A. Dias³⁹, T. Dias Do Vale^{136a},
M.A. Diaz^{144a}, J. Dickinson¹⁸, E.B. Diehl¹⁰³, J. Dietrich¹⁹, S. Díez Cornell⁴⁴,
A. Dimitrievska¹⁸, J. Dingfelder²⁴, F. Dittus³⁵, F. Djama⁹⁹, T. Djobava^{156b},
J.I. Djuvsland^{59a}, M.A.B. Do Vale^{78c}, M. Dobre^{27b}, D. Dodsworth²⁶, C. Doglioni⁹⁴,
J. Dolejsi¹³⁹, Z. Dolezal¹³⁹, M. Donadelli^{78d}, J. Donini³⁷, A. D’Onofrio⁹⁰, M. D’Onofrio⁸⁸,
J. Dopke¹⁴¹, A. Doria^{67a}, M.T. Dova⁸⁶, A.T. Doyle⁵⁵, E. Drechsler⁵¹, E. Dreyer¹⁴⁹,
T. Dreyer⁵¹, Y. Du^{58b}, J. Duarte-Campderros¹⁵⁸, F. Dubinin¹⁰⁸, M. Dubovsky^{28a},
A. Dubreuil⁵², E. Duchovni¹⁷⁷, G. Duckeck¹¹², A. Ducourthial¹³², O.A. Ducu^{107,v},
D. Duda¹¹³, A. Dudarev³⁵, A.C. Dudder⁹⁷, E.M. Duffield¹⁸, L. Duflot¹²⁸, M. Dührssen³⁵,
C. Dülse¹⁷⁹, M. Dumancic¹⁷⁷, A.E. Dumitriu^{27b,d}, A.K. Duncan⁵⁵, M. Dunford^{59a},
A. Duperrin⁹⁹, H. Duran Yildiz^{4a}, M. Düren⁵⁴, A. Durglishvili^{156b}, D. Duschinger⁴⁶,
B. Dutta⁴⁴, D. Duvnjak¹, M. Dyndal⁴⁴, S. Dysch⁹⁸, B.S. Dziedzic⁸², C. Eckardt⁴⁴,
K.M. Ecker¹¹³, R.C. Edgar¹⁰³, T. Eifert³⁵, G. Eigen¹⁷, K. Einsweiler¹⁸, T. Ekelof¹⁶⁹,
M. El Kacimi^{34c}, R. El Kosseifi⁹⁹, V. Ellajosyula⁹⁹, M. Ellert¹⁶⁹, F. Ellinghaus¹⁷⁹,
A.A. Elliot⁹⁰, N. Ellis³⁵, J. Elmsheuser²⁹, M. Elsing³⁵, D. Emelianov¹⁴¹, Y. Enari¹⁶⁰,
J.S. Ennis¹⁷⁵, M.B. Epland⁴⁷, J. Erdmann⁴⁵, A. Ereditato²⁰, S. Errede¹⁷⁰, M. Escalier¹²⁸,
C. Escobar¹⁷¹, O. Estrada Pastor¹⁷¹, A.I. Etienne¹⁴², E. Etzion¹⁵⁸, H. Evans⁶³,
A. Ezhilov¹³⁴, M. Ezzi^{34e}, F. Fabbri⁵⁵, L. Fabbri^{23b,23a}, V. Fabiani¹¹⁷, G. Facini⁹²,
R.M. Faisca Rodrigues Pereira^{136a}, R.M. Fakhruddinov¹⁴⁰, S. Falciano^{70a}, P.J. Falke⁵,
S. Falke⁵, J. Faltova¹³⁹, Y. Fang^{15a}, M. Fanti^{66a,66b}, A. Farbin⁸, A. Farilla^{72a},
E.M. Farina^{68a,68b}, T. Farooque¹⁰⁴, S. Farrell¹⁸, S.M. Farrington¹⁷⁵, P. Farthouat³⁵,
F. Fassi^{34e}, P. Fassnacht³⁵, D. Fassouliotis⁹, M. Faucci Giannelli⁴⁸, A. Favareto^{53b,53a},
W.J. Fawcett³¹, L. Fayard¹²⁸, O.L. Fedin^{134,o}, W. Fedorko¹⁷², M. Feickert⁴¹, S. Feigl¹³⁰,
L. Feligioni⁹⁹, C. Feng^{58b}, E.J. Feng³⁵, M. Feng⁴⁷, M.J. Fenton⁵⁵, A.B. Fenyuk¹⁴⁰,
L. Feremenga⁸, J. Ferrando⁴⁴, A. Ferrari¹⁶⁹, P. Ferrari¹¹⁸, R. Ferrari^{68a},
D.E. Ferreira de Lima^{59b}, A. Ferrer¹⁷¹, D. Ferrere⁵², C. Ferretti¹⁰³, F. Fiedler⁹⁷,
A. Filipčič⁸⁹, F. Filthaut¹¹⁷, K.D. Finelli²⁵, M.C.N. Fiolhais^{136a,136c,a}, L. Fiorini¹⁷¹,
C. Fischer¹⁴, W.C. Fisher¹⁰⁴, N. Flaschel⁴⁴, I. Fleck¹⁴⁸, P. Fleischmann¹⁰³,
R.R.M. Fletcher¹³³, T. Flick¹⁷⁹, B.M. Flierl¹¹², L.M. Flores¹³³, L.R. Flores Castillo^{61a},
F.M. Follega^{73a,73b}, N. Fomin¹⁷, G.T. Forcolin⁹⁸, A. Formica¹⁴², F.A. Förster¹⁴,
A.C. Forti⁹⁸, A.G. Foster²¹, D. Fournier¹²⁸, H. Fox⁸⁷, S. Fracchia¹⁴⁶, P. Francavilla^{69a,69b},
M. Franchini^{23b,23a}, S. Franchino^{59a}, D. Francis³⁵, L. Franconi¹³⁰, M. Franklin⁵⁷,
M. Frate¹⁶⁸, M. Fraternali^{68a,68b}, D. Freeborn⁹², S.M. Fressard-Batraneanu³⁵,
B. Freund¹⁰⁷, W.S. Freund^{78b}, D.C. Frizzell¹²⁴, D. Froidevaux³⁵, J.A. Frost¹³¹,
C. Fukunaga¹⁶¹, E. Fullana Torregrosa¹⁷¹, T. Fusayasu¹¹⁴, J. Fuster¹⁷¹, O. Gabizon¹⁵⁷,
A. Gabrielli^{23b,23a}, A. Gabrielli¹⁸, G.P. Gach^{81a}, S. Gadatsch⁵², P. Gadow¹¹³,
G. Gagliardi^{53b,53a}, L.G. Gagnon¹⁰⁷, C. Galea^{27b}, B. Galhardo^{136a,136c}, E.J. Gallas¹³¹,
B.J. Gallop¹⁴¹, P. Gallus¹³⁸, G. Galster³⁹, R. Gamboa Goni⁹⁰, K.K. Gan¹²²,
S. Ganguly¹⁷⁷, J. Gao^{58a}, Y. Gao⁸⁸, Y.S. Gao^{150,l}, C. García¹⁷¹, J.E. García Navarro¹⁷¹,
J.A. García Pascual^{15a}, M. Garcia-Sciveres¹⁸, R.W. Gardner³⁶, N. Garelli¹⁵⁰,
V. Garonne¹³⁰, K. Gasnikova⁴⁴, A. Gaudiello^{53b,53a}, G. Gaudio^{68a}, I.L. Gavrilenko¹⁰⁸,
A. Gavriluk¹⁰⁹, C. Gay¹⁷², G. Gaycken²⁴, E.N. Gazis¹⁰, C.N.P. Gee¹⁴¹, J. Geisen⁵¹,
M. Geisen⁹⁷, M.P. Geisler^{59a}, K. Gellerstedt^{43a,43b}, C. Gemme^{53b}, M.H. Genest⁵⁶,

C. Geng¹⁰³, S. Gentile^{70a,70b}, S. George⁹¹, D. Gerbaudo¹⁴, G. Gessner⁴⁵, S. Ghasemi¹⁴⁸, M. Ghasemi Bostanabad¹⁷³, M. Ghneimat²⁴, B. Giacobbe^{23b}, S. Giagu^{70a,70b}, N. Giangiacomi^{23b,23a}, P. Giammetti^{69a}, A. Giannini^{67a,67b}, S.M. Gibson⁹¹, M. Gignac¹⁴³, D. Gillberg³³, G. Gilles¹⁷⁹, D.M. Gingrich^{3,aq}, M.P. Giordani^{64a,64c}, F.M. Giorgi^{23b}, P.F. Giraud¹⁴², P. Giromini⁵⁷, G. Giuliani^{64a,64c}, D. Giugni^{66a}, F. Giuli¹³¹, M. Giulini^{59b}, S. Gkaitatzis¹⁵⁹, I. Gkialas^{9,i}, E.L. Gkougkousis¹⁴, P. Gkoutoumis¹⁰, L.K. Gladilin¹¹¹, C. Glasman⁹⁶, J. Glatzer¹⁴, P.C.F. Glaysheer⁴⁴, A. Glazov⁴⁴, M. Goblirsch-Kolb²⁶, J. Godlewski⁸², S. Goldfarb¹⁰², T. Golling⁵², D. Golubkov¹⁴⁰, A. Gomes^{136a,136b,136d}, R. Goncalves Gama^{78a}, R. Gonalo^{136a}, G. Gonella⁵⁰, L. Gonella²¹, A. Gongadze⁷⁷, F. Gonnella²¹, J.L. Gonski⁵⁷, S. Gonzlez de la Hoz¹⁷¹, S. Gonzalez-Sevilla⁵², L. Goossens³⁵, P.A. Gorbounov¹⁰⁹, H.A. Gordon²⁹, B. Gorini³⁵, E. Gorini^{65a,65b}, A. Gorišek⁸⁹, A.T. Goshaw⁴⁷, C. Gssling⁴⁵, M.I. Gostkin⁷⁷, C.A. Gottardo²⁴, C.R. Goudet¹²⁸, D. Goudami^{34c}, A.G. Goussiou¹⁴⁵, N. Govender^{32b,b}, C. Goy⁵, E. Gozani¹⁵⁷, I. Grabowska-Bold^{81a}, P.O.J. Gradin¹⁶⁹, E.C. Graham⁸⁸, J. Gramling¹⁶⁸, E. Gramstad¹³⁰, S. Grancagnolo¹⁹, V. Gratchev¹³⁴, P.M. Gravila^{27f}, F.G. Gravili^{65a,65b}, C. Gray⁵⁵, H.M. Gray¹⁸, Z.D. Greenwood^{93,ag}, C. Grefe²⁴, K. Gregersen⁹⁴, I.M. Gregor⁴⁴, P. Grenier¹⁵⁰, K. Grevtsov⁴⁴, N.A. Grieser¹²⁴, J. Griffiths⁸, A.A. Grillo¹⁴³, K. Grimm¹⁵⁰, S. Grinstein^{14,x}, Ph. Gris³⁷, J.-F. Grivaz¹²⁸, S. Groh⁹⁷, E. Gross¹⁷⁷, J. Grosse-Knetter⁵¹, G.C. Grossi⁹³, Z.J. Grout⁹², C. Grud¹⁰³, A. Grummer¹¹⁶, L. Guan¹⁰³, W. Guan¹⁷⁸, J. Guenther³⁵, A. Guerguichon¹²⁸, F. Guescini^{165a}, D. Guest¹⁶⁸, R. Gugel⁵⁰, B. Gui¹²², T. Guillemin⁵, S. Guindon³⁵, U. Gul⁵⁵, C. Gumpert³⁵, J. Guo^{58c}, W. Guo¹⁰³, Y. Guo^{58a,q}, Z. Guo⁹⁹, R. Gupta⁴¹, S. Gurbuz^{12c}, G. Gustavino¹²⁴, B.J. Gutelman¹⁵⁷, P. Gutierrez¹²⁴, C. Gutsche⁹², C. Guyot¹⁴², M.P. Guzik^{81a}, C. Gwenlan¹³¹, C.B. Gwilliam⁸⁸, A. Haas¹²¹, C. Haber¹⁸, H.K. Hadavand⁸, N. Haddad^{34e}, A. Hader^{58a}, S. Hagebock²⁴, M. Hagihara¹⁶⁶, H. Hakobyan^{181,*}, M. Haleem¹⁷⁴, J. Haley¹²⁵, G. Halladjian¹⁰⁴, G.D. Hallewell⁹⁹, K. Hamacher¹⁷⁹, P. Hamal¹²⁶, K. Hamano¹⁷³, A. Hamilton^{32a}, G.N. Hamity¹⁴⁶, K. Han^{58a,af}, L. Han^{58a}, S. Han^{15d}, K. Hanagaki^{79,t}, M. Hance¹⁴³, D.M. Handl¹¹², B. Haney¹³³, R. Hankache¹³², P. Hanke^{59a}, E. Hansen⁹⁴, J.B. Hansen³⁹, J.D. Hansen³⁹, M.C. Hansen²⁴, P.H. Hansen³⁹, K. Hara¹⁶⁶, A.S. Hard¹⁷⁸, T. Harenberg¹⁷⁹, S. Harkusha¹⁰⁵, P.F. Harrison¹⁷⁵, N.M. Hartmann¹¹², Y. Hasegawa¹⁴⁷, A. Hasib⁴⁸, S. Hassani¹⁴², S. Haug²⁰, R. Hauser¹⁰⁴, L. Hauswald⁴⁶, L.B. Havener³⁸, M. Havranek¹³⁸, C.M. Hawkes²¹, R.J. Hawkins³⁵, D. Hayden¹⁰⁴, C. Hayes¹⁵², C.P. Hays¹³¹, J.M. Hays⁹⁰, H.S. Hayward⁸⁸, S.J. Haywood¹⁴¹, M.P. Heath⁴⁸, V. Hedberg⁹⁴, L. Heelan⁸, S. Heer²⁴, K.K. Heidegger⁵⁰, J. Heilman³³, S. Heim⁴⁴, T. Heim¹⁸, B. Heinemann^{44,al}, J.J. Heinrich¹¹², L. Heinrich¹²¹, C. Heinz⁵⁴, J. Hejbal¹³⁷, L. Helary³⁵, A. Held¹⁷², S. Hellesund¹³⁰, S. Hellman^{43a,43b}, C. Helsens³⁵, R.C.W. Henderson⁸⁷, Y. Heng¹⁷⁸, S. Henkelmann¹⁷², A.M. Henriques Correia³⁵, G.H. Herbert¹⁹, H. Herde²⁶, V. Herget¹⁷⁴, Y. Hernndez Jimnez^{32c}, H. Herr⁹⁷, M.G. Herrmann¹¹², G. Herten⁵⁰, R. Hertenberger¹¹², L. Hervas³⁵, T.C. Herwig¹³³, G.G. Hesketh⁹², N.P. Hessey^{165a}, J.W. Hetherly⁴¹, S. Higashino⁷⁹, E. Hign-Rodríguez¹⁷¹, K. Hildebrand³⁶, E. Hill¹⁷³, J.C. Hill³¹, K.K. Hill²⁹, K.H. Hiller⁴⁴, S.J. Hillier²¹, M. Hils⁴⁶, I. Hinchliffe¹⁸, M. Hirose¹²⁹, D. Hirschbuehl¹⁷⁹, B. Hiti⁸⁹, O. Hladik¹³⁷, D.R. Hlaluku^{32c}, X. Hoad⁴⁸,

J. Hobbs¹⁵², N. Hod^{165a}, M.C. Hodgkinson¹⁴⁶, A. Hoecker³⁵, M.R. Hoferkamp¹¹⁶,
 F. Hoenig¹¹², D. Hohn²⁴, D. Hohov¹²⁸, T.R. Holmes³⁶, M. Holzbock¹¹², M. Homann⁴⁵,
 S. Honda¹⁶⁶, T. Honda⁷⁹, T.M. Hong¹³⁵, A. Hönle¹¹³, B.H. Hooberman¹⁷⁰,
 W.H. Hopkins¹²⁷, Y. Horii¹¹⁵, P. Horn⁴⁶, A.J. Horton¹⁴⁹, L.A. Horyn³⁶, J.-Y. Hostachy⁵⁶,
 A. Hostiuc¹⁴⁵, S. Hou¹⁵⁵, A. Hoummada^{34a}, J. Howarth⁹⁸, J. Hoya⁸⁶, M. Hrabovsky¹²⁶,
 J. Hrdinka³⁵, I. Hristova¹⁹, J. Hrivnac¹²⁸, A. Hrynevich¹⁰⁶, T. Hryn'ova⁵, P.J. Hsu⁶²,
 S.-C. Hsu¹⁴⁵, Q. Hu²⁹, S. Hu^{58c}, Y. Huang^{15a}, Z. Hubacek¹³⁸, F. Hubaut⁹⁹, M. Huebner²⁴,
 F. Huegging²⁴, T.B. Huffman¹³¹, E.W. Hughes³⁸, M. Huhtinen³⁵, R.F.H. Hunter³³,
 P. Huo¹⁵², A.M. Hupe³³, N. Huseynov^{77,ad}, J. Huston¹⁰⁴, J. Huth⁵⁷, R. Hyneman¹⁰³,
 G. Iacobucci⁵², G. Iakovidis²⁹, I. Ibragimov¹⁴⁸, L. Iconomidou-Fayard¹²⁸, Z. Idrissi^{34e},
 P. Iengo³⁵, R. Ignazzi³⁹, O. Igonkina^{118,z}, R. Iguchi¹⁶⁰, T. Iizawa⁵², Y. Ikegami⁷⁹,
 M. Ikeno⁷⁹, D. Iliadis¹⁵⁹, N. Ilic¹⁵⁰, F. Iltzsche⁴⁶, G. Introzzi^{68a,68b}, M. Iodice^{72a},
 K. Iordanidou³⁸, V. Ippolito^{70a,70b}, M.F. Isacson¹⁶⁹, N. Ishijima¹²⁹, M. Ishino¹⁶⁰,
 M. Ishitsuka¹⁶², W. Islam¹²⁵, C. Issever¹³¹, S. Istin^{12c,ak}, F. Ito¹⁶⁶, J.M. Iturbe Ponce^{61a},
 R. Iuppa^{73a,73b}, A. Ivina¹⁷⁷, H. Iwasaki⁷⁹, J.M. Izen⁴², V. Izzo^{67a}, P. Jacka¹³⁷,
 P. Jackson¹, R.M. Jacobs²⁴, V. Jain², G. Jäkel¹⁷⁹, K.B. Jakobi⁹⁷, K. Jakobs⁵⁰,
 S. Jakobsen⁷⁴, T. Jakoubek¹³⁷, D.O. Jamin¹²⁵, D.K. Jana⁹³, R. Jansky⁵², J. Janssen²⁴,
 M. Janus⁵¹, P.A. Janus^{81a}, G. Jarlskog⁹⁴, N. Javadov^{77,ad}, T. Javůrek³⁵, M. Javurkova⁵⁰,
 F. Jeanneau¹⁴², L. Jeanty¹⁸, J. Jejelava^{156a,ae}, A. Jelinskas¹⁷⁵, P. Jenni^{50,c}, J. Jeong⁴⁴,
 S. Jézéquel⁵, H. Ji¹⁷⁸, J. Jia¹⁵², H. Jiang⁷⁶, Y. Jiang^{58a}, Z. Jiang¹⁵⁰, S. Jiggins⁵⁰,
 F.A. Jimenez Morales³⁷, J. Jimenez Pena¹⁷¹, S. Jin^{15b}, A. Jinaru^{27b}, O. Jinnouchi¹⁶²,
 H. Jivan^{32c}, P. Johansson¹⁴⁶, K.A. Johns⁷, C.A. Johnson⁶³, W.J. Johnson¹⁴⁵,
 K. Jon-And^{43a,43b}, R.W.L. Jones⁸⁷, S.D. Jones¹⁵³, S. Jones⁷, T.J. Jones⁸⁸,
 J. Jongmanns^{59a}, P.M. Jorge^{136a,136b}, J. Jovicevic^{165a}, X. Ju¹⁸, J.J. Junggeburth¹¹³,
 A. Juste Rozas^{14,x}, A. Kaczmarska⁸², M. Kado¹²⁸, H. Kagan¹²², M. Kagan¹⁵⁰, T. Kaji¹⁷⁶,
 E. Kajomovitz¹⁵⁷, C.W. Kalderon⁹⁴, A. Kaluza⁹⁷, S. Kama⁴¹, A. Kamenshchikov¹⁴⁰,
 L. Kanjir⁸⁹, Y. Kano¹⁶⁰, V.A. Kantserov¹¹⁰, J. Kanzaki⁷⁹, B. Kaplan¹²¹, L.S. Kaplan¹⁷⁸,
 D. Kar^{32c}, M.J. Kareem^{165b}, E. Karentzos¹⁰, S.N. Karpov⁷⁷, Z.M. Karpova⁷⁷,
 V. Kartvelishvili⁸⁷, A.N. Karyukhin¹⁴⁰, L. Kashif¹⁷⁸, R.D. Kass¹²², A. Kastanas¹⁵¹,
 Y. Kataoka¹⁶⁰, C. Kato^{58d,58c}, J. Katzy⁴⁴, K. Kawade⁸⁰, K. Kawagoe⁸⁵, T. Kawamoto¹⁶⁰,
 G. Kawamura⁵¹, E.F. Kay⁸⁸, V.F. Kazanin^{120b,120a}, R. Keeler¹⁷³, R. Kehoe⁴¹,
 J.S. Keller³³, E. Kellermann⁹⁴, J.J. Kempster²¹, J. Kendrick²¹, O. Kepka¹³⁷,
 S. Kersten¹⁷⁹, B.P. Kerševan⁸⁹, R.A. Keyes¹⁰¹, M. Khader¹⁷⁰, F. Khalil-Zada¹³,
 A. Khanov¹²⁵, A.G. Kharlamov^{120b,120a}, T. Kharlamova^{120b,120a}, E.E. Khoda¹⁷²,
 A. Khodinov¹⁶³, T.J. Khoo⁵², E. Khramov⁷⁷, J. Khubua^{156b}, S. Kido⁸⁰, M. Kiehn⁵²,
 C.R. Kilby⁹¹, Y.K. Kim³⁶, N. Kimura^{64a,64c}, O.M. Kind¹⁹, B.T. King⁸⁸, D. Kirchmeier⁴⁶,
 J. Kirk¹⁴¹, A.E. Kiryunin¹¹³, T. Kishimoto¹⁶⁰, D. Kisielewska^{81a}, V. Kitali⁴⁴,
 O. Kivernyk⁵, E. Kladiva^{28b}, T. Klapdor-Kleingrothaus⁵⁰, M.H. Klein¹⁰³, M. Klein⁸⁸,
 U. Klein⁸⁸, K. Kleinknecht⁹⁷, P. Klimek¹¹⁹, A. Klimentov²⁹, R. Klingenberg^{45,*},
 T. Klingl²⁴, T. Klioutchnikova³⁵, F.F. Klitzner¹¹², P. Kluit¹¹⁸, S. Kluth¹¹³,
 E. Kneringer⁷⁴, E.B.F.G. Knoops⁹⁹, A. Knue⁵⁰, A. Kobayashi¹⁶⁰, D. Kobayashi⁸⁵,
 T. Kobayashi¹⁶⁰, M. Kobel⁴⁶, M. Kocian¹⁵⁰, P. Kodys¹³⁹, P.T. Koenig²⁴, T. Koffas³³,
 E. Koffeman¹¹⁸, N.M. Köhler¹¹³, T. Koi¹⁵⁰, M. Kolb^{59b}, I. Koletsou⁵, T. Kondo⁷⁹,

N. Kondrashova^{58c}, K. Köneke⁵⁰, A.C. König¹¹⁷, T. Kono⁷⁹, R. Konoplich^{121,ah},
V. Konstantinides⁹², N. Konstantinidis⁹², B. Konya⁹⁴, R. Kopeliansky⁶³, S. Koperny^{81a},
K. Korcyl⁸², K. Kordas¹⁵⁹, G. Koren¹⁵⁸, A. Korn⁹², I. Korolkov¹⁴, E.V. Korolkova¹⁴⁶,
N. Korotkova¹¹¹, O. Kortner¹¹³, S. Kortner¹¹³, T. Kosek¹³⁹, V.V. Kostyukhin²⁴,
A. Kotwal⁴⁷, A. Koulouris¹⁰, A. Kourkoulouli-Charalampidi^{68a,68b}, C. Kourkoulouli⁹,
E. Kourlitis¹⁴⁶, V. Kouskoura²⁹, A.B. Kowalewska⁸², R. Kowalewski¹⁷³, T.Z. Kowalski^{81a},
C. Kozakai¹⁶⁰, W. Kozanecki¹⁴², A.S. Kozhin¹⁴⁰, V.A. Kramarenko¹¹¹, G. Kramberger⁸⁹,
D. Krasnopevtsev^{58a}, M.W. Krasny¹³², A. Krasznahorkay³⁵, D. Krauss¹¹³,
J.A. Kremer^{81a}, J. Kretschmar⁸⁸, P. Krieger¹⁶⁴, K. Krizka¹⁸, K. Kroeninger⁴⁵,
H. Kroha¹¹³, J. Kroll¹³⁷, J. Kroll¹³³, J. Krstic¹⁶, U. Kruchonak⁷⁷, H. Krüger²⁴,
N. Krumnack⁷⁶, M.C. Kruse⁴⁷, T. Kubota¹⁰², S. Kuday^{4b}, J.T. Kuechler¹⁷⁹, S. Kuehn³⁵,
A. Kugel^{59a}, F. Kuger¹⁷⁴, T. Kuhl⁴⁴, V. Kukhtin⁷⁷, R. Kukla⁹⁹, Y. Kulchitsky¹⁰⁵,
S. Kuleshov^{144b}, Y.P. Kulinich¹⁷⁰, M. Kuna⁵⁶, T. Kunigo⁸³, A. Kupco¹³⁷, T. Kupfer⁴⁵,
O. Kuprash¹⁵⁸, H. Kurashige⁸⁰, L.L. Kurchaninov^{165a}, Y.A. Kurochkin¹⁰⁵,
M.G. Kurth^{15d}, E.S. Kuwertz³⁵, M. Kuze¹⁶², J. Kvita¹²⁶, T. Kwan¹⁰¹, A. La Rosa¹¹³,
J.L. La Rosa Navarro^{78d}, L. La Rotonda^{40b,40a}, F. La Ruffa^{40b,40a}, C. Lacasta¹⁷¹,
F. Lacava^{70a,70b}, J. Lacey⁴⁴, D.P.J. Lack⁹⁸, H. Lacker¹⁹, D. Lacour¹³², E. Ladygin⁷⁷,
R. Lafaye⁵, B. Laforge¹³², T. Lagouri^{32c}, S. Lai⁵¹, S. Lammers⁶³, W. Lampl⁷,
E. Lançon²⁹, U. Landgraf⁵⁰, M.P.J. Landon⁹⁰, M.C. Lanfermann⁵², V.S. Lang⁴⁴,
J.C. Lange¹⁴, R.J. Langenberg³⁵, A.J. Lankford¹⁶⁸, F. Lanni²⁹, K. Lantzscht²⁴,
A. Lanza^{68a}, A. Lapertosa^{53b,53a}, S. Laplace¹³², J.F. Laporte¹⁴², T. Lari^{66a},
F. Lasagni Manghi^{23b,23a}, M. Lassnig³⁵, T.S. Lau^{61a}, A. Laudrain¹²⁸, M. Lavorgna^{67a,67b},
A.T. Law¹⁴³, P. Laycock⁸⁸, M. Lazzaroni^{66a,66b}, B. Le¹⁰², O. Le Dortz¹³²,
E. Le Guirriec⁹⁹, E.P. Le Quilleuc¹⁴², M. LeBlanc⁷, T. LeCompte⁶, F. Ledroit-Guillon⁵⁶,
C.A. Lee²⁹, G.R. Lee^{144a}, L. Lee⁵⁷, S.C. Lee¹⁵⁵, B. Lefebvre¹⁰¹, M. Lefebvre¹⁷³,
F. Legger¹¹², C. Leggett¹⁸, K. Lehmann¹⁴⁹, N. Lehmann¹⁷⁹, G. Lehmann Miotto³⁵,
W.A. Leight⁴⁴, A. Leisos^{159,u}, M.A.L. Leite^{78d}, R. Leitner¹³⁹, D. Lellouch¹⁷⁷,
B. Lemmer⁵¹, K.J.C. Leney⁹², T. Lenz²⁴, B. Lenzi³⁵, R. Leone⁷, S. Leone^{69a},
C. Leonidopoulos⁴⁸, G. Lerner¹⁵³, C. Leroy¹⁰⁷, R. Les¹⁶⁴, A.A.J. Lesage¹⁴², C.G. Lester³¹,
M. Levchenko¹³⁴, J. Levêque⁵, D. Levin¹⁰³, L.J. Levinson¹⁷⁷, D. Lewis⁹⁰, B. Li¹⁰³,
C-Q. Li^{58a}, H. Li^{58b}, L. Li^{58c}, Q. Li^{15d}, Q.Y. Li^{58a}, S. Li^{58d,58c}, X. Li^{58c}, Y. Li¹⁴⁸,
Z. Liang^{15a}, B. Liberti^{71a}, A. Liblong¹⁶⁴, K. Lie^{61c}, S. Liem¹¹⁸, A. Limosani¹⁵⁴,
C.Y. Lin³¹, K. Lin¹⁰⁴, T.H. Lin⁹⁷, R.A. Linck⁶³, J.H. Lindon²¹, B.E. Lindquist¹⁵²,
A.L. Lioni⁵², E. Lipeles¹³³, A. Lipniacka¹⁷, M. Lisovyi^{59b}, T.M. Liss^{170,an}, A. Lister¹⁷²,
A.M. Litke¹⁴³, J.D. Little⁸, B. Liu⁷⁶, B.L. Liu⁶, H.B. Liu²⁹, H. Liu¹⁰³, J.B. Liu^{58a},
J.K.K. Liu¹³¹, K. Liu¹³², M. Liu^{58a}, P. Liu¹⁸, Y. Liu^{15a}, Y.L. Liu^{58a}, Y.W. Liu^{58a},
M. Livan^{68a,68b}, A. Lleres⁵⁶, J. Llorente Merino^{15a}, S.L. Lloyd⁹⁰, C.Y. Lo^{61b},
F. Lo Sterzo⁴¹, E.M. Lobodzinska⁴⁴, P. Loch⁷, A. Loesle⁵⁰, T. Lohse¹⁹, K. Lohwasser¹⁴⁶,
M. Lokajicek¹³⁷, B.A. Long²⁵, J.D. Long¹⁷⁰, R.E. Long⁸⁷, L. Longo^{65a,65b},
K.A. Looper¹²², J.A. Lopez^{144b}, I. Lopez Paz¹⁴, A. Lopez Solis¹⁴⁶, J. Lorenz¹¹²,
N. Lorenzo Martinez⁵, M. Losada²², P.J. Lösel¹¹², X. Lou⁴⁴, X. Lou^{15a}, A. Lounis¹²⁸,
J. Love⁶, P.A. Love⁸⁷, J.J. Lozano Bahilo¹⁷¹, H. Lu^{61a}, M. Lu^{58a}, N. Lu¹⁰³, Y.J. Lu⁶²,
H.J. Lubatti¹⁴⁵, C. Luci^{70a,70b}, A. Lucotte⁵⁶, C. Luedtke⁵⁰, F. Luehring⁶³, I. Luise¹³²,

L. Luminari^{70a}, B. Lund-Jensen¹⁵¹, M.S. Lutz¹⁰⁰, P.M. Luzi¹³², D. Lynn²⁹, R. Lysak¹³⁷,
 E. Lytken⁹⁴, F. Lyu^{15a}, V. Lyubushkin⁷⁷, H. Ma²⁹, L.L. Ma^{58b}, Y. Ma^{58b},
 G. Maccarrone⁴⁹, A. Macchiolo¹¹³, C.M. Macdonald¹⁴⁶, J. Machado Miguens^{133,136b},
 D. Madaffari¹⁷¹, R. Madar³⁷, W.F. Mader⁴⁶, A. Madsen⁴⁴, N. Madysa⁴⁶, J. Maeda⁸⁰,
 K. Maekawa¹⁶⁰, S. Maeland¹⁷, T. Maeno²⁹, A.S. Maevskiy¹¹¹, V. Magerl⁵⁰,
 C. Maidantchik^{78b}, T. Maier¹¹², A. Maio^{136a,136b,136d}, O. Majersky^{28a}, S. Majewski¹²⁷,
 Y. Makida⁷⁹, N. Makovec¹²⁸, B. Malaescu¹³², Pa. Malecki⁸², V.P. Maleev¹³⁴, F. Malek⁵⁶,
 U. Mallik⁷⁵, D. Malon⁶, C. Malone³¹, S. Maltezos¹⁰, S. Malyukov³⁵, J. Mamuzic¹⁷¹,
 G. Mancini⁴⁹, I. Mandić⁸⁹, J. Maneira^{136a}, L. Manhaes de Andrade Filho^{78a},
 J. Manjarres Ramos⁴⁶, K.H. Mankinen⁹⁴, A. Mann¹¹², A. Manousos⁷⁴, B. Mansoulie¹⁴²,
 J.D. Mansour^{15a}, M. Mantoani⁵¹, S. Manzoni^{66a,66b}, G. Marceca³⁰, L. March⁵²,
 L. Marchese¹³¹, G. Marchiori¹³², M. Marcisovsky¹³⁷, C.A. Marin Tobon³⁵,
 M. Marjanovic³⁷, D.E. Marley¹⁰³, F. Marroquim^{78b}, Z. Marshall¹⁸, M.U.F. Martensson¹⁶⁹,
 S. Marti-Garcia¹⁷¹, C.B. Martin¹²², T.A. Martin¹⁷⁵, V.J. Martin⁴⁸,
 B. Martin dit Latour¹⁷, M. Martinez^{14,x}, V.I. Martinez Outschoorn¹⁰⁰,
 S. Martin-Haugh¹⁴¹, V.S. Martoiu^{27b}, A.C. Martyniuk⁹², A. Marzin³⁵, L. Masetti⁹⁷,
 T. Mashimo¹⁶⁰, R. Mashinistov¹⁰⁸, J. Masik⁹⁸, A.L. Maslennikov^{120b,120a}, L.H. Mason¹⁰²,
 L. Massa^{71a,71b}, P. Massarotti^{67a,67b}, P. Mastrandrea⁵, A. Mastroberardino^{40b,40a},
 T. Masubuchi¹⁶⁰, P. Mättig¹⁷⁹, J. Maurer^{27b}, B. Maček⁸⁹, S.J. Maxfield⁸⁸,
 D.A. Maximov^{120b,120a}, R. Mazini¹⁵⁵, I. Maznas¹⁵⁹, S.M. Mazza¹⁴³, N.C. Mc Fadden¹¹⁶,
 G. Mc Goldrick¹⁶⁴, S.P. Mc Kee¹⁰³, A. McCarn¹⁰³, T.G. McCarthy¹¹³, L.I. McClymont⁹²,
 E.F. McDonald¹⁰², J.A. Mcfayden³⁵, G. Mchedlidze⁵¹, M.A. McKay⁴¹, K.D. McLean¹⁷³,
 S.J. McMahon¹⁴¹, P.C. McNamara¹⁰², C.J. McNicol¹⁷⁵, R.A. McPherson^{173,ab},
 J.E. Mdhluli^{32c}, Z.A. Meadows¹⁰⁰, S. Meehan¹⁴⁵, T. Megy⁵⁰, S. Mehlhase¹¹², A. Mehta⁸⁸,
 T. Meideck⁵⁶, B. Meirose⁴², D. Melini^{171,g}, B.R. Mellado Garcia^{32c}, J.D. Mellenthin⁵¹,
 M. Melo^{28a}, F. Meloni⁴⁴, A. Melzer²⁴, S.B. Menary⁹⁸, E.D. Mendes Gouveia^{136a},
 L. Meng⁸⁸, X.T. Meng¹⁰³, A. Mengarelli^{23b,23a}, S. Menke¹¹³, E. Meoni^{40b,40a},
 S. Mergelmeyer¹⁹, C. Merlassino²⁰, P. Mermod⁵², L. Merola^{67a,67b}, C. Meroni^{66a},
 F.S. Merritt³⁶, A. Messina^{70a,70b}, J. Metcalfe⁶, A.S. Mete¹⁶⁸, C. Meyer¹³³, J. Meyer¹⁵⁷,
 J-P. Meyer¹⁴², H. Meyer Zu Theenhausen^{59a}, F. Miano¹⁵³, R.P. Middleton¹⁴¹,
 L. Mijović⁴⁸, G. Mikenberg¹⁷⁷, M. Mikestikova¹³⁷, M. Mikuž⁸⁹, M. Milesi¹⁰², A. Milic¹⁶⁴,
 D.A. Millar⁹⁰, D.W. Miller³⁶, A. Milov¹⁷⁷, D.A. Milstead^{43a,43b}, A.A. Minaenko¹⁴⁰,
 M. Miñano Moya¹⁷¹, I.A. Minashvili^{156b}, A.I. Mincer¹²¹, B. Mindur^{81a}, M. Mineev⁷⁷,
 Y. Minegishi¹⁶⁰, Y. Ming¹⁷⁸, L.M. Mir¹⁴, A. Mirto^{65a,65b}, K.P. Mistry¹³³, T. Mitani¹⁷⁶,
 J. Mitrevski¹¹², V.A. Mitsou¹⁷¹, A. Miucci²⁰, P.S. Miyagawa¹⁴⁶, A. Mizukami⁷⁹,
 J.U. Mjörnmark⁹⁴, T. Mkrtchyan¹⁸¹, M. Mlynarikova¹³⁹, T. Moa^{43a,43b}, K. Mochizuki¹⁰⁷,
 P. Mogg⁵⁰, S. Mohapatra³⁸, S. Molander^{43a,43b}, R. Moles-Valls²⁴, M.C. Mondragon¹⁰⁴,
 K. Mönig⁴⁴, J. Monk³⁹, E. Monnier⁹⁹, A. Montalbano¹⁴⁹, J. Montejo Berlingen³⁵,
 F. Monticelli⁸⁶, S. Monzani^{66a}, N. Morange¹²⁸, D. Moreno²², M. Moreno Llácer³⁵,
 P. Morettini^{53b}, M. Morgenstern¹¹⁸, S. Morgenstern⁴⁶, D. Mori¹⁴⁹, M. Morii⁵⁷,
 M. Morinaga¹⁷⁶, V. Morisbak¹³⁰, A.K. Morley³⁵, G. Mornacchi³⁵, A.P. Morris⁹²,
 J.D. Morris⁹⁰, L. Morvaj¹⁵², P. Moschovakos¹⁰, M. Mosidze^{156b}, H.J. Moss¹⁴⁶,
 J. Moss^{150,m}, K. Motohashi¹⁶², R. Mount¹⁵⁰, E. Mountricha³⁵, E.J.W. Moyse¹⁰⁰,

S. Muanza⁹⁹, F. Mueller¹¹³, J. Mueller¹³⁵, R.S.P. Mueller¹¹², D. Muenstermann⁸⁷,
 G.A. Mullier²⁰, F.J. Munoz Sanchez⁹⁸, P. Murin^{28b}, W.J. Murray^{175,141},
 A. Murrone^{66a,66b}, M. Muškinja⁸⁹, C. Mwewa^{32a}, A.G. Myagkov^{140,ai}, J. Myers¹²⁷,
 M. Myska¹³⁸, B.P. Nachman¹⁸, O. Nackenhorst⁴⁵, K. Nagai¹³¹, K. Nagano⁷⁹,
 Y. Nagasaka⁶⁰, M. Nagel⁵⁰, E. Nagy⁹⁹, A.M. Nairz³⁵, Y. Nakahama¹¹⁵, K. Nakamura⁷⁹,
 T. Nakamura¹⁶⁰, I. Nakano¹²³, H. Nanjo¹²⁹, F. Napolitano^{59a}, R.F. Naranjo Garcia⁴⁴,
 R. Narayan¹¹, D.I. Narrias Villar^{59a}, I. Naryshkin¹³⁴, T. Naumann⁴⁴, G. Navarro²²,
 R. Nayyar⁷, H.A. Neal¹⁰³, P.Y. Nechaeva¹⁰⁸, T.J. Neep¹⁴², A. Negri^{68a,68b}, M. Negrini^{23b},
 S. Nektarijevic¹¹⁷, C. Nellist⁵¹, M.E. Nelson¹³¹, S. Nemecek¹³⁷, P. Nemethy¹²¹,
 M. Nessi^{35,e}, M.S. Neubauer¹⁷⁰, M. Neumann¹⁷⁹, P.R. Newman²¹, T.Y. Ng^{61c}, Y.S. Ng¹⁹,
 H.D.N. Nguyen⁹⁹, T. Nguyen Manh¹⁰⁷, E. Nibigira³⁷, R.B. Nickerson¹³¹,
 R. Nicolaidou¹⁴², J. Nielsen¹⁴³, N. Nikiforou¹¹, V. Nikolaenko^{140,ai}, I. Nikolic-Audit¹³²,
 K. Nikolopoulos²¹, P. Nilsson²⁹, Y. Ninomiya⁷⁹, A. Nisati^{70a}, N. Nishu^{58c}, R. Nisius¹¹³,
 I. Nitsche⁴⁵, T. Nitta¹⁷⁶, T. Nobe¹⁶⁰, Y. Noguchi⁸³, M. Nomachi¹²⁹, I. Nomidis¹³²,
 M.A. Nomura²⁹, T. Nooney⁹⁰, M. Nordberg³⁵, N. Norjoharuddeen¹³¹, T. Novak⁸⁹,
 O. Novgorodova⁴⁶, R. Novotny¹³⁸, L. Nozka¹²⁶, K. Ntekas¹⁶⁸, E. Nurse⁹², F. Nuti¹⁰²,
 F.G. Oakham^{33,aq}, H. Oberlack¹¹³, T. Obermann²⁴, J. Ocariz¹³², A. Ochi⁸⁰, I. Ochoa³⁸,
 J.P. Ochoa-Ricoux^{144a}, K. O'Connor²⁶, S. Oda⁸⁵, S. Odaka⁷⁹, S. Oerdek⁵¹, A. Oh⁹⁸,
 S.H. Oh⁴⁷, C.C. Ohm¹⁵¹, H. Oide^{53b,53a}, M.L. Ojeda¹⁶⁴, H. Okawa¹⁶⁶, Y. Okazaki⁸³,
 Y. Okumura¹⁶⁰, T. Okuyama⁷⁹, A. Olariu^{27b}, L.F. Oleiro Seabra^{136a},
 S.A. Olivares Pino^{144a}, D. Oliveira Damazio²⁹, J.L. Oliver¹, M.J.R. Olsson³⁶,
 A. Olszewski⁸², J. Olszowska⁸², D.C. O'Neil¹⁴⁹, A. Onofre^{136a,136e}, K. Onogi¹¹⁵,
 P.U.E. Onyisi¹¹, H. Oppen¹³⁰, M.J. Oreglia³⁶, Y. Oren¹⁵⁸, D. Orestano^{72a,72b},
 E.C. Orgill⁹⁸, N. Orlando^{61b}, A.A. O'Rourke⁴⁴, R.S. Orr¹⁶⁴, B. Osculati^{53b,53a,*},
 V. O'Shea⁵⁵, R. Ospanov^{58a}, G. Otero y Garzon³⁰, H. Otono⁸⁵, M. Ouchrif^{34d},
 F. Ould-Saada¹³⁰, A. Ouraou¹⁴², Q. Ouyang^{15a}, M. Owen⁵⁵, R.E. Owen²¹, V.E. Ozcan^{12c},
 N. Ozturk⁸, J. Pacalt¹²⁶, H.A. Pacey³¹, K. Pachal¹⁴⁹, A. Pacheco Pages¹⁴,
 L. Pacheco Rodriguez¹⁴², C. Padilla Aranda¹⁴, S. Pagan Griso¹⁸, M. Paganini¹⁸⁰,
 G. Palacino⁶³, S. Palazzo^{40b,40a}, S. Palestini³⁵, M. Palka^{81b}, D. Pallin³⁷, I. Panagoulas¹⁰,
 C.E. Pandini³⁵, J.G. Panduro Vazquez⁹¹, P. Pani³⁵, G. Panizzo^{64a,64c}, L. Paolozzi⁵²,
 T.D. Papadopoulou¹⁰, K. Papageorgiou^{9,i}, A. Paramonov⁶, D. Paredes Hernandez^{61b},
 S.R. Paredes Saenz¹³¹, B. Parida^{58c}, A.J. Parker⁸⁷, K.A. Parker⁴⁴, M.A. Parker³¹,
 F. Parodi^{53b,53a}, J.A. Parsons³⁸, U. Parzefall⁵⁰, V.R. Pascuzzi¹⁶⁴, J.M.P. Pasner¹⁴³,
 E. Pasqualucci^{70a}, S. Passaggio^{53b}, F. Pastore⁹¹, P. Pasuwan^{43a,43b}, S. Pataria⁹⁷,
 J.R. Pater⁹⁸, A. Pathak^{178,j}, T. Pauly³⁵, B. Pearson¹¹³, M. Pedersen¹³⁰,
 L. Pedraza Diaz¹¹⁷, R. Pedro^{136a,136b}, S.V. Peleganchuk^{120b,120a}, O. Penc¹³⁷, C. Peng^{15d},
 H. Peng^{58a}, B.S. Peralva^{78a}, M.M. Perego¹⁴², A.P. Pereira Peixoto^{136a}, D.V. Perepelitsa²⁹,
 F. Peri¹⁹, L. Perini^{66a,66b}, H. Pernegger³⁵, S. Perrella^{67a,67b}, V.D. Peshekhonov^{77,*},
 K. Peters⁴⁴, R.F.Y. Peters⁹⁸, B.A. Petersen³⁵, T.C. Petersen³⁹, E. Petit⁵⁶, A. Petridis¹,
 C. Petridou¹⁵⁹, P. Petroff¹²⁸, M. Petrov¹³¹, F. Petrucci^{72a,72b}, M. Pettee¹⁸⁰,
 N.E. Pettersson¹⁰⁰, A. Peyaud¹⁴², R. Pezoa^{144b}, T. Pham¹⁰², F.H. Phillips¹⁰⁴,
 P.W. Phillips¹⁴¹, G. Piacquadio¹⁵², E. Pianori¹⁸, A. Picazio¹⁰⁰, M.A. Pickering¹³¹,
 R.H. Pickles⁹⁸, R. Piegai³⁰, J.E. Pilcher³⁶, A.D. Pilkington⁹⁸, M. Pinamonti^{71a,71b},

J.L. Pinfold³, M. Pitt¹⁷⁷, M-A. Pleier²⁹, V. Pleskot¹³⁹, E. Plotnikova⁷⁷, D. Pluth⁷⁶, P. Podberezko^{120b,120a}, R. Poettgen⁹⁴, R. Poggi⁵², L. Poggioli¹²⁸, I. Pogrebnyak¹⁰⁴, D. Pohl²⁴, I. Pokharel⁵¹, G. Polesello^{68a}, A. Poley¹⁸, A. Policicchio^{70a,70b}, R. Polifka³⁵, A. Polini^{23b}, C.S. Pollard⁴⁴, V. Polychronakos²⁹, D. Ponomarenko¹¹⁰, L. Pontecorvo^{70a}, G.A. Popeneciu^{27d}, D.M. Portillo Quintero¹³², S. Pospisil¹³⁸, K. Potamianos⁴⁴, I.N. Potrap⁷⁷, C.J. Potter³¹, H. Potti¹¹, T. Poulsen⁹⁴, J. Poveda³⁵, T.D. Powell¹⁴⁶, M.E. Pozo Astigarraga³⁵, P. Pralavorio⁹⁹, S. Prell⁷⁶, D. Price⁹⁸, M. Primavera^{65a}, S. Prince¹⁰¹, N. Proklova¹¹⁰, K. Prokofiev^{61c}, F. Prokoshin^{144b}, S. Protopopescu²⁹, J. Proudfoot⁶, M. Przybycien^{81a}, A. Puri¹⁷⁰, P. Puzo¹²⁸, J. Qian¹⁰³, Y. Qin⁹⁸, A. Quadt⁵¹, M. Queitsch-Maitland⁴⁴, A. Qureshi¹, P. Rados¹⁰², F. Ragusa^{66a,66b}, G. Rahal⁹⁵, J.A. Raine⁵², S. Rajagopalan²⁹, A. Ramirez Morales⁹⁰, T. Rashid¹²⁸, S. Raspopov⁵, M.G. Ratti^{66a,66b}, D.M. Rauch⁴⁴, F. Rauscher¹¹², S. Rave⁹⁷, B. Ravina¹⁴⁶, I. Ravinovich¹⁷⁷, J.H. Rawling⁹⁸, M. Raymond³⁵, A.L. Read¹³⁰, N.P. Readioff⁵⁶, M. Reale^{65a,65b}, D.M. Rebuzzi^{68a,68b}, A. Redelbach¹⁷⁴, G. Redlinger²⁹, R. Reece¹⁴³, R.G. Reed^{32c}, K. Reeves⁴², L. Rehnisch¹⁹, J. Reichert¹³³, A. Reiss⁹⁷, C. Rembser³⁵, H. Ren^{15d}, M. Rescigno^{70a}, S. Resconi^{66a}, E.D. Resseguie¹³³, S. Rettie¹⁷², E. Reynolds²¹, O.L. Rezanova^{120b,120a}, P. Reznicek¹³⁹, E. Ricci^{73a,73b}, R. Richter¹¹³, S. Richter⁹², E. Richter-Was^{81b}, O. Ricken²⁴, M. Ridel¹³², P. Rieck¹¹³, C.J. Riegel¹⁷⁹, O. Rifki⁴⁴, M. Rijssenbeek¹⁵², A. Rimoldi^{68a,68b}, M. Rimoldi²⁰, L. Rinaldi^{23b}, G. Ripellino¹⁵¹, B. Ristić⁸⁷, E. Ritsch³⁵, I. Riu¹⁴, J.C. Rivera Vergara^{144a}, F. Rizatdinova¹²⁵, E. Rizvi⁹⁰, C. Rizzi¹⁴, R.T. Roberts⁹⁸, S.H. Robertson^{101,ab}, D. Robinson³¹, J.E.M. Robinson⁴⁴, A. Robson⁵⁵, E. Rocco⁹⁷, C. Roda^{69a,69b}, Y. Rodina⁹⁹, S. Rodriguez Bosca¹⁷¹, A. Rodriguez Perez¹⁴, D. Rodriguez Rodriguez¹⁷¹, A.M. Rodríguez Vera^{165b}, S. Roe³⁵, C.S. Rogan⁵⁷, O. Røhne¹³⁰, R. Röhrig¹¹³, C.P.A. Roland⁶³, J. Roloff⁵⁷, A. Romaniouk¹¹⁰, M. Romano^{23b,23a}, N. Rompotis⁸⁸, M. Ronzani¹²¹, L. Roos¹³², S. Rosati^{70a}, K. Rosbach⁵⁰, P. Rose¹⁴³, N-A. Rosien⁵¹, E. Rossi⁴⁴, E. Rossi^{67a,67b}, L.P. Rossi^{53b}, L. Rossini^{66a,66b}, J.H.N. Rosten³¹, R. Rosten¹⁴, M. Rotaru^{27b}, J. Rothberg¹⁴⁵, D. Rousseau¹²⁸, D. Roy^{32c}, A. Rozanov⁹⁹, Y. Rozen¹⁵⁷, X. Ruan^{32c}, F. Rubbo¹⁵⁰, F. Rühr⁵⁰, A. Ruiz-Martinez¹⁷¹, Z. Rurikova⁵⁰, N.A. Rusakovich⁷⁷, H.L. Russell¹⁰¹, J.P. Rutherford⁷, E.M. Rüttinger^{44,k}, Y.F. Ryabov¹³⁴, M. Rybar¹⁷⁰, G. Rybkin¹²⁸, S. Ryu⁶, A. Ryzhov¹⁴⁰, G.F. Rzehorz⁵¹, P. Sabatini⁵¹, G. Sabato¹¹⁸, S. Sacerdoti¹²⁸, H.F-W. Sadrozinski¹⁴³, R. Sadykov⁷⁷, F. Safai Tehrani^{70a}, P. Saha¹¹⁹, M. Sahinsoy^{59a}, A. Sahu¹⁷⁹, M. Saimpert⁴⁴, M. Saito¹⁶⁰, T. Saito¹⁶⁰, H. Sakamoto¹⁶⁰, A. Sakharov^{121,ah}, D. Salamani⁵², G. Salamanna^{72a,72b}, J.E. Salazar Loyola^{144b}, D. Salek¹¹⁸, P.H. Sales De Bruin¹⁶⁹, D. Salihagic¹¹³, A. Salnikov¹⁵⁰, J. Salt¹⁷¹, D. Salvatore^{40b,40a}, F. Salvatore¹⁵³, A. Salvucci^{61a,61b,61c}, A. Salzburger³⁵, J. Samarati³⁵, D. Sammel⁵⁰, D. Sampsonidis¹⁵⁹, D. Sampsonidou¹⁵⁹, J. Sánchez¹⁷¹, A. Sanchez Pineda^{64a,64c}, H. Sandaker¹³⁰, C.O. Sander⁴⁴, M. Sandhoff¹⁷⁹, C. Sandoval²², D.P.C. Sankey¹⁴¹, M. Sannino^{53b,53a}, Y. Sano¹¹⁵, A. Sansoni⁴⁹, C. Santoni³⁷, H. Santos^{136a}, I. Santoyo Castillo¹⁵³, A. Santra¹⁷¹, A. Saprionov⁷⁷, J.G. Saraiva^{136a,136d}, O. Sasaki⁷⁹, K. Sato¹⁶⁶, E. Sauvan⁵, P. Savard^{164,aq}, N. Savic¹¹³, R. Sawada¹⁶⁰, C. Sawyer¹⁴¹, L. Sawyer^{93,ag}, C. Sbarra^{23b}, A. Sbrizzi^{23b,23a}, T. Scanlon⁹², J. Schaarschmidt¹⁴⁵, P. Schacht¹¹³, B.M. Schachtner¹¹², D. Schaefer³⁶, L. Schaefer¹³³, J. Schaeffer⁹⁷, S. Schaepe³⁵, U. Schäfer⁹⁷, A.C. Schaffer¹²⁸, D. Schaile¹¹²,

R.D. Schamberger¹⁵², N. Scharmberg⁹⁸, V.A. Schegelsky¹³⁴, D. Scheirich¹³⁹,
F. Schenck¹⁹, M. Schernau¹⁶⁸, C. Schiavi^{53b,53a}, S. Schier¹⁴³, L.K. Schildgen²⁴,
Z.M. Schillaci²⁶, E.J. Schioppa³⁵, M. Schioppa^{40b,40a}, K.E. Schleicher⁵⁰, S. Schlenker³⁵,
K.R. Schmidt-Sommerfeld¹¹³, K. Schmieden³⁵, C. Schmitt⁹⁷, S. Schmitt⁴⁴, S. Schmitz⁹⁷,
J.C. Schmoeckel⁴⁴, U. Schnoor⁵⁰, L. Schoeffel¹⁴², A. Schoening^{59b}, E. Schopf²⁴,
M. Schott⁹⁷, J.F.P. Schouwenberg¹¹⁷, J. Schovancova³⁵, S. Schramm⁵², A. Schulte⁹⁷,
H-C. Schultz-Coulon^{59a}, M. Schumacher⁵⁰, B.A. Schumm¹⁴³, Ph. Schune¹⁴²,
A. Schwartzman¹⁵⁰, T.A. Schwarz¹⁰³, H. Schweiger⁹⁸, Ph. Schwemling¹⁴²,
R. Schwienhorst¹⁰⁴, A. Sciandra²⁴, G. Sciolla²⁶, M. Scornajenghi^{40b,40a}, F. Scuri^{69a},
F. Scutti¹⁰², L.M. Scyboz¹¹³, J. Searcy¹⁰³, C.D. Sebastiani^{70a,70b}, P. Seema²⁴,
S.C. Seidel¹¹⁶, A. Seiden¹⁴³, T. Seiss³⁶, J.M. Seixas^{78b}, G. Sekhniaidze^{67a}, K. Sekhon¹⁰³,
S.J. Sekula⁴¹, N. Semprini-Cesari^{23b,23a}, S. Sen⁴⁷, S. Senkin³⁷, C. Serfon¹³⁰, L. Serin¹²⁸,
L. Serkin^{64a,64b}, M. Sessa^{72a,72b}, H. Severini¹²⁴, F. Sforza¹⁶⁷, A. Sfyrila⁵², E. Shabalina⁵¹,
J.D. Shahinian¹⁴³, N.W. Shaikh^{43a,43b}, L.Y. Shan^{15a}, R. Shang¹⁷⁰, J.T. Shank²⁵,
M. Shapiro¹⁸, A.S. Sharma¹, A. Sharma¹³¹, P.B. Shatalov¹⁰⁹, K. Shaw¹⁵³, S.M. Shaw⁹⁸,
A. Shcherbakova¹³⁴, Y. Shen¹²⁴, N. Sherafati³³, A.D. Sherman²⁵, P. Sherwood⁹²,
L. Shi^{155,am}, S. Shimizu⁷⁹, C.O. Shimmin¹⁸⁰, M. Shimojima¹¹⁴, I.P.J. Shipsey¹³¹,
S. Shirabe⁸⁵, M. Shiyakova⁷⁷, J. Shlomi¹⁷⁷, A. Shmeleva¹⁰⁸, D. Shoaleh Saadi¹⁰⁷,
M.J. Shochet³⁶, S. Shojaii¹⁰², D.R. Shope¹²⁴, S. Shrestha¹²², E. Shulga¹¹⁰, P. Sicho¹³⁷,
A.M. Sickles¹⁷⁰, P.E. Sidebo¹⁵¹, E. Sideras Haddad^{32c}, O. Sidiropoulou³⁵, A. Sidoti^{23b,23a},
F. Siegert⁴⁶, Dj. Sijacki¹⁶, J. Silva^{136a}, M. Silva Jr.¹⁷⁸, M.V. Silva Oliveira^{78a},
S.B. Silverstein^{43a}, L. Simic⁷⁷, S. Simion¹²⁸, E. Simioni⁹⁷, M. Simon⁹⁷, R. Simoniello⁹⁷,
P. Sinervo¹⁶⁴, N.B. Sinev¹²⁷, M. Sioli^{23b,23a}, G. Siragusa¹⁷⁴, I. Siral¹⁰³,
S.Yu. Sivoklokov¹¹¹, J. Sjölin^{43a,43b}, P. Skubic¹²⁴, M. Slater²¹, T. Slavicek¹³⁸,
M. Slawinska⁸², K. Sliwa¹⁶⁷, R. Slovak¹³⁹, V. Smakhtin¹⁷⁷, B.H. Smart⁵, J. Smiesko^{28a},
N. Smirnov¹¹⁰, S.Yu. Smirnov¹¹⁰, Y. Smirnov¹¹⁰, L.N. Smirnova¹¹¹, O. Smirnova⁹⁴,
J.W. Smith⁵¹, M.N.K. Smith³⁸, M. Smizanska⁸⁷, K. Smolek¹³⁸, A. Smykiewicz⁸²,
A.A. Snesarev¹⁰⁸, I.M. Snyder¹²⁷, S. Snyder²⁹, R. Sobie^{173,ab}, A.M. Soffa¹⁶⁸, A. Soffer¹⁵⁸,
A. Søggaard⁴⁸, D.A. Soh¹⁵⁵, G. Sokhrannyi⁸⁹, C.A. Solans Sanchez³⁵, M. Solar¹³⁸,
E.Yu. Soldatov¹¹⁰, U. Soldevila¹⁷¹, A.A. Solodkov¹⁴⁰, A. Soloshenko⁷⁷,
O.V. Solovyanov¹⁴⁰, V. Solovyev¹³⁴, P. Sommer¹⁴⁶, H. Son¹⁶⁷, W. Song¹⁴¹,
W.Y. Song^{165b}, A. Sopczak¹³⁸, F. Sopkova^{28b}, D. Sosa^{59b}, C.L. Sotiropoulou^{69a,69b},
S. Sottocornola^{68a,68b}, R. Soualah^{64a,64c,h}, A.M. Soukharev^{120b,120a}, D. South⁴⁴,
B.C. Sowden⁹¹, S. Spagnolo^{65a,65b}, M. Spalla¹¹³, M. Spangenberg¹⁷⁵, F. Spanò⁹¹,
D. Sperlich¹⁹, F. Spettel¹¹³, T.M. Spieker^{59a}, R. Spighi^{23b}, G. Spigo³⁵, L.A. Spiller¹⁰²,
D.P. Spiteri⁵⁵, M. Spousta¹³⁹, A. Stabile^{66a,66b}, R. Stamen^{59a}, S. Stamm¹⁹, E. Stanecka⁸²,
R.W. Stanek⁶, C. Stanescu^{72a}, B. Stanislaus¹³¹, M.M. Stanitzki⁴⁴, B.S. Stapf¹¹⁸,
S. Stapnes¹³⁰, E.A. Starchenko¹⁴⁰, G.H. Stark³⁶, J. Stark⁵⁶, S.H. Stark³⁹, P. Staroba¹³⁷,
P. Starovoitov^{59a}, S. Stärz³⁵, R. Staszewski⁸², M. Stegler⁴⁴, P. Steinberg²⁹, B. Stelzer¹⁴⁹,
H.J. Stelzer³⁵, O. Stelzer-Chilton^{165a}, H. Stenzel⁵⁴, T.J. Stevenson⁹⁰, G.A. Stewart⁵⁵,
M.C. Stockton¹²⁷, G. Stoicea^{27b}, P. Stolte⁵¹, S. Stonjek¹¹³, A. Straessner⁴⁶,
J. Strandberg¹⁵¹, S. Strandberg^{43a,43b}, M. Strauss¹²⁴, P. Strizenec^{28b}, R. Ströhmer¹⁷⁴,
D.M. Strom¹²⁷, R. Stroynowski⁴¹, A. Strubig⁴⁸, S.A. Stucci²⁹, B. Stugu¹⁷, J. Stupak¹²⁴,

N.A. Styles⁴⁴, D. Su¹⁵⁰, J. Su¹³⁵, S. Suchek^{59a}, Y. Sugaya¹²⁹, M. Suk¹³⁸, V.V. Sulin¹⁰⁸,
D.M.S. Sultan⁵², S. Sultansoy^{4c}, T. Sumida⁸³, S. Sun¹⁰³, X. Sun³, K. Suruliz¹⁵³,
C.J.E. Suster¹⁵⁴, M.R. Sutton¹⁵³, S. Suzuki⁷⁹, M. Svatos¹³⁷, M. Swiatlowski³⁶,
S.P. Swift², A. Sydorenko⁹⁷, I. Sykora^{28a}, T. Sykora¹³⁹, D. Ta⁹⁷, K. Tackmann^{44,y},
J. Taenzer¹⁵⁸, A. Taffard¹⁶⁸, R. Tafirout^{165a}, E. Tahirovic⁹⁰, N. Taiblum¹⁵⁸, H. Takai²⁹,
R. Takashima⁸⁴, E.H. Takasugi¹¹³, K. Takeda⁸⁰, T. Takeshita¹⁴⁷, Y. Takubo⁷⁹,
M. Talby⁹⁹, A.A. Talyshev^{120b,120a}, J. Tanaka¹⁶⁰, M. Tanaka¹⁶², R. Tanaka¹²⁸,
B.B. Tannenwald¹²², S. Tapia Araya^{144b}, S. Tapprogge⁹⁷,
A. Tarek Abouelfadl Mohamed¹³², S. Tarem¹⁵⁷, G. Tarna^{27b,d}, G.F. Tartarelli^{66a},
P. Tas¹³⁹, M. Tasevsky¹³⁷, T. Tashiro⁸³, E. Tassi^{40b,40a}, A. Tavares Delgado^{136a,136b},
Y. Tayalati^{34e}, A.C. Taylor¹¹⁶, A.J. Taylor⁴⁸, G.N. Taylor¹⁰², P.T.E. Taylor¹⁰²,
W. Taylor^{165b}, A.S. Tee⁸⁷, P. Teixeira-Dias⁹¹, H. Ten Kate³⁵, P.K. Teng¹⁵⁵, J.J. Teoh¹¹⁸,
F. Tepel¹⁷⁹, S. Terada⁷⁹, K. Terashi¹⁶⁰, J. Terron⁹⁶, S. Terzo¹⁴, M. Testa⁴⁹,
R.J. Teuscher^{164,ab}, S.J. Thais¹⁸⁰, T. Theveneaux-Pelzer⁴⁴, F. Thiele³⁹, D.W. Thomas⁹¹,
J.P. Thomas²¹, A.S. Thompson⁵⁵, P.D. Thompson²¹, L.A. Thomsen¹⁸⁰, E. Thomson¹³³,
Y. Tian³⁸, R.E. Ticse Torres⁵¹, V.O. Tikhomirov^{108,aj}, Yu.A. Tikhonov^{120b,120a},
S. Timoshenko¹¹⁰, P. Tipton¹⁸⁰, S. Tisserant⁹⁹, K. Todome¹⁶², S. Todorova-Nova⁵,
S. Todt⁴⁶, J. Tojo⁸⁵, S. Tokár^{28a}, K. Tokushuku⁷⁹, E. Tolley¹²², K.G. Tomiwa^{32c},
M. Tomoto¹¹⁵, L. Tompkins¹⁵⁰, K. Toms¹¹⁶, B. Tong⁵⁷, P. Tornambe⁵⁰, E. Torrence¹²⁷,
H. Torres⁴⁶, E. Torró Pastor¹⁴⁵, C. Toscirì¹³¹, J. Toth^{99,aa}, F. Touchard⁹⁹, D.R. Tovey¹⁴⁶,
C.J. Treado¹²¹, T. Trefzger¹⁷⁴, F. Tresoldi¹⁵³, A. Tricoli²⁹, I.M. Trigger^{165a},
S. Trincaz-Duvoid¹³², M.F. Tripiana¹⁴, W. Trischuk¹⁶⁴, B. Trocme⁵⁶, A. Trofymov¹²⁸,
C. Troncon^{66a}, M. Trovatelli¹⁷³, F. Trovato¹⁵³, L. Truong^{32b}, M. Trzebinski⁸²,
A. Trzupek⁸², F. Tsai⁴⁴, J.C-L. Tseng¹³¹, P.V. Tsiareshka¹⁰⁵, A. Tsirigotis¹⁵⁹,
N. Tsirintanis⁹, V. Tsiskaridze¹⁵², E.G. Tskhadadze^{156a}, I.I. Tsukerman¹⁰⁹, V. Tsulaia¹⁸,
S. Tsuno⁷⁹, D. Tsybychev¹⁵², Y. Tu^{61b}, A. Tudorache^{27b}, V. Tudorache^{27b},
T.T. Tulbure^{27a}, A.N. Tuna⁵⁷, S. Turchikhin⁷⁷, D. Turgeman¹⁷⁷, I. Turk Cakir^{4b,s},
R. Turra^{66a}, P.M. Tuts³⁸, E. Tzovara⁹⁷, G. Ucchielli^{23b,23a}, I. Ueda⁷⁹, M. Ughetto^{43a,43b},
F. Ukegawa¹⁶⁶, G. Unal³⁵, A. Undrus²⁹, G. Unel¹⁶⁸, F.C. Ungaro¹⁰², Y. Unno⁷⁹,
K. Uno¹⁶⁰, J. Urban^{28b}, P. Urquijo¹⁰², P. Urrejola⁹⁷, G. Usai⁸, J. Usui⁷⁹, L. Vacavant⁹⁹,
V. Vacek¹³⁸, B. Vachon¹⁰¹, K.O.H. Vadla¹³⁰, A. Vaidya⁹², C. Valderanis¹¹²,
E. Valdes Santurio^{43a,43b}, M. Valente⁵², S. Valentinetti^{23b,23a}, A. Valero¹⁷¹, L. Valéry⁴⁴,
R.A. Vallance²¹, A. Vallier⁵, J.A. Valls Ferrer¹⁷¹, T.R. Van Daalen¹⁴,
H. Van der Graaf¹¹⁸, P. Van Gemmeren⁶, J. Van Nieuwkoop¹⁴⁹, I. Van Vulpen¹¹⁸,
M. Vanadia^{71a,71b}, W. Vandelli³⁵, A. Vaniachine¹⁶³, P. Vankov¹¹⁸, R. Vari^{70a},
E.W. Varnes⁷, C. Varni^{53b,53a}, T. Varol⁴¹, D. Varouchas¹²⁸, K.E. Varvell¹⁵⁴,
G.A. Vasquez^{144b}, J.G. Vasquez¹⁸⁰, F. Vazeille³⁷, D. Vazquez Furelos¹⁴,
T. Vazquez Schroeder¹⁰¹, J. Veatch⁵¹, V. Vecchio^{72a,72b}, L.M. Veloce¹⁶⁴,
F. Veloso^{136a,136c}, S. Veneziano^{70a}, A. Ventura^{65a,65b}, M. Venturi¹⁷³, N. Venturi³⁵,
V. Vercesi^{68a}, M. Verducci^{72a,72b}, C.M. Vergel Infante⁷⁶, C. Vergis²⁴, W. Verkerke¹¹⁸,
A.T. Vermeulen¹¹⁸, J.C. Vermeulen¹¹⁸, M.C. Vetterli^{149,aq}, N. Viaux Maira^{144b},
M. Vicente Barreto Pinto⁵², I. Vichou^{170,*}, T. Vickey¹⁴⁶, O.E. Vickey Boeriu¹⁴⁶,
G.H.A. Viehhauser¹³¹, S. Viel¹⁸, L. Vigani¹³¹, M. Villa^{23b,23a}, M. Villaplana Perez^{66a,66b},

E. Vilucchi⁴⁹, M.G. Vinciter³³, V.B. Vinogradov⁷⁷, A. Vishwakarma⁴⁴, C. Vittori^{23b,23a}, I. Vivarelli¹⁵³, S. Vlachos¹⁰, M. Vogel¹⁷⁹, P. Vokac¹³⁸, G. Volpi¹⁴, S.E. Von Buddenbrock^{32c}, E. Von Toerne²⁴, V. Vorobel¹³⁹, K. Vorobev¹¹⁰, M. Vos¹⁷¹, J.H. Vossebeld⁸⁸, N. Vranjes¹⁶, M. Vranjes Milosavljevic¹⁶, V. Vrba¹³⁸, M. Vreeswijk¹¹⁸, T. Šfiligoj⁸⁹, R. Vuillermet³⁵, I. Vukotic³⁶, T. Ženiš^{28a}, L. Živković¹⁶, P. Wagner²⁴, W. Wagner¹⁷⁹, J. Wagner-Kuhr¹¹², H. Wahlberg⁸⁶, S. Wahrmund⁴⁶, K. Wakamiya⁸⁰, V.M. Walbrecht¹¹³, J. Walder⁸⁷, R. Walker¹¹², S.D. Walker⁹¹, W. Walkowiak¹⁴⁸, V. Wallangen^{43a,43b}, A.M. Wang⁵⁷, C. Wang^{58b,d}, F. Wang¹⁷⁸, H. Wang¹⁸, H. Wang³, J. Wang¹⁵⁴, J. Wang^{59b}, P. Wang⁴¹, Q. Wang¹²⁴, R.-J. Wang¹³², R. Wang^{58a}, R. Wang⁶, S.M. Wang¹⁵⁵, W.T. Wang^{58a}, W. Wang^{15b,ac}, W.X. Wang^{58a,ac}, Y. Wang^{58a}, Z. Wang^{58c}, C. Wanotayaroj⁴⁴, A. Warburton¹⁰¹, C.P. Ward³¹, D.R. Wardrope⁹², A. Washbrook⁴⁸, P.M. Watkins²¹, A.T. Watson²¹, M.F. Watson²¹, G. Watts¹⁴⁵, S. Watts⁹⁸, B.M. Waugh⁹², A.F. Webb¹¹, S. Webb⁹⁷, C. Weber¹⁸⁰, M.S. Weber²⁰, S.A. Weber³³, S.M. Weber^{59a}, A.R. Weidberg¹³¹, B. Weinert⁶³, J. Weingarten⁵¹, M. Weirich⁹⁷, C. Weiser⁵⁰, P.S. Wells³⁵, T. Wenaus²⁹, T. Wengler³⁵, S. Wenig³⁵, N. Vermes²⁴, M.D. Werner⁷⁶, P. Werner³⁵, M. Wessels^{59a}, T.D. Weston²⁰, K. Whalen¹²⁷, N.L. Whallon¹⁴⁵, A.M. Wharton⁸⁷, A.S. White¹⁰³, A. White⁸, M.J. White¹, R. White^{144b}, D. Whiteson¹⁶⁸, B.W. Whitmore⁸⁷, F.J. Wickens¹⁴¹, W. Wiedenmann¹⁷⁸, M. Wielers¹⁴¹, C. Wiglesworth³⁹, L.A.M. Wiik-Fuchs⁵⁰, A. Wildauer¹¹³, F. Wilk⁹⁸, H.G. Wilkens³⁵, L.J. Wilkins⁹¹, H.H. Williams¹³³, S. Williams³¹, C. Willis¹⁰⁴, S. Willocq¹⁰⁰, J.A. Wilson²¹, I. Wingerter-Seez⁵, E. Winkels¹⁵³, F. Winklmeier¹²⁷, O.J. Winston¹⁵³, B.T. Winter²⁴, M. Wittgen¹⁵⁰, M. Wobisch⁹³, A. Wolf⁹⁷, T.M.H. Wolf¹¹⁸, R. Wolff⁹⁹, M.W. Wolter⁸², H. Wolters^{136a,136c}, V.W.S. Wong¹⁷², N.L. Woods¹⁴³, S.D. Worm²¹, B.K. Wosiek⁸², K.W. Woźniak⁸², K. Wraight⁵⁵, M. Wu³⁶, S.L. Wu¹⁷⁸, X. Wu⁵², Y. Wu^{58a}, T.R. Wyatt⁹⁸, B.M. Wynne⁴⁸, S. Xella³⁹, Z. Xi¹⁰³, L. Xia¹⁷⁵, D. Xu^{15a}, H. Xu^{58a}, L. Xu²⁹, T. Xu¹⁴², W. Xu¹⁰³, B. Yabsley¹⁵⁴, S. Yacoob^{32a}, K. Yajima¹²⁹, D.P. Yallup⁹², D. Yamaguchi¹⁶², Y. Yamaguchi¹⁶², A. Yamamoto⁷⁹, T. Yamanaka¹⁶⁰, F. Yamane⁸⁰, M. Yamatani¹⁶⁰, T. Yamazaki¹⁶⁰, Y. Yamazaki⁸⁰, Z. Yan²⁵, H.J. Yang^{58c,58d}, H.T. Yang¹⁸, S. Yang⁷⁵, Y. Yang¹⁶⁰, Z. Yang¹⁷, W.-M. Yao¹⁸, Y.C. Yap⁴⁴, Y. Yasu⁷⁹, E. Yatsenko^{58c,58d}, J. Ye⁴¹, S. Ye²⁹, I. Yeletsikh⁷⁷, E. Yigitbasi²⁵, E. Yildirim⁹⁷, K. Yorita¹⁷⁶, K. Yoshihara¹³³, C.J.S. Young³⁵, C. Young¹⁵⁰, J. Yu⁸, J. Yu⁷⁶, X. Yue^{59a}, S.P.Y. Yuen²⁴, B. Zabinski⁸², G. Zacharis¹⁰, E. Zaffaroni⁵², R. Zaidan¹⁴, A.M. Zaitsev^{140,ai}, T. Zakareishvili^{156b}, N. Zakharchuk⁴⁴, J. Zalieckas¹⁷, S. Zambito⁵⁷, D. Zanzi³⁵, D.R. Zaripovas⁵⁵, S.V. Zeißner⁴⁵, C. Zeitnitz¹⁷⁹, G. Zemaityte¹³¹, J.C. Zeng¹⁷⁰, Q. Zeng¹⁵⁰, O. Zenin¹⁴⁰, D. Zerwas¹²⁸, M. Zgubić¹³¹, D.F. Zhang^{58b}, D. Zhang¹⁰³, F. Zhang¹⁷⁸, G. Zhang^{58a}, H. Zhang^{15b}, J. Zhang⁶, L. Zhang^{15b}, L. Zhang^{58a}, M. Zhang¹⁷⁰, P. Zhang^{15b}, R. Zhang^{58a}, R. Zhang²⁴, X. Zhang^{58b}, Y. Zhang^{15d}, Z. Zhang¹²⁸, X. Zhao⁴¹, Y. Zhao^{58b,128,af}, Z. Zhao^{58a}, A. Zhemchugov⁷⁷, B. Zhou¹⁰³, C. Zhou¹⁷⁸, L. Zhou⁴¹, M.S. Zhou^{15d}, M. Zhou¹⁵², N. Zhou^{58c}, Y. Zhou⁷, C.G. Zhu^{58b}, H.L. Zhu^{58a}, H. Zhu^{15a}, J. Zhu¹⁰³, Y. Zhu^{58a}, X. Zhuang^{15a}, K. Zhukov¹⁰⁸, V. Zhulanov^{120b,120a}, A. Zibell¹⁷⁴, D. Zieminska⁶³, N.I. Zimine⁷⁷, S. Zimmermann⁵⁰, Z. Zinonos¹¹³, M. Zinser⁹⁷, M. Ziolkowski¹⁴⁸, G. Zobernig¹⁷⁸, A. Zoccoli^{23b,23a}, K. Zoch⁵¹, T.G. Zorbas¹⁴⁶, R. Zou³⁶, M. Zur Nedden¹⁹, L. Zwalinski³⁵

- ¹ *Department of Physics, University of Adelaide, Adelaide; Australia*
- ² *Physics Department, SUNY Albany, Albany NY; United States of America*
- ³ *Department of Physics, University of Alberta, Edmonton AB; Canada*
- ⁴ *Department of Physics^(a), Ankara University, Ankara; Istanbul Aydin University^(b), Istanbul; Division of Physics^(c), TOBB University of Economics and Technology, Ankara; Turkey*
- ⁵ *LAPP, Université Grenoble Alpes, Université Savoie Mont Blanc, CNRS/IN2P3, Annecy; France*
- ⁶ *High Energy Physics Division, Argonne National Laboratory, Argonne IL; United States of America*
- ⁷ *Department of Physics, University of Arizona, Tucson AZ; United States of America*
- ⁸ *Department of Physics, University of Texas at Arlington, Arlington TX; United States of America*
- ⁹ *Physics Department, National and Kapodistrian University of Athens, Athens; Greece*
- ¹⁰ *Physics Department, National Technical University of Athens, Zografou; Greece*
- ¹¹ *Department of Physics, University of Texas at Austin, Austin TX; United States of America*
- ¹² *Bahcesehir University^(a), Faculty of Engineering and Natural Sciences, Istanbul; Istanbul Bilgi University^(b), Faculty of Engineering and Natural Sciences, Istanbul; Department of Physics^(c), Bogazici University, Istanbul; Department of Physics Engineering^(d), Gaziantep University, Gaziantep; Turkey*
- ¹³ *Institute of Physics, Azerbaijan Academy of Sciences, Baku; Azerbaijan*
- ¹⁴ *Institut de Física d'Altes Energies (IFAE), Barcelona Institute of Science and Technology, Barcelona; Spain*
- ¹⁵ *Institute of High Energy Physics^(a), Chinese Academy of Sciences, Beijing; Department of Physics^(b), Nanjing University, Nanjing; Physics Department^(c), Tsinghua University, Beijing; University of Chinese Academy of Science (UCAS)^(d), Beijing; China*
- ¹⁶ *Institute of Physics, University of Belgrade, Belgrade; Serbia*
- ¹⁷ *Department for Physics and Technology, University of Bergen, Bergen; Norway*
- ¹⁸ *Physics Division, Lawrence Berkeley National Laboratory and University of California, Berkeley CA; United States of America*
- ¹⁹ *Institut für Physik, Humboldt Universität zu Berlin, Berlin; Germany*
- ²⁰ *Albert Einstein Center for Fundamental Physics and Laboratory for High Energy Physics, University of Bern, Bern; Switzerland*
- ²¹ *School of Physics and Astronomy, University of Birmingham, Birmingham; United Kingdom*
- ²² *Centro de Investigaciones, Universidad Antonio Nariño, Bogota; Colombia*
- ²³ *Dipartimento di Fisica e Astronomia^(a), Università di Bologna, Bologna; INFN Sezione di Bologna; Italy*
- ²⁴ *Physikalisches Institut^(b), Universität Bonn, Bonn; Germany*
- ²⁵ *Department of Physics, Boston University, Boston MA; United States of America*
- ²⁶ *Department of Physics, Brandeis University, Waltham MA; United States of America*
- ²⁷ *Transilvania University of Brasov^(a), Brasov; Horia Hulubei National Institute of Physics and Nuclear Engineering^(b), Bucharest; Department of Physics^(c), Alexandru Ioan Cuza University of Iasi, Iasi; National Institute for Research and Development of Isotopic and Molecular Technologies^(d), Physics Department, Cluj-Napoca; University Politehnica Bucharest^(e), Bucharest; West University in Timisoara^(f), Timisoara; Romania*
- ²⁸ *Faculty of Mathematics^(a), Physics and Informatics, Comenius University, Bratislava; Department of Subnuclear Physics^(b), Institute of Experimental Physics of the Slovak Academy of Sciences, Kosice; Slovak Republic*
- ²⁹ *Physics Department, Brookhaven National Laboratory, Upton NY; United States of America*
- ³⁰ *Departamento de Física, Universidad de Buenos Aires, Buenos Aires; Argentina*
- ³¹ *Cavendish Laboratory, University of Cambridge, Cambridge; United Kingdom*
- ³² *Department of Physics^(a), University of Cape Town, Cape Town; Department of Mechanical Engineering Science^(b), University of Johannesburg, Johannesburg; School of Physics^(c), University of the Witwatersrand, Johannesburg; South Africa*
- ³³ *Department of Physics, Carleton University, Ottawa ON; Canada*
- ³⁴ *Faculté des Sciences Ain Chock^(a), Réseau Universitaire de Physique des Hautes Energies —*

- Université Hassan II, Casablanca; Centre National de l'Energie des Sciences Techniques Nucleaires (CNESTEN)^(b), Rabat; Faculté des Sciences Semlalia^(c), Université Cadi Ayyad, LPHEA-Marrakech; Faculté des Sciences^(d), Université Mohamed Premier and LPTPM, Oujda; Faculté des sciences^(e), Université Mohammed V, Rabat; Morocco
 35 CERN, Geneva; Switzerland
 36 Enrico Fermi Institute, University of Chicago, Chicago IL; United States of America
 37 LPC, Université Clermont Auvergne, CNRS/IN2P3, Clermont-Ferrand; France
 38 Nevis Laboratory, Columbia University, Irvington NY; United States of America
 39 Niels Bohr Institute, University of Copenhagen, Copenhagen; Denmark
 40 Dipartimento di Fisica^(a), Università della Calabria, Rende; INFN Gruppo Collegato di Cosenza^(b), Laboratori Nazionali di Frascati; Italy
 41 Physics Department, Southern Methodist University, Dallas TX; United States of America
 42 Physics Department, University of Texas at Dallas, Richardson TX; United States of America
 43 Department of Physics^(a), Stockholm University; Oskar Klein Centre^(b), Stockholm; Sweden
 44 Deutsches Elektronen-Synchrotron DESY, Hamburg and Zeuthen; Germany
 45 Lehrstuhl für Experimentelle Physik IV, Technische Universität Dortmund, Dortmund; Germany
 46 Institut für Kern- und Teilchenphysik, Technische Universität Dresden, Dresden; Germany
 47 Department of Physics, Duke University, Durham NC; United States of America
 48 SUPA — School of Physics and Astronomy, University of Edinburgh, Edinburgh; United Kingdom
 49 INFN e Laboratori Nazionali di Frascati, Frascati; Italy
 50 Physikalisches Institut, Albert-Ludwigs-Universität Freiburg, Freiburg; Germany
 51 II. Physikalisches Institut, Georg-August-Universität Göttingen, Göttingen; Germany
 52 Département de Physique Nucléaire et Corpusculaire, Université de Genève, Genève; Switzerland
 53 Dipartimento di Fisica^(a), Università di Genova, Genova; INFN Sezione di Genova^(b); Italy
 54 II. Physikalisches Institut, Justus-Liebig-Universität Giessen, Giessen; Germany
 55 SUPA — School of Physics and Astronomy, University of Glasgow, Glasgow; United Kingdom
 56 LPSC, Université Grenoble Alpes, CNRS/IN2P3, Grenoble INP, Grenoble; France
 57 Laboratory for Particle Physics and Cosmology, Harvard University, Cambridge MA; United States of America
 58 Department of Modern Physics and State Key Laboratory of Particle Detection and Electronics^(a), University of Science and Technology of China, Hefei; Institute of Frontier and Interdisciplinary Science and Key Laboratory of Particle Physics and Particle Irradiation (MOE)^(b), Shandong University, Qingdao; School of Physics and Astronomy^(c), Shanghai Jiao Tong University, KLPPAC-MoE, SKLPPC, Shanghai; Tsung-Dao Lee Institute^(d), Shanghai; China
 59 Kirchhoff-Institut für Physik^(a), Ruprecht-Karls-Universität Heidelberg, Heidelberg; Physikalisches Institut^(b), Ruprecht-Karls-Universität Heidelberg, Heidelberg; Germany
 60 Faculty of Applied Information Science, Hiroshima Institute of Technology, Hiroshima; Japan
 61 Department of Physics^(a), Chinese University of Hong Kong, Shatin, N.T., Hong Kong; Department of Physics^(b), University of Hong Kong, Hong Kong; Department of Physics and Institute for Advanced Study^(c), Hong Kong University of Science and Technology, Clear Water Bay, Kowloon, Hong Kong; China
 62 Department of Physics, National Tsing Hua University, Hsinchu; Taiwan
 63 Department of Physics, Indiana University, Bloomington IN; United States of America
 64 INFN Gruppo Collegato di Udine^(a), Sezione di Trieste, Udine; ICTP^(b), Trieste; Dipartimento di Chimica^(c), Fisica e Ambiente, Università di Udine, Udine; Italy
 65 INFN Sezione di Lecce^(a); Dipartimento di Matematica e Fisica^(b), Università del Salento, Lecce; Italy
 66 INFN Sezione di Milano^(a); Dipartimento di Fisica^(b), Università di Milano, Milano; Italy
 67 INFN Sezione di Napoli^(a); Dipartimento di Fisica^(b), Università di Napoli, Napoli; Italy
 68 INFN Sezione di Pavia^(a); Dipartimento di Fisica^(b), Università di Pavia, Pavia; Italy
 69 INFN Sezione di Pisa^(a); Dipartimento di Fisica E. Fermi^(b), Università di Pisa, Pisa; Italy
 70 INFN Sezione di Roma^(a); Dipartimento di Fisica^(b), Sapienza Università di Roma, Roma; Italy

- ⁷¹ INFN Sezione di Roma Tor Vergata^(a); Dipartimento di Fisica^(b), Università di Roma Tor Vergata, Roma; Italy
- ⁷² INFN Sezione di Roma Tre^(a); Dipartimento di Matematica e Fisica^(b), Università Roma Tre, Roma; Italy
- ⁷³ INFN-TIFPA^(a); Università degli Studi di Trento^(b), Trento; Italy
- ⁷⁴ Institut für Astro- und Teilchenphysik, Leopold-Franzens-Universität, Innsbruck; Austria
- ⁷⁵ University of Iowa, Iowa City IA; United States of America
- ⁷⁶ Department of Physics and Astronomy, Iowa State University, Ames IA; United States of America
- ⁷⁷ Joint Institute for Nuclear Research, Dubna; Russia
- ⁷⁸ Departamento de Engenharia Elétrica^(a), Universidade Federal de Juiz de Fora (UFJF), Juiz de Fora; Universidade Federal do Rio De Janeiro COPPE/EE/IF^(b), Rio de Janeiro; Universidade Federal de São João del Rei (UFSJ)^(c), São João del Rei; Instituto de Física^(d), Universidade de São Paulo, São Paulo; Brazil
- ⁷⁹ KEK, High Energy Accelerator Research Organization, Tsukuba; Japan
- ⁸⁰ Graduate School of Science, Kobe University, Kobe; Japan
- ⁸¹ AGH University of Science and Technology^(a), Faculty of Physics and Applied Computer Science, Krakow; Marian Smoluchowski Institute of Physics^(b), Jagiellonian University, Krakow; Poland
- ⁸² Institute of Nuclear Physics Polish Academy of Sciences, Krakow; Poland
- ⁸³ Faculty of Science, Kyoto University, Kyoto; Japan
- ⁸⁴ Kyoto University of Education, Kyoto; Japan
- ⁸⁵ Research Center for Advanced Particle Physics and Department of Physics, Kyushu University, Fukuoka; Japan
- ⁸⁶ Instituto de Física La Plata, Universidad Nacional de La Plata and CONICET, La Plata; Argentina
- ⁸⁷ Physics Department, Lancaster University, Lancaster; United Kingdom
- ⁸⁸ Oliver Lodge Laboratory, University of Liverpool, Liverpool; United Kingdom
- ⁸⁹ Department of Experimental Particle Physics, Jožef Stefan Institute and Department of Physics, University of Ljubljana, Ljubljana; Slovenia
- ⁹⁰ School of Physics and Astronomy, Queen Mary University of London, London; United Kingdom
- ⁹¹ Department of Physics, Royal Holloway University of London, Egham; United Kingdom
- ⁹² Department of Physics and Astronomy, University College London, London; United Kingdom
- ⁹³ Louisiana Tech University, Ruston LA; United States of America
- ⁹⁴ Fysiska institutionen, Lunds universitet, Lund; Sweden
- ⁹⁵ Centre de Calcul de l'Institut National de Physique Nucléaire et de Physique des Particules (IN2P3), Villeurbanne; France
- ⁹⁶ Departamento de Física Teórica C-15 and CIAFF, Universidad Autónoma de Madrid, Madrid; Spain
- ⁹⁷ Institut für Physik, Universität Mainz, Mainz; Germany
- ⁹⁸ School of Physics and Astronomy, University of Manchester, Manchester; United Kingdom
- ⁹⁹ CPPM, Aix-Marseille Université, CNRS/IN2P3, Marseille; France
- ¹⁰⁰ Department of Physics, University of Massachusetts, Amherst MA; United States of America
- ¹⁰¹ Department of Physics, McGill University, Montreal QC; Canada
- ¹⁰² School of Physics, University of Melbourne, Victoria; Australia
- ¹⁰³ Department of Physics, University of Michigan, Ann Arbor MI; United States of America
- ¹⁰⁴ Department of Physics and Astronomy, Michigan State University, East Lansing MI; United States of America
- ¹⁰⁵ B.I. Stepanov Institute of Physics, National Academy of Sciences of Belarus, Minsk; Belarus
- ¹⁰⁶ Research Institute for Nuclear Problems of Byelorussian State University, Minsk; Belarus
- ¹⁰⁷ Group of Particle Physics, University of Montreal, Montreal QC; Canada
- ¹⁰⁸ P.N. Lebedev Physical Institute of the Russian Academy of Sciences, Moscow; Russia
- ¹⁰⁹ Institute for Theoretical and Experimental Physics (ITEP), Moscow; Russia
- ¹¹⁰ National Research Nuclear University MEPhI, Moscow; Russia
- ¹¹¹ D.V. Skobeltsyn Institute of Nuclear Physics, M.V. Lomonosov Moscow State University, Moscow;

- Russia
- ¹¹² Fakultät für Physik, Ludwig-Maximilians-Universität München, München; Germany
- ¹¹³ Max-Planck-Institut für Physik (Werner-Heisenberg-Institut), München; Germany
- ¹¹⁴ Nagasaki Institute of Applied Science, Nagasaki; Japan
- ¹¹⁵ Graduate School of Science and Kobayashi-Maskawa Institute, Nagoya University, Nagoya; Japan
- ¹¹⁶ Department of Physics and Astronomy, University of New Mexico, Albuquerque NM; United States of America
- ¹¹⁷ Institute for Mathematics, Astrophysics and Particle Physics, Radboud University Nijmegen/Nikhef, Nijmegen; Netherlands
- ¹¹⁸ Nikhef National Institute for Subatomic Physics and University of Amsterdam, Amsterdam; Netherlands
- ¹¹⁹ Department of Physics, Northern Illinois University, DeKalb IL; United States of America
- ¹²⁰ Budker Institute of Nuclear Physics^(a), SB RAS, Novosibirsk; Novosibirsk State University Novosibirsk^(b); Russia
- ¹²¹ Department of Physics, New York University, New York NY; United States of America
- ¹²² Ohio State University, Columbus OH; United States of America
- ¹²³ Faculty of Science, Okayama University, Okayama; Japan
- ¹²⁴ Homer L. Dodge Department of Physics and Astronomy, University of Oklahoma, Norman OK; United States of America
- ¹²⁵ Department of Physics, Oklahoma State University, Stillwater OK; United States of America
- ¹²⁶ Palacký University, RCPTM, Joint Laboratory of Optics, Olomouc; Czech Republic
- ¹²⁷ Center for High Energy Physics, University of Oregon, Eugene OR; United States of America
- ¹²⁸ LAL, Université Paris-Sud, CNRS/IN2P3, Université Paris-Saclay, Orsay; France
- ¹²⁹ Graduate School of Science, Osaka University, Osaka; Japan
- ¹³⁰ Department of Physics, University of Oslo, Oslo; Norway
- ¹³¹ Department of Physics, Oxford University, Oxford; United Kingdom
- ¹³² LPNHE, Sorbonne Université, Paris Diderot Sorbonne Paris Cité, CNRS/IN2P3, Paris; France
- ¹³³ Department of Physics, University of Pennsylvania, Philadelphia PA; United States of America
- ¹³⁴ Konstantinov Nuclear Physics Institute of National Research Centre "Kurchatov Institute", PNPI, St. Petersburg; Russia
- ¹³⁵ Department of Physics and Astronomy, University of Pittsburgh, Pittsburgh PA; United States of America
- ¹³⁶ Laboratório de Instrumentação e Física Experimental de Partículas — LIP^(a); Departamento de Física^(b), Faculdade de Ciências, Universidade de Lisboa, Lisboa; Departamento de Física^(c), Universidade de Coimbra, Coimbra; Centro de Física Nuclear da Universidade de Lisboa^(d), Lisboa; Departamento de Física^(e), Universidade do Minho, Braga; Departamento de Física Teórica y del Cosmos^(f), Universidad de Granada, Granada (Spain); Dep Física and CEFITEC of Faculdade de Ciências e Tecnologia^(g), Universidade Nova de Lisboa, Caparica; Portugal
- ¹³⁷ Institute of Physics, Academy of Sciences of the Czech Republic, Prague; Czech Republic
- ¹³⁸ Czech Technical University in Prague, Prague; Czech Republic
- ¹³⁹ Charles University, Faculty of Mathematics and Physics, Prague; Czech Republic
- ¹⁴⁰ State Research Center Institute for High Energy Physics, NRC KI, Protvino; Russia
- ¹⁴¹ Particle Physics Department, Rutherford Appleton Laboratory, Didcot; United Kingdom
- ¹⁴² IRFU, CEA, Université Paris-Saclay, Gif-sur-Yvette; France
- ¹⁴³ Santa Cruz Institute for Particle Physics, University of California Santa Cruz, Santa Cruz CA; United States of America
- ¹⁴⁴ Departamento de Física^(a), Pontificia Universidad Católica de Chile, Santiago; Departamento de Física^(b), Universidad Técnica Federico Santa María, Valparaíso; Chile
- ¹⁴⁵ Department of Physics, University of Washington, Seattle WA; United States of America
- ¹⁴⁶ Department of Physics and Astronomy, University of Sheffield, Sheffield; United Kingdom
- ¹⁴⁷ Department of Physics, Shinshu University, Nagano; Japan
- ¹⁴⁸ Department Physik, Universität Siegen, Siegen; Germany

- 149 *Department of Physics, Simon Fraser University, Burnaby BC; Canada*
 150 *SLAC National Accelerator Laboratory, Stanford CA; United States of America*
 151 *Physics Department, Royal Institute of Technology, Stockholm; Sweden*
 152 *Departments of Physics and Astronomy, Stony Brook University, Stony Brook NY; United States of America*
 153 *Department of Physics and Astronomy, University of Sussex, Brighton; United Kingdom*
 154 *School of Physics, University of Sydney, Sydney; Australia*
 155 *Institute of Physics, Academia Sinica, Taipei; Taiwan*
 156 *E. Andronikashvili Institute of Physics^(a), Iv. Javakhishvili Tbilisi State University, Tbilisi; High Energy Physics Institute^(b), Tbilisi State University, Tbilisi; Georgia*
 157 *Department of Physics, Technion, Israel Institute of Technology, Haifa; Israel*
 158 *Raymond and Beverly Sackler School of Physics and Astronomy, Tel Aviv University, Tel Aviv; Israel*
 159 *Department of Physics, Aristotle University of Thessaloniki, Thessaloniki; Greece*
 160 *International Center for Elementary Particle Physics and Department of Physics, University of Tokyo, Tokyo; Japan*
 161 *Graduate School of Science and Technology, Tokyo Metropolitan University, Tokyo; Japan*
 162 *Department of Physics, Tokyo Institute of Technology, Tokyo; Japan*
 163 *Tomsk State University, Tomsk; Russia*
 164 *Department of Physics, University of Toronto, Toronto ON; Canada*
 165 *TRIUMF^(a), Vancouver BC; Department of Physics and Astronomy^(b), York University, Toronto ON; Canada*
 166 *Division of Physics and Tomonaga Center for the History of the Universe, Faculty of Pure and Applied Sciences, University of Tsukuba, Tsukuba; Japan*
 167 *Department of Physics and Astronomy, Tufts University, Medford MA; United States of America*
 168 *Department of Physics and Astronomy, University of California Irvine, Irvine CA; United States of America*
 169 *Department of Physics and Astronomy, University of Uppsala, Uppsala; Sweden*
 170 *Department of Physics, University of Illinois, Urbana IL; United States of America*
 171 *Instituto de Física Corpuscular (IFIC), Centro Mixto Universidad de Valencia — CSIC, Valencia; Spain*
 172 *Department of Physics, University of British Columbia, Vancouver BC; Canada*
 173 *Department of Physics and Astronomy, University of Victoria, Victoria BC; Canada*
 174 *Fakultät für Physik und Astronomie, Julius-Maximilians-Universität Würzburg, Würzburg; Germany*
 175 *Department of Physics, University of Warwick, Coventry; United Kingdom*
 176 *Waseda University, Tokyo; Japan*
 177 *Department of Particle Physics, Weizmann Institute of Science, Rehovot; Israel*
 178 *Department of Physics, University of Wisconsin, Madison WI; United States of America*
 179 *Fakultät für Mathematik und Naturwissenschaften, Fachgruppe Physik, Bergische Universität Wuppertal, Wuppertal; Germany*
 180 *Department of Physics, Yale University, New Haven CT; United States of America*
 181 *Yerevan Physics Institute, Yerevan; Armenia*

^a *Also at Borough of Manhattan Community College, City University of New York, NY; United States of America*

^b *Also at Centre for High Performance Computing, CSIR Campus, Rosebank, Cape Town; South Africa*

^c *Also at CERN, Geneva; Switzerland*

^d *Also at CPPM, Aix-Marseille Université, CNRS/IN2P3, Marseille; France*

^e *Also at Département de Physique Nucléaire et Corpusculaire, Université de Genève, Genève; Switzerland*

- ^f Also at Departament de Física de la Universitat Autònoma de Barcelona, Barcelona; Spain
- ^g Also at Departamento de Física Teórica y del Cosmos, Universidad de Granada, Granada (Spain); Spain
- ^h Also at Department of Applied Physics and Astronomy, University of Sharjah, Sharjah; United Arab Emirates
- ⁱ Also at Department of Financial and Management Engineering, University of the Aegean, Chios; Greece
- ^j Also at Department of Physics and Astronomy, University of Louisville, Louisville, KY; United States of America
- ^k Also at Department of Physics and Astronomy, University of Sheffield, Sheffield; United Kingdom
- ^l Also at Department of Physics, California State University, Fresno CA; United States of America
- ^m Also at Department of Physics, California State University, Sacramento CA; United States of America
- ⁿ Also at Department of Physics, King's College London, London; United Kingdom
- ^o Also at Department of Physics, St. Petersburg State Polytechnical University, St. Petersburg; Russia
- ^p Also at Department of Physics, University of Fribourg, Fribourg; Switzerland
- ^q Also at Department of Physics, University of Michigan, Ann Arbor MI; United States of America
- ^r Also at Dipartimento di Fisica E. Fermi, Università di Pisa, Pisa; Italy
- ^s Also at Giresun University, Faculty of Engineering, Giresun; Turkey
- ^t Also at Graduate School of Science, Osaka University, Osaka; Japan
- ^u Also at Hellenic Open University, Patras; Greece
- ^v Also at Horia Hulubei National Institute of Physics and Nuclear Engineering, Bucharest; Romania
- ^w Also at II. Physikalisches Institut, Georg-August-Universität Göttingen, Göttingen; Germany
- ^x Also at Institutio Catalana de Recerca i Estudis Avancats, ICREA, Barcelona; Spain
- ^y Also at Institut für Experimentalphysik, Universität Hamburg, Hamburg; Germany
- ^z Also at Institute for Mathematics, Astrophysics and Particle Physics, Radboud University Nijmegen/Nikhef, Nijmegen; Netherlands
- ^{aa} Also at Institute for Particle and Nuclear Physics, Wigner Research Centre for Physics, Budapest; Hungary
- ^{ab} Also at Institute of Particle Physics (IPP); Canada
- ^{ac} Also at Institute of Physics, Academia Sinica, Taipei; Taiwan
- ^{ad} Also at Institute of Physics, Azerbaijan Academy of Sciences, Baku; Azerbaijan
- ^{ae} Also at Institute of Theoretical Physics, Ilia State University, Tbilisi; Georgia
- ^{af} Also at LAL, Université Paris-Sud, CNRS/IN2P3, Université Paris-Saclay, Orsay; France
- ^{ag} Also at Louisiana Tech University, Ruston LA; United States of America
- ^{ah} Also at Manhattan College, New York NY; United States of America
- ^{ai} Also at Moscow Institute of Physics and Technology State University, Dolgoprudny; Russia
- ^{aj} Also at National Research Nuclear University MEPhI, Moscow; Russia
- ^{ak} Also at Near East University, Nicosia, North Cyprus, Mersin; Turkey
- ^{al} Also at Physikalisches Institut, Albert-Ludwigs-Universität Freiburg, Freiburg; Germany
- ^{am} Also at School of Physics, Sun Yat-sen University, Guangzhou; China
- ^{an} Also at The City College of New York, New York NY; United States of America
- ^{ao} Also at The Collaborative Innovation Center of Quantum Matter (CICQM), Beijing; China
- ^{ap} Also at Tomsk State University, Tomsk, and Moscow Institute of Physics and Technology State University, Dolgoprudny; Russia
- ^{aq} Also at TRIUMF, Vancouver BC; Canada
- ^{ar} Also at Università di Napoli Parthenope, Napoli; Italy
- * Deceased